

83-31-9

83-31-9

Technical Report

Modeling the Fate of Aluminum in a Watershed
Under Acidified Conditions

Drew C. McAvoy
Graduate Research Assistant

James W. Male
Professor of Civil Engineering

November 1986
Env. ENg. Reprt. No.105-89-1

Technical Report

MODELING THE FATE OF ALUMINUM IN A
WATERSHED SYSTEM UNDER ACIDIFIED CONDITIONS

by

Drew C. McAvoy, Graduate Research Assistant
James W. Male, Professor

Environmental Engineering Program
Department of Civil Engineering
University of Massachusetts
Amherst, MA 01003

Submitted to the
Massachusetts Department Environmental Quality Engineering
Division of Water Pollution Control
S. Russell Sylva, Commissioner
Thomas C. McMahon, Director

November 1986 |

TABLE OF CONTENTS

	Page
LIST OF TABLES	iv
LIST OF FIGURES	v
PREFACE.....	xi
 CHAPTER	
I. INTRODUCTION	1
Background	1
Scope and Objectives	3
Site Description	5
Experimental Design	7
II. LITERATURE REVIEW	12
Aluminum Transport Mechanisms	12
Mineral Weathering and Solubility	13
Cation Exchange	18
Anion Adsorption	19
Complexation	20
Existing Aluminum Transport Models	23
Birkenes Model	23
ILWAS Model	29
MAGIC Model	38
pH and Aluminum Effects on Aquatic Biota	42
III. MATERIALS AND METHODS	47
Field Sampling	47
Precipitation	47
Streamwater	47
Soil	52
Laboratory Analysis	52
Precipitation and Streamwater Chemistry	52
Aluminum	53
pH	54
Acid Neutralizing Capacity	55
Major Inorganic Cations	57
Major Inorganic Anions	58
Fluoride	59
Dissolved Organic Carbon	60
Conductivity and Temperature	62

Soil Chemistry	62
Soil pH	62
Organic Matter Content	63
Exchangeable Base Cations	64
Exchangeable Acid Cations	64
Cation Exchange Capacity	65
Soil Moisture Characteristics	65
IV. MODEL DEVELOPMENT	67
Chemical Equilibrium Model	67
Mass-Action Equilibrium Equations	68
Temperature Correction	69
Ionic Strength Adjustment	72
Mass Balance Equations	74
Solution Technique	74
Transport Simulation Model	76
Hydrologic Submodel	78
Soil Compartment	82
Stream Compartment	85
Soil Chemistry Submodel	87
Stream Chemistry Submodel	96
Summary of Simulation Model	105
V. RESULTS AND DISCUSSION	108
Seasonal Streamwater Chemistry	108
Intensive Surveys	131
May, 1985	131
November, 1985	145
Soil Chemistry Analysis	157
Simulation Model	161
Input Parameter Estimations	162
Results and Discussion	168
VI. CONCLUSIONS AND RECOMMENDATIONS	183
Conclusions	183
Recommendations	186
BIBLIOGRAPHY	188

APPENDICES

- A. ANC Computer Program listing with Sample Input and Output
- B. Equilibrium Constants and Enthalpy Data Used in this Study
- C. Equal Computer Program Listing with Sample Input and Output
- D. Simulation Model Computer Program Listing with Sample Input and Output
- E. Raw Data Collected for This Study
- F. Plots of Streamwater Ions

LIST OF TABLES

Tables	Page
1. Summary of processes included in the Birkenes Model (from Christophersen <u>et al.</u> , 1982)	27
2. Biogeochemical processes considered in the ILWAS Model (from Chen <u>et al.</u> , 1983)	34
3. Summary of the model equations, parameters, and inputs used in the MAGIC Model (from Cosby <u>et al.</u> , 1985b)	40
4. Equations used in EQUAL computer program	70
5. Equations used in soil chemistry submodel	93
6. Equations used in stream chemistry submodel	100
7. Summary of the soil analytical results where depth is in centimeters, pH_w is water pH, pH_s is salt pH, %org is percent organic matter content, Ca is exchangeable calcium (meq/100 g soil), Mg is exchangeable magnesium (meq/100 g soil), K is exchangeable potassium (meq/100 g soil), Na is exchangeable sodium (meq/100 g soil), Fe is exchangeable iron (meq/100 g soil), Al is exchangeable aluminum (meq/100 g soil), H is exchangeable hydrogen ion (meq/100 g soil)	158
8. Simulation model inputs	163
9. Summary of the soil physical properties where depth is in centimeters, sden is density of solids (gm/cm^3), bden is dry bulk density (gm/cm^3), wet is moisture content (%), fwet is field moisture content (%), swet is saturated moisture content (%)	164

LIST OF FIGURES

Figure	Page
1. Location of study area within the Commonwealth of Massachusetts. The West Wachusett Brook is located in the Bickford Subwatershed	6
2. Detailed map of the West Wachusett Brook Catchment. Stream monitoring site 1 originates from Wachusett Mountain, stream monitoring site 2 passes through a wetland, and stream monitoring site 3 is approximately one kilometer downstream of the two upstream monitoring sites	9
3. Hydrologic submodel for the Birkenes Model. Q_a and Q_b drainage from upper and lower reservoir, E_a and E_b evapotranspiration, P precipitation, A_{sig} routing parameter (from Christophersen <u>et al.</u> , 1982)	24
4. Storgama hydrologic reservoir model (from Christophersen <u>et al.</u> , 1984)	28
5. Horizontal segmentation of a lake-watershed system into land subcatchments, stream segments, and a lake (after Chen <u>et al.</u> , 1983)	31
6. Idealization of system compartments along the flowpath of water within a subcatchment (from Chen <u>et al.</u> , 1983)	32
7. Idealized flowpaths of ILWAS Model (from Chen <u>et al.</u> , 1983)	33
8. Aluminum dissolution and complexation with hydroxide (OH^-), fluoride (F^-), sulfate (SO_4^{2-}), and organic acid ligand (R^{3-}) (from Chen <u>et al.</u> , 1983)	37
9. Stage-discharge relationship for site 1 the mountain stream site. Stage is measured in feet and streamflow is measured in cubic feet per second (cfs)	49
10. Stage-discharge relationship for site 2 the wetland stream site. Stage is measured in feet and streamflow is measured in cubic feet per second (cfs)	50
11. Stage-discharge relationship for site 3 the downstream site. Stage is measured in feet and streamflow is measured in cubic feet per second (cfs)	51

12.	Plot of the surrogate variable UV absorbance (at 254 nm) against dissolved organic carbon (DOC) in milligrams per liter	61
13.	Flow Chart for EQUAL	75
14.	Physical configuration and flowpaths for the transport simulation model	79
15.	Conceptual depiction of the hydrologic submodel	80
16.	Conceptual depiction of the soil and stream compartment submodels	81
17.	Semi-log plot of streamflow verses time for the November storm. The recession curve has two first order release rates, presumably interflow and base flow	84
18.	Schematic of soil sulfate model. P is precipitation volume flux ($L-T^{-1}$), A is drainage area (L^2), $SO_4(\text{precip})$ is precipitation sulfate concentration ($M-L^{-3}$), $SO_4(\text{sol})$ is soil solution sulfate concentration ($M-L^{-3}$), $SO_4(\text{sor})$ is soil sorbed sulfate concentration ($M-M^{-1}$), L is lateral flow (L^3-T^{-1})	89
19.	Flow Chart for Simulation Model	107
20.	Stream flows, in cubic feet per second (cfs), for site 1 the mountain stream site, site 2 the wetland stream site, and site 3 the downstream site	110
21.	Streamwater temperatures, in degrees Centigrade, for site 1 the mountain stream site, site 2 the wetland stream site, and site 3 the downstream site	111
22.	Streamwater pH values, for site 1 the mountain stream site, site 2 the wetland stream site, and site 3 the downstream site	112
23.	Streamwater acid neutralizing capacity (ANC) levels, in micro-equivalents per liter, for site 1 the mountain stream site, site 2 the wetland stream site, and site 3 the downstream site	114

24.	Streamwater dissolved organic carbon (DOC) concentrations, in milligrams per liter, for site 1 the mountain stream site, site 2 the wetland stream site, and site 3 the downstream site	117
25.	Electoneutrality plot for site 1 the mountain stream site. AL equals the total inorganic monomeric aluminum equivalence charge, H equals the hydrogen ion equivalence charge, CB equals the base cations (Ca, Mg, Na, K) equivalence charge, CL equals the chloride ion equivalence charge, SO ₄ equals the sulfate ion equivalence charge	118
26.	Electoneutrality plot for site 2 the wetland stream site. AL equals the total inorganic monomeric aluminum equivalence charge, H equals the hydrogen ion equivalence charge, CB equals the base cations (Ca, Mg, Na, K) equivalence charge, CL equals the chloride ion equivalence charge, SO ₄ equals the sulfate ion equivalence charge	119
27.	Electoneutrality plot for site 3 the downstream site. AL equals the total inorganic monomeric aluminum equivalence charge, H equals the hydrogen ion equivalence charge, CB equals the base cations (Ca, Mg, Na, K) equivalence charge, CL equals the chloride ion equivalence charge, SO ₄ equals the sulfate ion equivalence charge	120
28.	Measured streamwater aluminum fractions, in milli-grams per liter, for site 1 the mountain stream site	122
29.	Measured streamwater aluminum fractions, in milli-grams per liter, for site 2 the wetland stream site	123
30.	Measured streamwater aluminum fractions, in milli-grams per liter, for site 3 the downstream site	124
31.	Monomeric aluminum fractions, in micro-moles per liter, as estimated from the EQUAL program for site 1 the mountain stream site	127
32.	Monomeric aluminum fractions, in micro-moles per liter, as estimated from the EQUAL program for site 2 the wetland stream site	128
33.	Monomeric aluminum fractions, in micro-moles per liter, as estimated from the EQUAL program for site 3 the downstream site	129
34.	Rainfall intensity recorded at the Worcester Municipal Airport during May 1985	132

35.	Streamflow at the downstream site, in cubic feet per second (cfs), during May 1985	132
36.	Streamwater temperature, in degrees Centigrade, during May 1985 for site 1 the mountain stream site, site 2 the wetland stream site, and site 3 the downstream site	133
37.	Streamwater pH response during May 1985 for site 1 the mountain stream site, site 2 the wetland stream site, and site 3 the downstream site	135
38.	Monomeric aluminum fractions, in micro-moles per liter, as estimated from EQUAL during May 1985 for site 1 the mountain stream site	136
39.	Monomeric aluminum fractions, in micro-moles per liter, as estimated from EQUAL during May 1985 for site 2 the wetland stream site	137
40.	Monomeric aluminum fractions, in micro-moles per liter, as estimated from EQUAL during May 1985 for site 3 the downstream site	139
41.	Dissolved organic carbon (DOC), in milli-grams per liter, during May 1985 for site 1 the mountain stream site, site 2 the wetland stream site, and site 3 the downstream site	140
42.	Charge equivalence, in micro-equivalence per liter, of base cations to strong acid anions for site 1 the mountain stream ..	141
43.	Charge equivalence, in micro-equivalence per liter, of base cations to strong acid anions for site 2 the wetland stream ..	142
44.	Charge equivalence, in micro-equivalence per liter, of base cations to strong acid anions for site 3 the downstream site ..	143
45.	Rainfall intensity recorded at the Worcester Municipal Airport during November 1985	145
46.	Streamflow at site 3 the downstream site, in cubic feet per second (cfs)	145
47.	Streamwater temperature, in degrees Centigrade, during November 1985 for site 1 the mountain stream site, site 2 the wetland stream site, and site 3 the downstream site	146
48.	Streamwater pH response during November 1985 for site 1 the mountain stream site, site 2 the wetland stream site, and site 3 the downstream site	147

49.	Monomeric aluminum fractions, in micro-moles per liter, as estimated from EQUAL during November 1985 for site 1 the mountain stream site	148
50.	Monomeric aluminum fractions, in micro-moles per liter, as estimated from EQUAL during November 1985 for site 2 the wetland stream site	149
51.	Monomeric aluminum fractions, in micro-moles per liter, as estimated from EQUAL during November 1985 for site 3 the downstream site	150
52.	Dissolved organic carbon (DOC), in milli-grams per liter, during November 1985 for site 1 the mountain stream site, site 2 the wetland stream site, and site 3 the downstream site	152
53.	Charge equivalence, in micro-equivalence per liter, of base cations to strong acid anions for site 1 the mountain stream site	154
54.	Charge equivalence, in micro-equivalence per liter, of base cations to strong acid anions for site 2 the wetland stream site	155
55.	Charge equivalence, in micro-equivalence per liter, of base cations to strong acid anions for site 3 the downstream site .	156
56.	Simulated versus measured streamflow at the downstream site. Time starts on 4 November 1985	169
57.	Simulated versus measured groundwater flow. Time starts on 4 November 1985	170
58.	Simulated versus measured sulfate concentration at the downstream site. Time starts on 4 November 1985	173
59.	Simulated versus measured divalent cation concentration at the downstream site. Time starts on 4 November 1985	174
60.	Simulated versus measured potassium concentration at the downstream site. Time starts on 4 November 1985	175
61.	Simulated versus measured pH levels at the downstream site. Time starts on 4 November 1985	177
62.	Simulated versus measured acid neutralizing capacity (ANC) at the downstream site. Time starts on 4 November 1985	178

- 63. Simulated versus measured total monomeric aluminum at the downstream site. Time starts on 4 November 1985 179
- 64. Simulated versus measured organic monomeric aluminum at the downstream site. Time starts on 4 November 1985 180
- 65. Solubility plot for the downstream site with $-\log\{Al^{3+}\}$ plotted against $-\log\{H^+\}$ 181

PREFACE

This report represents the research performed by Drew C. McAvoy as part of his Ph.D. degree. A second report titled "Computer Programming and Data for Modeling the Fate of Aluminum in a Watershed System Under Acidified Conditions" contains the detailed computer program listings and raw data. The contents of this second report are listed in the Table of Contents of this report under APPENDICES.

A number of people contributed their expertise, advice and labor toward the completion of this research. Dr. James K. Edzwald and Dr. John H. Baker provided guidance throughout the project. In addition, John Van Benschoten, Martin Scheackler, and Dave Popielarczyk provided laboratory assistance, particularly during the intensive sampling periods. Appreciation also goes to Steve Bodine for his technical assistance in soil sampling and analysis techniques, and to Dan Wagner for his technical assistance in aquatic analytical laboratory techniques. Dr. O.T. Zajicek and his assistants Irene Ellis and Bill Brooks analyzed the major cations and anions in this study, and Dr. Joseph Horowitz provided statistical consulting and modeling advice. Continuous flow data was provided by Dr. Harry Hemond and modeling advice was received from Dr. Nils Christophersen. William Alsop, Alan Van Arsdale and Dr. Harry Hemond are also acknowledged for the critical review of this technical report.

The work was supported by the Massachusetts Division of Water Pollution Control, Research and Demonstration Program, Contract Number 83-31.

CHAPTER I
INTRODUCTION

Background

Acid deposition, consisting of both wet and dry deposition, has had a profound impact on surface water quality in northern Europe and eastern North America. One major consequence has been the altering of the biogeochemical cycle in many watershed systems. The impact on surface water quality depends highly on the catchment's bedrock geology, surficial geology, and hydrologic flowpath. Acid-sensitive areas usually consists of shallow surficial material with a granitic bedrock. Surface waters in these particular watersheds typically have low pH and elevated aluminum levels. These conditions may affect aquatic organisms, with fish kills during acidic episodes being well documented (Overrein et al., 1981).

Wet deposition is considered acidic if its pH value is less than 7.0, but enhanced acidic if less than 5.64, i.e., the pH level at which atmospheric carbon dioxide is in equilibrium with pure water (25°C), thus having no influence either by mineral acidity or by bases (Stumm et al., 1983). Dry deposition consists of strong acid precursors such as sulfur dioxide gas (SO₂) or sulfate and nitrate aerosol particulates. While it is relatively easy to measure wet deposition, the assessment of dry deposition is extremely difficult with currently no direct way of

measurement. Estimates, however, of dry deposition range from 10 to 50% of the total sulfate deposition (Kerr, 1981).

Some researchers have suggested that the increase in streamwater acidity attributed to acid precipitation is minor when compared to the increase of acidity caused by land use changes (Rosenqvist, 1978; Klug and Frink, 1983). The major land use change in New England is reforestation with forest floor development in humid climates known to be an acidifying process (Frink and Voight, 1977; Johnson et al., 1982). Acidification of surface waters, though, seems to occur only in regions receiving acid precipitation. Studies conducted in remote areas of Norway, with relatively small land use changes, showed drastic decreases of fish populations along with acidification of surface waters in recent years (SNSF, 1981). Thus, evidence is not conclusive that land use changes are indeed a major cause of acidified fresh water systems.

The study presented in this document focuses on the more important mechanisms that control neutralization of acid deposition and the subsequent mobilization of aluminum within a watershed system. In addition, the effects of streamwater acidity on aquatic biota are addressed.

Scope and Objectives

The effects of acid rain on small watersheds have been studied extensively by many researchers for a number of years, but few have focused on the episodic short-term transport of aluminum. In addition, the development and testing of mathematical models that describe the fate of aluminum under acidified streamwater conditions, especially during short-term periods, have been limited. Existing models that simulate streamwater aluminum have been developed by Johnson et al. (1969), which use a stochastic modeling approach, as well as the Birkenes Model by Christophersen et al. (1982), the ILWAS Model by Chen et al. (1983), and the MAGIC Model by Cosby et al. (1985b), which use a deterministic modeling approach. These models describe streamwater aluminum under acidified conditions, but none have been tested for short-term aluminum transport responses along a stream segment. Thus, it is the purpose of this research to develop a watershed aluminum-chemistry transport model that describes short-term aluminum responses and to test this model by obtaining field data from the West Wachusett Brook catchment, Massachusetts. Once the model is verified it can be used to further study aluminum mobility and its effect on the aquatic biota.

The West Wachusett Brook appears to have been adversely affected by acid deposition over the last 20 years. One result has been the loss of fisheries in this stream with a healthy population reported as late as

the mid-60's (Screpetis, personal communication). It has been hypothesized that the decline of fisheries in this acid-sensitive brook was due in part to acid deposition mobilizing aluminum from the soil to the aquatic environment under high flow, low pH conditions. An in-situ fish bioassay study testing this hypothesis was performed cooperatively by several participants during March, 1983. It was determined from this inquiry that stream conditions were toxic to fish, as none of the caged brook trout survived in the upper reach of the stream during the 14 day study period (Bickford Pond Fish Bioassay Study, unpublished data). Furthermore, 80% mortality was observed in the lower reach of the stream. Streamwater total aluminum concentrations from this study ranged from 0.4 to 0.9 mg/l with pH values ranging from 4.5 to 5.0. Laboratory bioassays have shown that over the ranges of aluminum and pH levels observed, detrimental effects to fish may occur (Cleveland et al., 1986; Baker and Schofield, 1982; Schofield and Trojnar, 1980).

Thus, the overall objectives of this research are:

1. to develop an instream aluminum fate and transport model by utilizing and improving upon existing model approaches,
2. to test the instream model with actual field data from a small watershed,
3. to gain insight into the transformation and transport processes of aluminum under acidified soil and stream conditions,
4. to relate the fate of aluminum to its toxicological effects on the aquatic biota.

Site Description

The West Wachusett Brook catchment is located in the central part of Massachusetts as seen in Figure 1. The stream originates from the western slope of Mt. Wachusett (elevation approximately 580 m above mean sea level) and flows in a westerly direction for roughly three kilometers before entering the Bickford Reservoir. This reservoir serves as a water supply for the city of Fitchburg, Massachusetts. It was completed in 1971 with a total capacity of 3.74 million cubic meters and, when full, encompasses a surface area of 80 hectares at an elevation of 318.5 meters above mean sea level (USDA, 1973). The Bickford Reservoir watershed encompasses a drainage area of 890 hectares with the West Wachusett Brook subwatershed comprising nearly two-thirds of this area at 578 hectares.

A large portion of the watershed consists of protected lands (Wachusett Mountain State Reservation and Minns Wildlife Sanctuary) with a northern hardwood forest covering more than 95% of the total watershed area (Eshleman, 1982). The predominant tree species are red oak, red maple, white pine, and eastern hemlock with some beech and birch found on the mountain slopes.

A surficial geology survey of the watershed by Stone (1978) showed the western slope of Mt. Wachusett to be predominately covered with glacial till. The soils are primarily inceptisols and spodosols (Soil

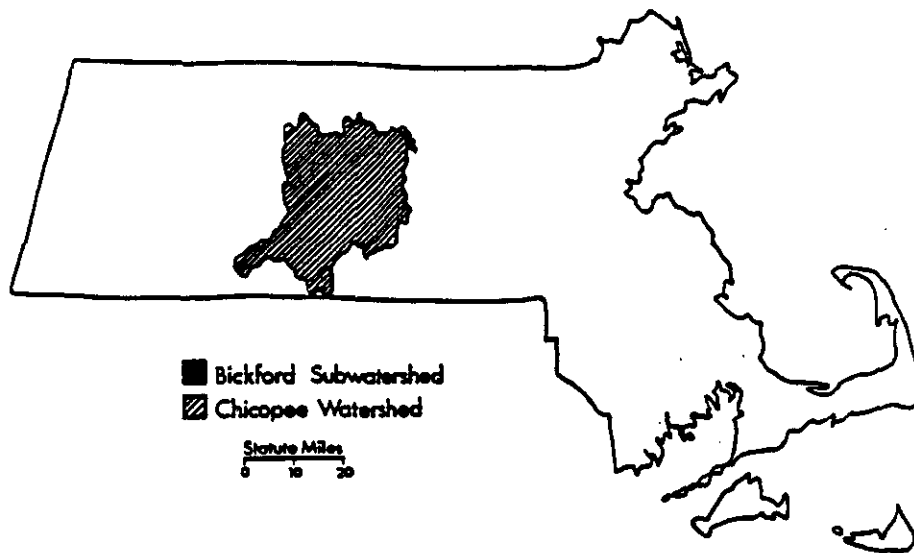


Figure 1. Location of study area within the Commonwealth of Massachusetts. The West Wachusett Brook is located in the Bickford Subwatershed.

Conservation Service, unpublished data). Soil types range from well drained soils (e.g., Paxton, Woodbridge, or Scituate) to poorly drained or muck soils (e.g., Raypole, Ridgebury, or Whitman). Most of the soils in the watershed have a dense fragipan layer approximately 70-90 cm from the surface. The Soil Conservation Service is currently in the process of mapping the entire watershed area.

The underlying bedrock of the study area consists mainly of two different types: 1) an undifferentiated biotite granofels, calc-silicate granofels, and sulfidic schist or 2) a black to gray aluminous mica schist, quarzone schist, and aluminous phyllite (USGS, 1983).

Experimental Design

Watershed data are essential for assessing the fate of instream aluminum chemistry during episodic rainfall periods. This type of information is useful in gaining a better understanding of aluminum mobility, in determining the more important neutralization reactions, and in assessing short-term or acute toxicity to aquatic organisms. Moreover, short-term data are needed for calibration and verification of mathematical models. Once calibrated, a simulation model can be used to test various acidification hypotheses and gain a quantitative insight into the transport mechanisms.

The field survey for this study was conducted in the West Wachusett Brook catchment, Massachusetts. A detailed map of the study area is

presented in Figure 2. This brook was selected for investigation because of its history of high instream concentration of Al, and conditions of low pH during high flow periods. Sampling was conducted at three stream sites within the watershed as indicated on the map of the study area. The two upstream sites were chosen because of their characteristic differences. Site 1 originates from a mountainous terrain whereas site 2 passes through a wetland area. Therefore, these two sites should have significantly different pH, aluminum, and organic content levels. Site 3 provides information of the stream's condition after the two upstream branches have mixed together, thus including stream transport as well as groundwater addition. A precipitation collection station was also set up in the catchment and used during intensive monitoring periods.

Intensive field surveys were conducted during the months of May and November, 1985. These typically have been high runoff periods and therefore thought to be the most critical times of the year. Furthermore, focusing on these particular time periods simplified the modeling effort by allowing the following assumptions:

1. snow hydrology was ignored since the surveys were conducted during periods of no snowmelt runoff,
2. biological activity, especially vegetation effects, was assumed unimportant because of low temperatures during the survey period,

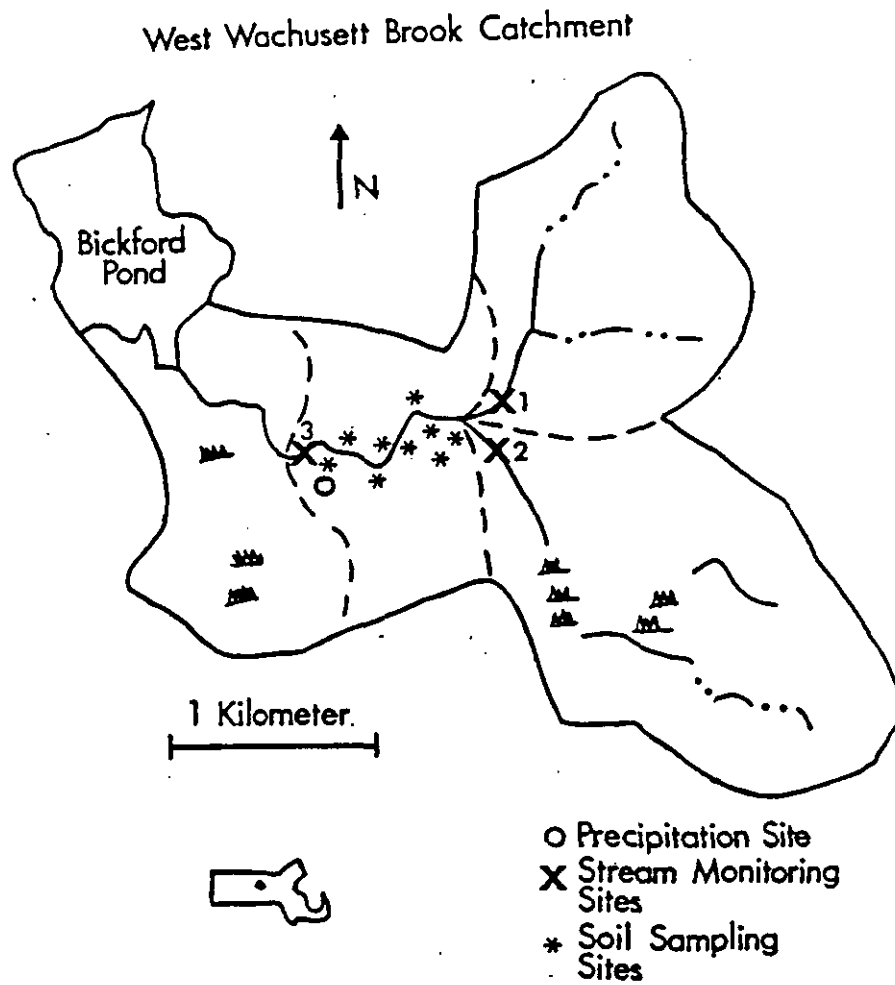


Figure 2. Detailed map of the West Wachusett Brook Catchment. Stream monitoring site 1 originates from Wachusett Mountain, stream monitoring site 2 passes through a wetland, and stream monitoring site 3 is approximately one kilometer downstream of the two upstream monitoring sites.

3. canopy reactions and interception losses were assumed to be small during these time periods because the deciduous trees were bare.

During intensive rainfall events streamwater monitoring sites were sampled every six hours for approximately two weeks. This frequency of sampling was needed to accurately assess the acute toxicity of the streamwater to fish as well as for testing the mathematical simulation model. All the major cations and anions that were thought to be important in terms of the ionic balance as well as the aluminum transport process were monitored. Sampling and analytical protocols used for this study may be found in the materials and methods chapter.

In addition to the intensive sampling periods, monthly grab samples were collected from March, 1985 to January, 1986 so that gross seasonal effects could be assessed. The results of this survey are discussed in Chapter V.

Besides water quality sampling, water quantity was monitored within the West Wachusett Brook catchment. Stream flows and precipitation volumes were needed in order to determine the mass balance of ions within the watershed system. Staff gauges were installed at each of the stream monitoring sites and a stage-discharge relationship determined. Stream flow and precipitation measurements were monitored manually during the survey period.

MIT, as part of a grant from the Northeast Electric Utility Companies, has also established two continuous stream flow gauges within

the West Wachusett Brook catchment. In addition, the National Weather Service maintains a rain gauging station at the Worcester Municipal Airport located approximately 25 kilometers from the study area. A comparison of precipitation inputs and stream flow measurements can be made among these various monitoring stations.

In addition to the streamwater and precipitation monitoring, a soil survey of the area was conducted. Approximate locations of the sampling sites may be seen in Figure 2. This survey was conducted to help assess the source of aluminum in this particular watershed.

In summary, it was the purpose of the field investigation:

1. to gather information that further explains the phenomenon of aluminum mobility,
2. to collect calibration data for a mathematical simulation model that tests the various hypothesized mechanisms of aluminum transport,
3. to assess the acute toxicity of this stream to fish under high Al, low pH conditions by comparing the information obtained to that of existing bioassay studies.

CHAPTER II
LITERATURE REVIEW

A basic understanding of the transformation and transport mechanisms, in both soil and stream environments, is fundamental to developing a mathematical model that describes the fate of aluminum in a watershed system. Major processes thought to control the fate of aluminum in northern temperate humid regions are mineral weathering and solubility, cation exchange, anion adsorption, and complexation with organic and inorganic ligands. These major mechanisms will be reviewed first, followed by a discussion of existing aluminum transport models that incorporate these various mechanisms in a quantitative fashion. Finally, the toxicological effects of aluminum and pH to aquatic organisms will be addressed.

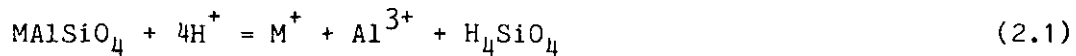
Aluminum Transport Mechanisms

Two theories of aluminum mobility have been postulated for northern temperate regions. The first involves the natural soil development of spodosols, a typical New England soil. Spodosols are common to cold temperate, humid climates and are usually associated with hardwood forests. These soils are extremely acidic and have an abundance of organic matter in the upper soil horizons. The development process of spodosols involves the mobilization of aluminum from the upper organic horizon, commonly in the form of an organo-metallic complex, to the

lower inorganic horizon where it precipitates out of solution (Bohn et al., 1979). Cronan and Schofield (1979) have hypothesized, though, that the mineral acidity from acid deposition remobilizes the previously deposited aluminum by altering the natural soil development process. The second theory, postulated by Driscoll (1985) suggests that biocycling (i.e., vegetation assimilation and microbial decomposition) is an important component of aluminum cycling in a northern temperate forested region. Other investigations have also concluded that forest floor development or biocycling is a significant source of mobile aluminum (David and Driscoll, 1984; Driscoll et al., 1985). Thus, these two postulations suggest that surface water organic and inorganic aluminum may originate from different soil processes, i.e., podsolization and biocycling.

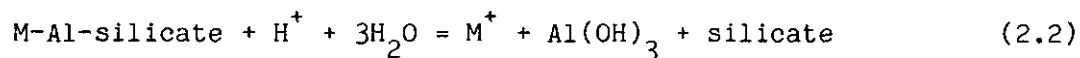
Mineral Weathering and Solubility

The ultimate sink for deposition acidity as well as a source for aluminum is the process of mineral weathering (Johnson, 1984). Basic cations may also be resupplied to the soil environment by this process. Aluminosilicate minerals weather by consuming acidity (H^+) and in turn release alkali cations and aluminum into solution. A general formula for an aluminosilicate mineral is MA_2SiO_4 , where M may consist of the cations Ca, Mg, Na, K, or Fe (Johnson, 1984). The dissolution of this mineral can be expressed mathematically as:



where H^+ represents acidity. The order of mobility for basic cations in granitic and basaltic soils is generally $Ca > Mg > Na > K$ (Holland, 1978).

Voight (1980) hypothesized that the aluminosilicate dissolution reaction increases the soil water pH near the mineral surface to levels as high as 9.5, even though the bulk solution is still acidic. Under these alkaline conditions the solubility of silica increases, thus increasing the breakdown of the aluminosilicate mineral lattice. Once the dissolved silica enters the more acidic bulk solution it precipitates back out of solution leaving aluminum free, under proper conditions, to form secondary minerals such as clays (e.g., kaolinite or vermiculite) or gibbsite ($Al(OH)_3$). The formation of these metastable secondary minerals are important in terms of acid neutralization and aluminum mobility as they react faster than the primary aluminosilicate minerals. The incongruent dissolution of granitic minerals to gibbsite may be represented as:



The abundant gibbsite in highly weathered soils is believed to control the free aluminum activity only after the cation exchange capacity has

been saturated with aluminum ions (Bohn et al., 1979). Gibbsite's congruent equilibrium reaction with acidity can be expressed as:



This reaction proceeds rapidly and is reversible (Johnson, 1984). This process does not neutralize acidity but only changes its form (i.e., from H^+ acidity to Al acidity). This shift in acidity was observed in the Falls Brook watershed when the rain's mineral acidity was converted to streamwater aluminum acidity (Johnson et al., 1981).

Several studies have observed that streamwater aluminum levels increase with decreasing pH (Schofield and Trojnar, 1980; Driscoll et al., 1982), thus supporting the idea that gibbsite solubility controls streamwater aluminum. Because of these observations most watershed acidification models have used this assumption in their formulation. Other investigations have observed a disequilibrium with respect to the solubility of Al(OH)_3 (Hooper and Shoemaker, 1985; Nordstrom and Ball, 1986). Researchers have suggested that this disequilibrium under low pH conditions may be attributed to an aluminum-sulfate mineral phase, such as alunogen ($\text{Al}_2(\text{SO}_4)_3$), alunite ($\text{KAl}_3(\text{SO}_4)_2(\text{OH})_6$), jurbanite ($\text{Al}(\text{SO}_4)(\text{OH})$), or basaluminite ($\text{Al}_4(\text{SO}_4)(\text{OH})_{10}$), controlling aqueous aluminum levels (Nordstrom, 1982; Nilsson and Bergkvist, 1983).

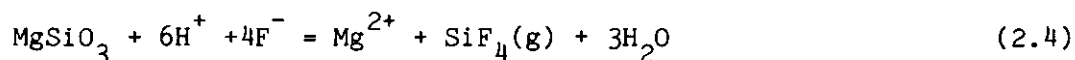
Nordstrom and Ball (1986) demonstrated a transition from gibbsite equilibrium when aqueous systems were above pH 4.6-4.9 to a

disequilibrium when below these levels. This transition is near the first hydrolysis constant for Al^{3+} and it is thought that this hydrolysis helps initiate gibbsite precipitation. Thus, the disequilibrium when streamwater pH levels are less than 4.6 may be caused by either the rate limiting weathering reaction of aluminosilicate minerals and/or the change in controlling mineral phase like the solubility with an aluminum-sulfate mineral (Nordstrom and Ball, 1986).

The potential capacity to neutralize acidity by mineral weathering is enormous considering the amount of silicate and carbonate bedrock in the earth's crust. For areas underlain by calcite or carbonate alkalinity, dissolution of inorganic carbon could potentially neutralize acid rain quickly because of its fast reaction rate. Therefore, these areas are less sensitive to acid deposition than predominantly silicate mineral watersheds. On the other hand, the weathering of aluminosilicate minerals are thermodynamically favorable, but the weathering rate of these minerals can be quite slow and depends greatly on their intrinsic crystalline structure (Johnson, 1984). Deju (1971) showed the rate of silicate mineral weathering to be faster for minerals with higher oxygen-to-silica ratios. Moreover, the substitution of aluminum into the silicate structure (e.g., feldspars) increases the susceptibility of the mineral to hydrolysis and acid attack because of weaker aluminum-oxygen bonds (Johnson, 1984).

The weathering rate process not only depends on the acidity of the aquatic solution and intrinsic structure of the mineral phase, but also

on the anions present in the bulk solution. For instance, the presence of F^- can act as a catalyst and speed up the rate of aluminosilicate mineral weathering (Johnson, 1984). A typical reaction utilizing F^- as the anion for silica depolymerization is:



Johnson (1984) suggests that if acid deposition was made up of HF instead of H_2SO_4 or HNO_3 , the environmental impact would be profoundly different.

The extent of acid neutralization and the release of metallic cations is not only dependent on the type of soil and bedrock, but also on the hydrologic pathway. The importance of contact time is seen during periods of peak runoff when much of the rainwater penetrates only the top few centimeters of the soil. With short retention times the soil neutralizing mechanisms are unable to keep up with the acidic inputs. Thus, higher streamwater acidity would be expected under these conditions as compared to a gentle rain that has time to percolate to greater depths. Johnson et al. (1981) demonstrated this point in a small New England watershed in which a decrease of downstream acidity was thought to be due to an increase in contact time with the silicate minerals. Since silicate minerals react slowly, especially at low temperatures typical of groundwater systems, the capacity to neutralize acidity may not be utilized during an individual storm event (Berner,

1981). Hence, kinetic factors should be considered when assessing the long-term effects of mineral weathering.

Cation Exchange

Cation exchange is an important short-term soil process that influences aluminum transport and soil acidity. The cation exchange capacity (CEC) of a soil is a function of physical and chemical properties. CEC is caused by soil particles, in particular silicate clays and organic matter, having a negative charge and thereby attracting cations. Clays that have been formed by incongruent isomorphic substitution exhibit a relatively constant permanent negative charge, whereas organic soils have a variable, pH-dependent negative charge. Cations may interchange freely on the exchange sites, but are influenced by the soil particle preference. Cation valence and hydration size also affect the preference of exchangeable cations. Cation exchange reactions can either increase or decrease the runoff acidity depending on the soil's base saturation, i.e., the percent of base cations on the exchange sites (Siep, 1983; Krug and Frink, 1983).

Cation exchange reactions are typically rapid and reversible (Bohn et al., 1979). These reactions have been modeled quantitatively by using a selectivity coefficient approach, e.g., the Gaines-Thomas (Gaines and Thomas, 1953) or Gapon (Bohn et al., 1979) models. The problem with this approach is that selectivity coefficients involving aluminum are affected by pH, surface composition, and hydrolysis of aluminum (Pleysier et al., 1979). In addition, selectivity coefficients

may vary considerably between soil types or even with pH changes within the same soil type (McBride and Bloom, 1977). Therefore, selectivity coefficients are usually treated as calibration parameters in models because of their variability. This type of formulation may be adequate over short-term simulations when soil pH is relatively constant, but may be inappropriate for long-term predictions (Hooper and Driscoll, 1986).

Anion Adsorption

Anion adsorption, particularly SO_4^{2-} , is an important mechanism controlling the fate of aluminum in a soil system. Sulfate is usually the predominant anion balancing and mobilizing the acid and base cations in soil and surface waters (Siep, 1983). In low pH soils, sulfate ions can be retained by adsorption/desorption with the retention of SO_4^{2-} being strongly correlated to acidity (Bohn et al., 1979). The adsorption of sulfate is thought to be primarily associated with the positive charged aluminum and iron hydroxide minerals.

Singh (1980) reported that the sorption of sulfate fit the Langmuir isotherm quite well for iron-podzol soils. These experiments showed two distinct linear portions to the isotherm curve, one at lower (<100 g/ml) and the other at higher (>100 g/ml) equilibrium sulfate concentrations. In addition, two separate sorption rates were observed, i.e., a rapid one of a few hours and a slow one of several days. Furthermore, Singh et al. (1980) observed the soil retention of sulfate to be proportional to the aluminum content.

Nordstrom (1982) suggests that sulfate is retained in the unsaturated zone as an aluminum-sulfate complex. He hypothesized, though, that when groundwater rises into the unsaturated zone during a storm event, the higher pH saturated groundwater releases sulfate, as well as aluminum from the aluminum-sulfate complex. Thus, he concluded that sulfate can influence aluminum mobility either by acting as a mobile anion or by complexation reactions.

Complexation

Aluminum forms strong complexes with hydroxide, fluoride, sulfate, and organic anions (Hem, 1968). These complexes are important in terms of aluminum transport within a watershed system and in turn affect the buffering properties of dilute acidic systems (Johannessen, 1980). Moreover, the degree of aluminum complexation affects the toxicity of aluminum to aquatic biota (Baker and Schofield, 1982).

Driscoll (1980) found that organically complexed aluminum was generally the predominant soluble form in selected Adirondack surface waters. He also found organically bound aluminum to be significantly correlated to total organic carbon (TOC). TOC and organo-aluminum complexes were also observed to be greatest during the summer months corresponding with the greatest microbial decomposition period. In general, aluminum-fluoride complexes were the major inorganic form with free aluminum and aluminum-hydroxide complexes being less significant. At pH levels less than 5.5 fluoride ions were almost entirely complexed by aluminum. At higher pH levels, though, hydroxide ligands out-compete

fluoride ligands for the available aluminum. Aluminum-sulfate complexes in these surface waters were insignificant. Aluminum appeared to be regulated by solubility with an aluminum trihydroxide ($\text{Al}(\text{OH})_3$) mineral phase.

Johnson et al. (1981) reported a shift in aluminum speciation along a Hubbard Brook, with aluminum-organic complexes increasing, while free aluminum ion and hydroxide complexes decreasing, with increasing stream order. Aluminum-fluoride complexes remained constant throughout the stream's reach. They also found that an $\text{Al}(\text{OH})_3$ model adequately describes aluminum levels in this brook.

Organic compounds or humic substances in the upper soil horizons are also an important mechanism for mobilizing aluminum. Humic substances (i.e., humic acids, fulvic acids, and humins) are largely derived from the decay of plant matter and give a distinctive color to soil and stream waters. The various humic fractions can be differentiated by means of their solubilities. Humic acids are soluble only in alkali solutions while fulvic acids are soluble under both alkali and acidic conditions (Stevenson and Butler, 1969). Humins are the most stable form of humus and are insoluble in both acidic and basic solutions. Hence, fulvic acids are the most soluble and hydrophilic of the humic substances under low pH conditions. In general, fulvic acids have lower molecular weights and contain more oxygen than humic acids, which leads to greater solubility as well as greater metal-complexing capacity (Stevenson and Butler, 1969). Metal-complexation with fulvic acids also depends on pH, as hydrogen ions compete with metal ions for

the available organic anion binding sites (Saar and Weber, 1982). Unfortunately, a specific formula for humic materials is not available because of their variable and complex structural composition, though general formulae have been assumed. A chemical formula would be helpful when trying to study their reactions quantitatively.

Organic complexation is an important aluminum transport mechanism in the soil environment. A Swedish study by Nilsson and Berkvist (1983) showed the soil solution from an A horizon to consist of 83 to 97% organically bound aluminum whereas the B horizon leachate had an organic-aluminum fraction varying between 8 and 20% of the total aluminum measured. In addition, an increase of total aluminum with depth was observed. They concluded that fulvic acids released aluminum in the upper soil horizons, but other mechanisms like mineral solubility control aluminum in the lower soil horizons.

Existing Aluminum Transport Models

Birkenes Model

The Birkenes model was developed with the intent to explain variations in streamwater chemistry in acidified areas of Norway (Christophersen and Wright, 1981; Christophersen et al., 1982). Two components are used, a hydrologic model and a chemical model, in describing the streamwater's response to acidic loadings. The modeling effort first focused on the Birkenes catchment, thus its name, and then on the Storgama catchment.

A hydrologic model was included because most of the chemical components entering and leaving the catchment are in an aqueous form. At Birkenes a simple two-compartment model was used to describe the flowpath through the drainage basin. The upper reservoir represents the organic soil horizon and provides quickflow to the stream whereas the lower reservoir incorporates the inorganic layers and simulates base flow. A schematic of the hydrologic pathways is presented in Figure 3. The model includes percolation from the upper to the lower soil compartment as well as evapotranspiration. Inputs to the hydrologic model are precipitation volume and daily mean temperature.

The chemical model utilizes the results from the hydrologic model to transport chemical constituents from the soil to the stream environment. Several assumptions are made to simplify the chemical model. First, it is assumed that sodium and chloride are conservative elements occurring at equivalent amounts, and thus omitted since they

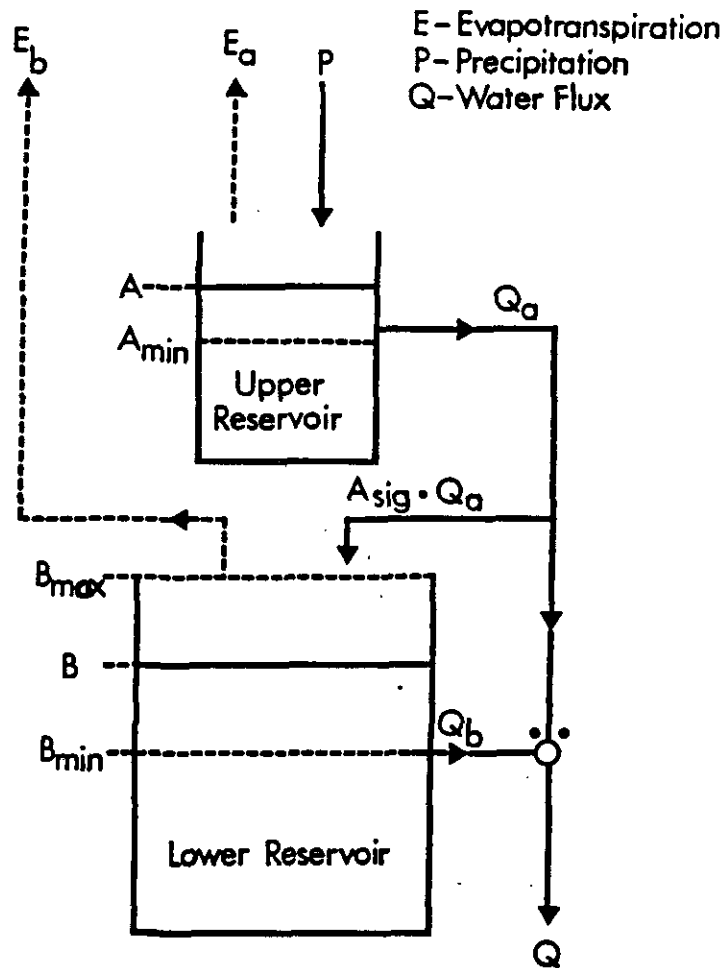


Figure 3. Hydrologic submodel for the Birkenes Model. Q_a and Q_b drainage from upper and lower reservoir, E_a and E_b evapotranspiration, P precipitation, A_{sig} routing parameter (from Christophersen et al., 1982).

balance each other. Second, the model ignores bicarbonate, nitrate, ammonium, potassium, and organic anions because their presence is small at Birkenes. These assumptions leave SO_4^{2-} as the predominant anion balancing the cations H^+ , Ca^{2+} , Mg^{2+} , and Al^{3+} . Therefore, sulfate is a crucial component of the Birkenes model since it determines the cations composition.

The sulfate submodel has adsorption and desorption controlling sulfate in both the upper and lower soil compartments. Sulfate enters the upper reservoir by both wet and dry deposition while sulfate leaving the upper compartment is assumed proportional to the total sulfate in the solid phase. The upper reservoir also includes mineralization, important during dry summer months, by incrementally increasing sulfate every day that the upper compartment is empty. The only process involving sulfate in the lower reservoir is adsorption/desorption. During dry periods, i.e., when the upper reservoir is empty, the lower compartment sulfate concentration follows an exponential path toward a fixed equilibrium value.

The cation submodel assumes that the anion SO_4^{2-} exactly balances the cations H^+ , Ca^{2+} , Mg^{2+} , and Al^{3+} . Thus, the overall levels of the cations are governed by the sulfate concentration. For simplicity the divalent cations Ca^{2+} and Mg^{2+} are assumed to behave similarly and are lumped together as a single variable M^{2+} . The upper organic soil compartment regulates the divalent cations, M^{2+} , by ion exchange with

H⁺. Cation exchange is modeled using the Gapon formulation (Gapon, 1933). Chemical weathering controls M²⁺ by a rate dependent formulation in the lower inorganic soil compartment. The free aluminum ion is regulated by equilibrium with the mineral phase aluminum trihydroxide (gibbsite) in both reservoirs. Inorganic aluminum complexes are assumed unimportant while organic aluminum is assumed constant. A summary of the processes included in the Birkenes model are presented in Table 1.

A secondary test of the Birkenes model was made at the Storgama watershed (Christophersen et al., 1983). Modification of the hydrologic model at Storgama included the addition of two more compartments: a snowpack reservoir and a streamwater reservoir. The snowpack reservoir allows for winter simulation and the streamwater reservoir accounts for the catchment's small pool outlet. The Storgama hydrologic model is illustrated in Figure 4.

The chemical model at Storgama is similar to that for Birkenes. Modification to the sulfate submodel includes a reduction process in the upper soil organic compartment. This process is important during wet periods when reducing conditions are favorable. Nitrate and bicarbonate are also incorporated in the Storgama version of the model. The cation formulation of the model is not changed.

The Birkenes model simulates the streamwater chemistry of two catchments in southern Norway quite well, considering the small number of physical and chemical processes included. Inputs to the model consist only of precipitation volume and sulfate concentration, both wet and dry deposition, as well as temperature on a daily basis. Some of

Table 1

Summary of Processes Included in the Birkenes Model
(from Christophersen et al., 1982)

	Processes	
	Upper Reservoir	Lower Reservoir
H_2O	precipitation, evapotranspiration, infiltration to lower reservoir, discharge to stream	infiltration, evapotranspiration, discharge to stream
SO_4^{2-}	wet + dry deposition, adsorption/desorption, mineralization	adsorption/desorption
$Ca^{2+} Mg^{2+}$	ion-exchange	release by weathering, adsorption/desorption
H^+	ion-exchange and equilibrium with gibbsite	consumption by weathering adsorption/desorption, equilibrium with gibbsite
Al^{3+}	equilibrium with gibbsite	equilibrium with gibbsite, adsorption/desorption

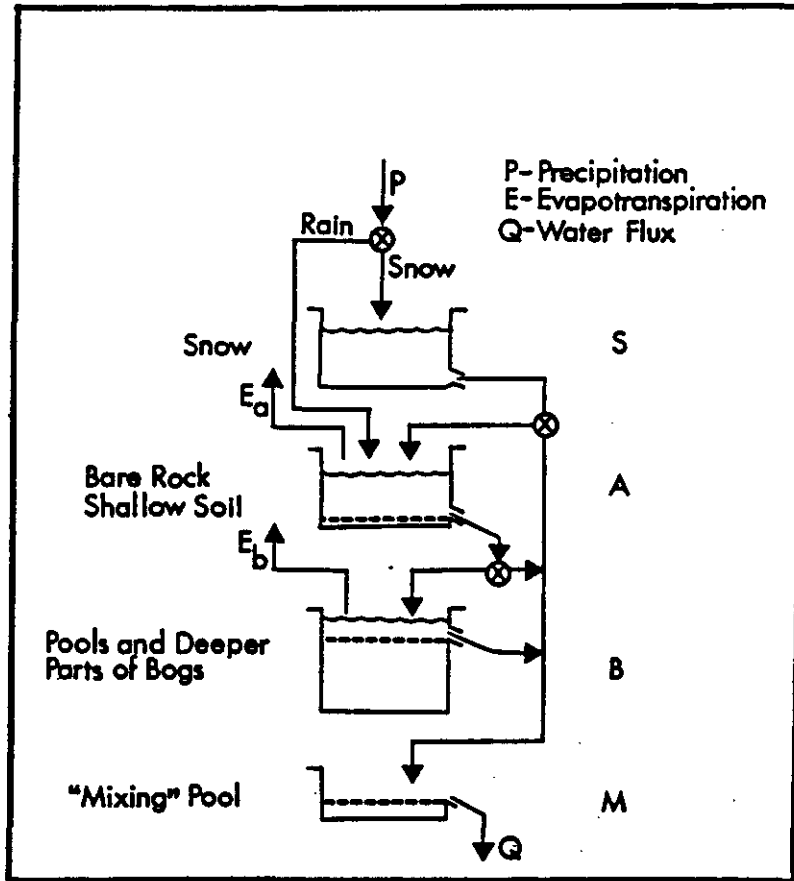


Figure 4. Storgama hydrologic reservoir model (from Christophersen et al., 1984).

the rate constants and initial conditions to the model were altered to simulate Storgama, but essentially the same processes accounted for the streamwater chemistry variation at both study areas.

ILWAS Model

The Integrated Lake-Watershed Acidification Study (ILWAS) was a large interdisciplinary study sponsored by the Electric Power Research Institute (EPRI) with the objective of providing a quantitative link between atmospheric acid deposition and surface water acidity. A deterministic mathematical approach, the ILWAS model (Chen et al., 1983), was developed to simulate the biogeochemical processes of an entire lake-watershed system. This ambitious endeavor incorporates processes from the forest canopy, soil horizons, streams, bogs, and lakes. Inputs to the model include precipitation quantity and quality, ambient air quality, and basin properties, with outputs of flow rates as well as concentrations of all major cations and anions, monomeric aluminum, total inorganic carbon, and organic acids.

The ILWAS model, like the Birkenes model, is divided into two components: hydrologic and chemical. The hydrologic model incorporates the physical processes of interception, throughfall, evaporation, freezing and thawing of the soil, snow accumulation and melt, soil and surface water hydraulics (Chen et al., 1983). The chemical model determines the concentrations of cations, anions, and other constituents by simulating: 1) the canopy processes of wet and dry deposition, exudation, and washoff; 2) the snowpack processes of ion-accumulation

and ion-leaching; 3) the soil processes of organic matter decomposition, nitrification, mineral weathering, cation exchange, and anion adsorption; 4) the plant processes of root respiration, nutrient uptake and nutrient cycling through litter fall; and 5) the chemical equilibria occurring in the aqueous phase (Chen et al., 1983).

Conceptually the ILWAS model divides the runoff basin into several compartments, routing water from one compartment to another, and calculates the chemical constituent concentrations in each compartment. The compartmentalized system is in both the horizontal and the vertical direction. Segmentation in the horizontal direction is divided into three major components, i.e., land, stream, and lake, as illustrated in Figure 5. Each subcatchment is further segmented in the vertical direction as depicted in Figure 6. Stream segments are assumed to be completely mixed and are not segmented vertically. The lake component, however, may be segmented into a series of horizontal mixed layers so that depth profiles can be simulated. A schematic of the model's flowpaths is presented in Figure 7.

The ILWAS model uses alkalinity as a master variable. Hence, the prediction of pH is dependent on all the biogeochemical processes that may produce or consume alkalinity. A summary of the biogeochemical processes used in the ILWAS model are listed in Table 2. The mathematic formulations of the various biogeochemical processes are presented in detail by Chen et al. (1983).

ILWAS models the fate of aluminum in the soil horizons by precipitation/dissolution reactions with a controlling mineral phase

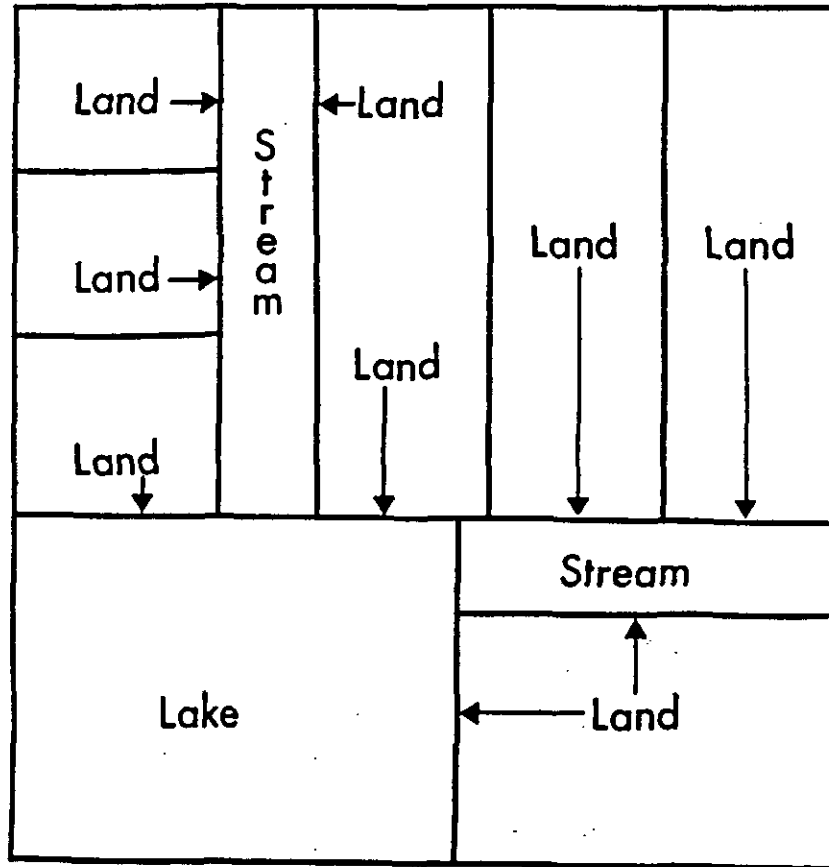


Figure 5. Horizontal segmentation of a lake-watershed system into land subcatchments, stream segments, and a lake (after Chen et al., 1983).

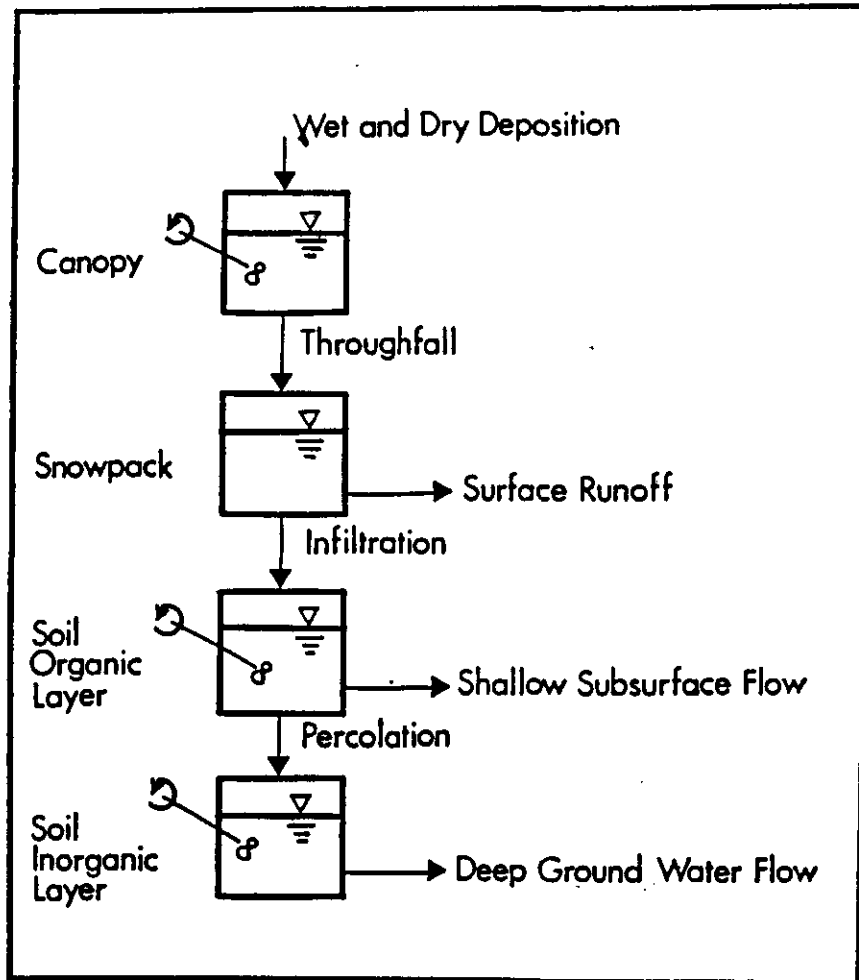


Figure 6. Idealization of system compartments along the flowpath of water within a subcatchment (from Chen *et al.*, 1983).

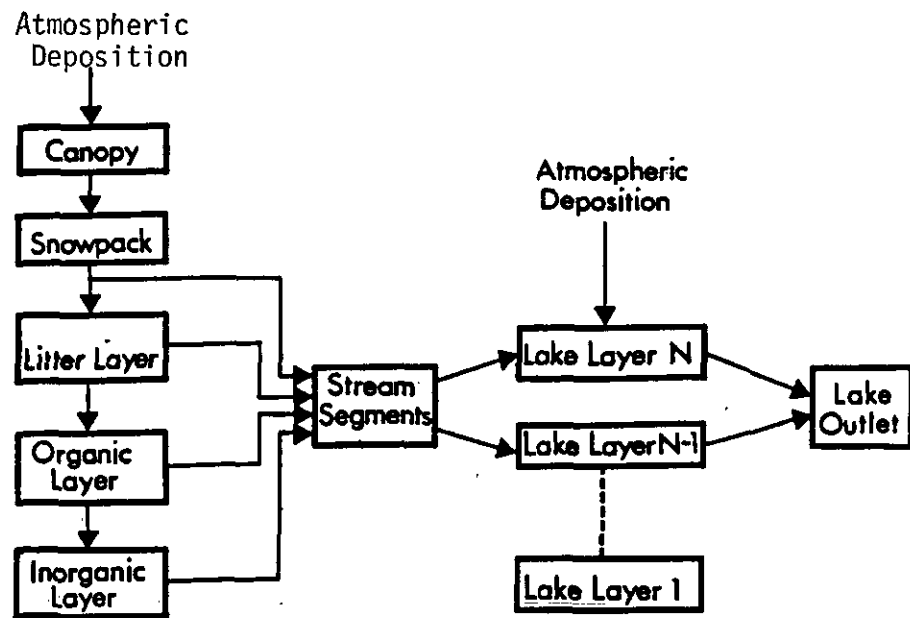


Figure 7. Idealized flowpaths of ILWAS Model (from Chen et al., 1983).

Table 2

Biogeochemical Processes Considered in the ILWAS Model
(from Chen et al., 1983)

<u>Process</u>	<u>Key Variables</u>
Canopy	
dry deposition	air quality, leaf area index
oxidation	SO ₂ , NO _x , temperature, alkalinity
nitrification	NH ₄ ⁺ , NO ₃ ⁻ , temperature, alkalinity
foliar exudation	leaf chemical composition, alkalinity
wet deposition	precipitation
interception and evap.	temperature, humidity
pH - equilibrium	alkalinity, TIC
wash-off	interception storage, precipitation
Snowpack	
accumulation	precipitation, temperature
dry deposition	air quality
nitrification	NH ₄ ⁺ , temperature
leaching	temperature, snowmelt
Litter Layer	
accumulation	litter fall rate
leaching	leaf chemical composition, alkalinity
breakdown	litter mass
decomposition	fine litter
evaporation	temperature, humidity

Table 2 (continued)

<u>Process</u>	<u>Key Variables</u>
Organic Layer	
evapotranspiration	temperature, humidity
decomposition	humus mass, temperature organic acids, CO ₂ , ions
nitrification	NH ₄ ⁺ , temperature, pH
nutrient uptake	NH ₄ ⁺ , NO ₃ ⁻ , Ca ²⁺ , K ⁺ , ...
root respiration	CO ₂
aluminum dissolution	pH, Al _T
CO ₂ -exchange	CO ₂
cation exchange	cations, CEC
chemical equilibrium	pH, alkalinity, Al _T , organic acids
Inorganic Layers	
evapotranspiration	temperature, humidity
decomposition	organic acids, temperature
nitrification	NH ₄ ⁺ , temperature, alkalinity
nutrient uptake	NH ₄ ⁺ , NO ₃ ⁻ , Ca ²⁺ , K ⁺ , ...
weathering	pH, minerals
anion sorption	SO ₄ ²⁻ , PO ₄ ³⁻ , organic acids
cation exchange	cations, CEC, base saturation
aluminum dynamics	pH, Al _T , organic acids
chemical equilibrium	pH, Al _T , alkalinity, organic acids
CO ₂ -exchange	CO ₂

Table 2 (continued)

<u>Process</u>	<u>Key Variables</u>
Stream Segment	
advection	flow
dilution	volume
evaporation	temperature, wind speed
CO ₂ -exchange	wind speed
heat budget	solar radiation
chemical equilibrium	pH, Al _T , alkalinity, organic acids
Lake Layers	
advection	flow
dilution	dispersion factor
evaporation	temperature, wind speed
diffusion	wind speed, density gradient
CO ₂ -exchange	wind speed
heat budget	solar radiation
algal uptake	NO ₃ ⁻ , PO ₄ ³⁻ , CO ₂ , alkalinity
aluminum precipitation	pH, Al _T
nitrification	NH ₄ ⁺ , temperature, alkalinity
decomposition	organic acids, CO ₂ , ions
chemical equilibrium	pH, Al _T , alkalinity, organic acids

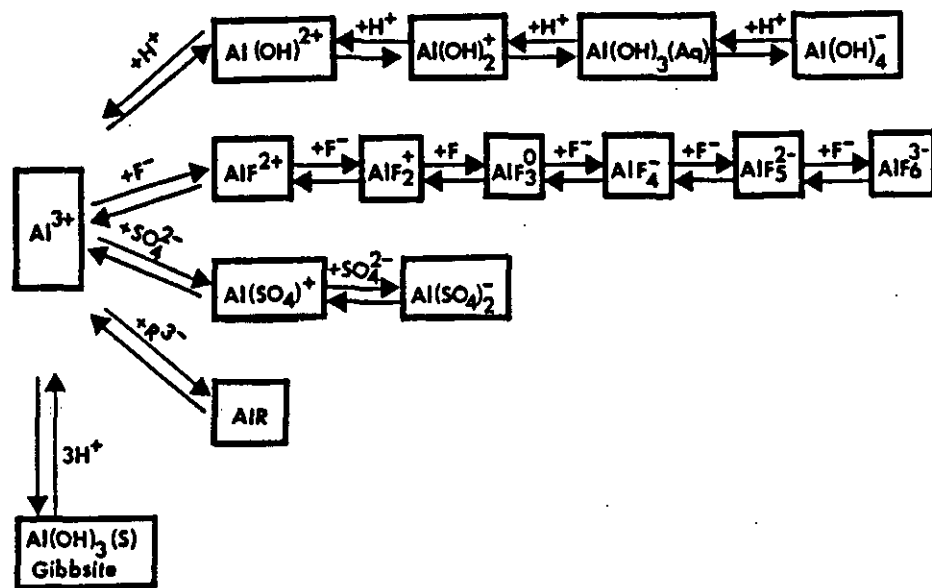


Figure 8. Aluminum dissolution and complexation with hydroxide (OH^-), fluoride (F^-), sulfate (SO_4^{2-}), and organic acid ligand (R^{3-}) (from Chen *et al.*, 1983).

(i.e., gibbsite) and by complexation with organic acids. In addition, inorganic aluminum complexes are determined for hydroxide, fluoride, and sulfate ligands. Figure 8 represents the aluminum system modeled in ILWAS. An option of simulating the dissolution of the aluminum solid phase as a rate limiting reaction is also available.

The ILWAS model is comprehensive in terms of including all the major processes influencing the acidification of a lake-watershed system. By being so rigorous, though, an extensive database is needed to run this model. Thus, its utility as a research tool is limited to only large research efforts.

MAGIC Model

The MAGIC model (Cosby et al., 1985b) was developed to estimate long-term catchment responses to acidic deposition. This relatively simple process-oriented mathematical model uses a lumped parameter approach with equilibrium soil processes controlling the pH, alkalinity, and ionic concentrations in both soil and stream waters. The MAGIC model links long-term dynamic mass balance equations with equilibrium equations to describe catchment soil and stream water quality. Soil processes included in the MAGIC model are: 1) anion retention by catchment soils (e.g., soil sulfate adsorption); 2) cation exchange by catchment soils; 3) alkalinity generation by carbonic acid dissolution; 4) dissolution of aluminum minerals in the catchment soils; and 5) mineral weathering (Cosby et al., 1985b).

Essentially, this model is an expansion of the Reuss-Johnson conceptual system (Reuss and Johnson, 1985; Reuss, 1983; Reuss, 1980) which assumes that streamwater chemistry is controlled by bedrock and soil horizon reactions. Surface water chemistry is determined by degassing the excess soil water CO_2 and resolving the equilibrium equations minus the soil matrix reactions.

Aluminum is modeled by equilibrium reactions. Soil aluminum processes include cation exchange reactions (using a Gaines-Thomas expression), inorganic aluminum complexation reactions (involving hydroxyl, fluoride, and sulfate ligands), and a soluble aluminum solid phase (gibbsite). Streamwater aluminum includes all of the above except the cation exchange reactions. A summary of all the equations used in the MAGIC model is presented in Table 3. A detailed discussion of their derivation can be found in Cosby et al. (1985a).

Sequentially, the model first obtains a solution to the entire set of equilibrium equations (including soil matrix reactions), and then routes the soil water to the stream channel and resolves the equilibrium equation excluding the soil-water cation exchange reactions. A mass balance of the major cations and anions is determined for each time step. Inputs needed for model simulation are atmospheric deposition, and net uptake-release fluxes of the base cations and the acid anions. Since long-term responses are modeled, mean annual precipitation volumes and ion concentrations are used in determining these fluxes. The atmospheric sulfate flux is corrected for dry deposition. Streamflow

Table 3

Summary of Model Equations, Parameters, and Inputs used in the MAGIC Model.

Equilibrium Equations		
<i>Solid Water Cation Exchange Reactions</i>		
1. $E_{Al} + E_{Ca} + E_{Mg} + E_{Na} + E_{K} = 1$	3. $\frac{[Ca^{2+}]^2 E_{Al}^2}{[Al^{3+}]^2 E_{Ca}^2} = S_{AlCa}$	5. $\frac{[Na^+]^2 E_{Al}}{[Mg^{2+}]^2 E_{Na}} = S_{AlMg}$
2. $BS = E_{Ca} + E_{Mg} + E_{Na} + E_{K} = 1 - E_{Al}$	4. $\frac{[Na^+]^2 E_{Ca}}{[Ca^{2+}]^2 E_{Na}} = S_{CaNa}$	6. $\frac{[Na^+] E_{Al}}{[K^+] E_{Na}} = S_{AlK}$
<i>Inorganic Aluminum Reactions</i>		
7. $\frac{[Al^{3+}]}{[H^+]^3} = K_{Al}$	11. $\frac{[Al(OH)_2^+][H^+]^2}{[Al^{3+}]} = K_{Al1}$	15. $\frac{[AlF_6^{3-}]}{[Al^{3+}][F^-]^6} = K_{Al6}$
8. $\frac{[Al(OH)^+][H^+]}{[Al^{3+}]} = K_{Al2}$	12. $\frac{[AlF_5^{2-}]}{[Al^{3+}][F^-]^5} = K_{Al5}$	16. $\frac{[AlF_4^{1-}]}{[Al^{3+}][F^-]^4} = K_{Al4}$
9. $\frac{[Al(OH)_2^+][H^+]^2}{[Al^{3+}]} = K_{Al3}$	13. $\frac{[AlF_4^{1-}]}{[Al^{3+}][F^-]^4} = K_{Al4}$	17. $\frac{[AlF_3^{2-}]}{[Al^{3+}][F^-]^3} = K_{Al3}$
10. $\frac{[Al(OH)_3^0][H^+]^3}{[Al^{3+}]} = K_{Al4}$	14. $\frac{[AlF_3^0]}{[Al^{3+}][F^-]^3} = K_{Al3}$	18. $\frac{[AlSO_4^+]}{[Al^{3+}][SO_4^{2-}]} = K_{Al5}$
		19. $\frac{[AlSO_3^+]}{[Al^{3+}][SO_3^{2-}]} = K_{Al6}$
<i>Inorganic Carbon Reactions</i>		
20. $\frac{[CO_2(aq)]}{P_{CO_2}} = K_{CO_2}$	21. $\frac{[HCO_3^-][H^+]}{[CO_2(aq)]} = K_{CO_3}$	22. $\frac{[CO_3^{2-}][H^+]^2}{[HCO_3^-]} = K_{CO_3}$
Dissociation of Water and Ionic Balance		
23. $[H^+][OH^-] = K_w$		
24. $[H^+] - [OH^-] + 2[Ca^{2+}] + 2[Mg^{2+}] + [K^+] + [Na^+] + 3[Al^{3+}] + 3[Al(OH)^+] + [Al(OH)_2^+] + [Al(OH)_3^0] - [Al(OH)_4^-] + 2[AlF_6^{3-}] + [AlF_5^{2-}] - [AlF_4^{1-}] - 3[AlF_3^{2-}] - 3[AlF_2^{1-}] + [AlSO_4^+] - [AlSO_3^+] - [Cl^-] - [F^-] - [NO_3^-] - 3[SO_4^{2-}] - [HCO_3^-] - 2[CO_3^{2-}] = 0$		
<i>Mass Balance Equations</i>		
1. $dCa_T/dt = F_{Ca} + W_{Ca} - Q^{Ca} [Ca^{2+}]$		
2. $dMg_T/dt = F_{Mg} + W_{Mg} - Q^{Mg} [Mg^{2+}]$		
3. $dNa_T/dt = F_{Na} + W_{Na} - Q^{Na} [Na^+]$		
4. $dK_T/dt = F_K + W_K - Q^{K} [K^+]$		
5. $dSO_{4T}/dt = F_{SO_4} + W_{SO_4} - Q^{SO_4} [SO_4^{2-}] + [AlSO_4^+] + 2[AlSO_3^+]$		
6. $dCl_T/dt = F_{Cl} + W_{Cl} - Q^{Cl} [Cl^-]$		
7. $dNO_{3T}/dt = F_{NO_3} + W_{NO_3} - Q^{NO_3} [NO_3^-]$		
8. $dF_T/dt = F_F + W_F - Q^{F} [F^-] + [AlF_6^{3-}] + 3[AlF_5^{2-}] + 3[AlF_4^{1-}] + 4[AlF_3^{2-}] + 3[AlF_2^{1-}] + 6[AlF_3^0]$		
Definitions		
Sulfate adsorption		
1. $E_s = E_{Al} \cdot XSO_4^{2-} / (C + XSO_4^{2-})$		
Alkalinity		
2. $Alk = [HCO_3^-] + 2[CO_3^{2-}] + [OH^-] - [H^+] - 3[Al^{3+}] - 3[Al(OH)^+] - [Al(OH)_2^+] + [Al(OH)_3^0] - 3[AlF_6^{3-}] - 2[AlF_5^{2-}] - 3[AlF_4^{1-}] - 3[AlF_3^{2-}] - 3[AlF_2^{1-}] - 3[AlSO_4^+] - 3[AlSO_3^+]$		
Total ion amounts		
1. $Ca_T = SP^{Ca} CEC \cdot E_{Ca} + 2V^{Ca} [Ca^{2+}]$		
4. $Mg_T = SP^{Mg} CEC \cdot E_{Mg} + 2V^{Mg} [Mg^{2+}]$		
5. $Na_T = SP^{Na} CEC \cdot E_{Na} + V^{Na} [Na^+]$		
6. $K_T = SP^{K} CEC \cdot E_{K} + V^{K} [K^+]$		
7. $SO_{4T} = SP^{SO_4} CEC \cdot E_{SO_4} + [AlSO_4^+] + 2[AlSO_3^+]$		
8. $F_T = V^{F} [F^-] + [AlF_6^{3-}] + 3[AlF_5^{2-}] + 3[AlF_4^{1-}] + 4[AlF_3^{2-}] + 3[AlF_2^{1-}] + 6[AlF_3^0]$		
9. $Cl_T = V^{Cl} [Cl^-]$		
10. $NO_{3T} = V^{NO_3} [NO_3^-]$		
Sums of aqueous base cation and strong acid anion concentrations		
11. $SBC = 2[Ca^{2+}] + 2[Mg^{2+}] + [Na^+] + [K^+]$		
12. $SSA = XSO_4^{2-} + [Cl^-] + [NO_3^-] + [F^-]$		
Variables		
Base cations: $[Ca^{2+}]$, $[Mg^{2+}]$, $[Na^+]$, $[K^+]$		
Strong acid anions: $[Cl^-]$, $[F^-]$, $[NO_3^-]$, $[SO_4^{2-}]$		
Inorganic aluminum species: $[Al^{3+}]$, $[Al(OH)^+]$, $[Al(OH)_2^+]$, $[Al(OH)_3^0]$, $[Al(OH)_4^-]$, $[AlF_6^{3-}]$, $[AlF_5^{2-}]$, $[AlF_4^{1-}]$, $[AlF_3^{2-}]$, $[AlF_2^{1-}]$, $[AlF_3^0]$, $[AlSO_4^+]$, $[AlSO_3^+]$		
Inorganic carbon species: $[CO_2(aq)]$, $[HCO_3^-]$, $[CO_3^{2-}]$		
Dissociation of water: $[H^+]$, $[OH^-]$		
Exchangeable cation fractions: E_{Ca} , E_{Mg} , E_{Na} , E_{K} , E_{Al}		
Base saturation: BS		
Total ion amounts: Ca_T , Mg_T , Na_T , K_T , SO_{4T} , Cl_T , NO_{3T} , F_T		
Adsorbed sulfate: E_s		
Alkalinity: Alk		
Sums of base cations and strong acid anions: SBC, SSA		

volumes leaving the catchment must also be provided because this model does not have a hydrologic simulation component.

pH and Aluminum Effects on Aquatic Biota

The toxicological effects of aluminum to fish during acidified surface water conditions have been known for some time (Baker and Schofield, 1982; Muniz and Leivestad, 1980; Driscoll et al., 1980). Moreover, elevated levels of aluminum in acidified surface waters, due to mobilization from the soil environment have been shown to be toxic to fish at pH levels not considered to be harmful (Schofield and Trojnar, 1980; Cronan and Schofield, 1979; Dickson, 1978). Mucus accumulation and gill damage have been reported by many researchers as common reactions of fish when exposed to elevated toxic metal levels in laboratory bioassays (e.g., Mattiessen and Brafield, 1973; Freeman and Everhart, 1971; Mount, 1966). When mucus accumulates on the gill membrane surface of a fish a decrease in gaseous exchange (e.g., O₂ or CO₂) occurs, which under severe conditions may lead to suffocation.

The inability of fish to regulate their body salts under acidified surface water conditions is thought to be a major cause of mortality. This has been demonstrated under laboratory conditions in which fish subjected to low pH waters suffered from a reduction in blood salts (Fromm, 1980; Leivestad et al., 1976). Since fish exchange ions through their gill membranes, this effect is thought to be attributed to the impairment of salt uptake at the gill surface McWilliams et al., 1980).

Furthermore, the rate of ion exchange at the gill membrane is greatly influenced by the amount of dissolved salts in the aquatic environment. Brown (1981) observed that low aqueous calcium levels increase the permeability of fish gills by creating an influx of hydrogen ions and an efflux of blood salts (i.e., sodium and calcium). Moreover, other bioassay experiments have shown that increasing calcium levels in low pH test water leads to a decrease in salt loss and an increase in fish survival (Leivestad et al., 1980; McWilliams and Potts, 1978; Leivestad et al., 1976).

Laboratory experiments have also been performed to assess the effects of aluminum on the survival of fish in acidified surface waters. A study conducted by Baker (1981) and later presented by Baker and Schofield (1982) found aluminum toxicity to vary over different pH levels, thus supporting the concept that aluminum toxicity is related to speciation. Her bioassay experiments also showed aluminum to be most toxic to white sucker (Catostomus commersoni, Lacepede) and brook trout (Salvelinus fontinalis, Mitchill) in over-saturated aluminum solutions at pH levels between 5.2 and 5.4. Background ion levels for all laboratory experiments were similar to Adirondack Lake and streamwaters. The presence of aluminum, though, under low pH conditions appears to benefit the survival of both white sucker and brook trout embryos prior to hatching. Aluminum is highly toxic to larvae and postlarvae stages at concentrations as low as 0.1-0.2 mg/L. A decline in toxicity is observed when pH levels are greater than 5.5. This is probably due to the decrease of aluminum in the water column by precipitation as

aluminum hydroxides. In general, this research found that under low pH levels older life stages are less sensitive to aluminum toxicity than are younger. Baker suggests that the mechanism for toxicity may involve either the precipitation and coagulation of aluminum-hydroxides and/or the adsorption and nucleation of aluminum-polymers on the gill membrane.

Cleveland et al (1986) investigated the exposure of aluminum on the mortality, growth, behavior, and biochemical responses to brook trout (Salvelinus fontinalis) as a function of developmental stages. Eyed eggs and young brook trout were subjected to pH levels of 4.5, 5.5, and 7.2, with and without aluminum (300 µg/L) for 30 days. Background ion concentrations simulated headwater lakes and streams in the northeastern United States. Adverse effects generally increased as pH decreased. Embryos and fish older than 36 days were found to be more tolerant of aluminum and acidic conditions than were larvae less than 15 days old. They concluded that observed adverse effects on brook trout at pH 4.5 with and without 300 µg/L aluminum, and at pH 5.5 with 300 µg/L aluminum, would make survival improbable under similar natural conditions.

A study performed by Muniz and Leivestad (1980) found that brown trout mortality occurs when aluminum concentrations are greater than 0.2 mg/L and pH values between 4.5 and 5.5. A rapid loss of sodium and chloride from fish blood is also observed at all toxic aluminum levels. It should be noted that the rapid loss of blood salts is the same response found from hydrogen ion stress previously presented. The highest rate of salt loss (i.e., the maximum aluminum toxicity) for

brown trout fingerlings occurred around pH 5.0 with an aluminum level of 0.19 mg/L. At pH 4.0, an aluminum addition of 0.38 mg/L reduced the hydrogen ion stress, as measured by loss in blood salts. They also observed hyperventilation, coughing, and mucus clogging of the gills, and concluded the mode of toxicity to be due to impaired ion exchange and respiratory stress caused by mucus clogging of the gill membrane surface. Fish with the most severe mucus clogging were also those having the lowest plasma salt levels. When the affected fish were transferred back into neutral pH waters, most of the stressed individuals recovered with no apparent damage to their gill membranes.

Schofield and Trojnar (1980) also reported a decrease in survival of brook trout postlarvae when aluminum concentrations are greater than 0.2 mg/L. Their bioassay experiments were conducted at pH levels between 4.4 to 5.2 and aluminum levels between 0.0 to 0.5 mg/L. They observed minor gill damage as well as a reduction in fish growth at aluminum concentrations as low as 0.1 mg/L.

Driscoll et al. (1980) found inorganic forms of aluminum to be the most toxic than organic forms to white sucker and brook trout postlarvae. They found that complexing aluminum with citrate, an organic compound, significantly reduced its toxic effect. Furthermore, the addition of fluoride at typical Adirondack surface water levels, and pH values of 5.2 and 4.4 also showed a reduction in toxicity, but by not as much as the citrate complex. Thus, their study concluded that ligands forming strong complexes with aluminum (e.g., organics and fluoride) reduce its toxicological effect.

Acidification of surface waters can also affect the population and community structure of other aquatic organisms at all trophic levels in an aquatic ecosystem (Hall et al., 1980; Hendrey et al., 1976). Roff and Kwiatkowski (1977) found a significant reduction in diversity and numbers of zooplankton communities in acidified lakes with pH levels below 5.5. Zoobenthos populations also show a reduction in both diversity and abundance under acidified conditions (Raddum, 1980), though an increase of sphagnum moss (Grahn, 1977) was observed. Acidification of surface waters generally causes a shift in dominance as well as a decrease in diversity and abundance.

Surface water quality can vary considerably from season-to-season, day-to-day, or even within-a-day. Since bioassay tests are usually conducted under fixed conditions over a 96 hour period, it is difficult to assess the potential toxicological risk to a natural ecosystem based on laboratory experiments. Moreover, natural aquatic systems contain many possible complexing agents (usually not included in laboratory bioassay studies) as well as varying hardness concentrations which are important in terms of overall aluminum toxicity. Since total aluminum is generally measured, it becomes extremely difficult to separate antagonistic and synergistic effects under low pH, high Al conditions. Thus, a distinction of aluminum speciation as well as occurrence and duration are needed when accurately assessing the potential risk of aluminum toxicity. Modeling a natural ecosystem becomes beneficial under these circumstances since it can be used to describe the dynamics of an ecosystem.

CHAPTER III
MATERIALS AND METHODS

Field Sampling

The field sampling effort consisted of three major components: precipitation, streamwater, and soil sampling. This section describes procedures used to obtain field samples.

Precipitation

Precipitation samples for chemical analysis were obtained during intensive sampling periods on a daily basis. Plastic buckets, which had been acid washed, 10% HCl, and then rinsed at least 5 times with distilled and deionized water, were used to collect rain water at the precipitation sampling site (see Figure 2 for approximate location). Precipitation volume was also measured on a daily basis during intensive storm periods with an on-site gauge. In addition, hourly precipitation volumes were obtained from the NOAA National Weather Station located at the Worcester Municipal Airport approximately 25 kilometers from the study area.

Streamwater

Streamwater samples for chemical analysis were obtained either by taking grab samples or by utilizing an automatic sampler, depending on the frequency of samples needed. Grab samples were collected in 1 liter

polyethylene bottles. The sampling bottles had been acid washed and rinsed with distilled and deionized water before use. While at the site sample bottles were again rinsed several times with streamwater before a final sample was taken. The collected samples were immediately put on ice before being brought to the laboratory for analysis. During intensive sampling periods streamwater samples for chemical analysis were collected every six hours by automatic samplers. One Manning and two ISCO automatic samplers were used for this purpose. The automatic monitored samples were transferred daily to 1 liter polyethylene bottles and put on ice awaiting return to the laboratory for analysis. Daily on site analyses consisted of temperature and conductivity measurements.

Stream flows were measured at each of the sampling sites in addition to streamwater chemistry. A pigmy Price meter was used to a develop stage-discharge relationship for each stream site in accordance with the USGS six-tenths depth method (Buchanan and Somers, 1969). These curves, shown in Figures 9-11, were used to determine stream flow. During intensive sampling periods a continuous stream flow gauge, maintained by MIT, was utilized. Continuous stage was recorded with a Stevens Type F Recorder, equipped with a 32-day time base (Eshleman, 1982). The recorder used standard Stevens F-1 paper in conjunction with a four inch float, counterweight, and capillary pen. The intake was at an elevation lower than the channel, thus eliminating the possibility of negative values for gage height.

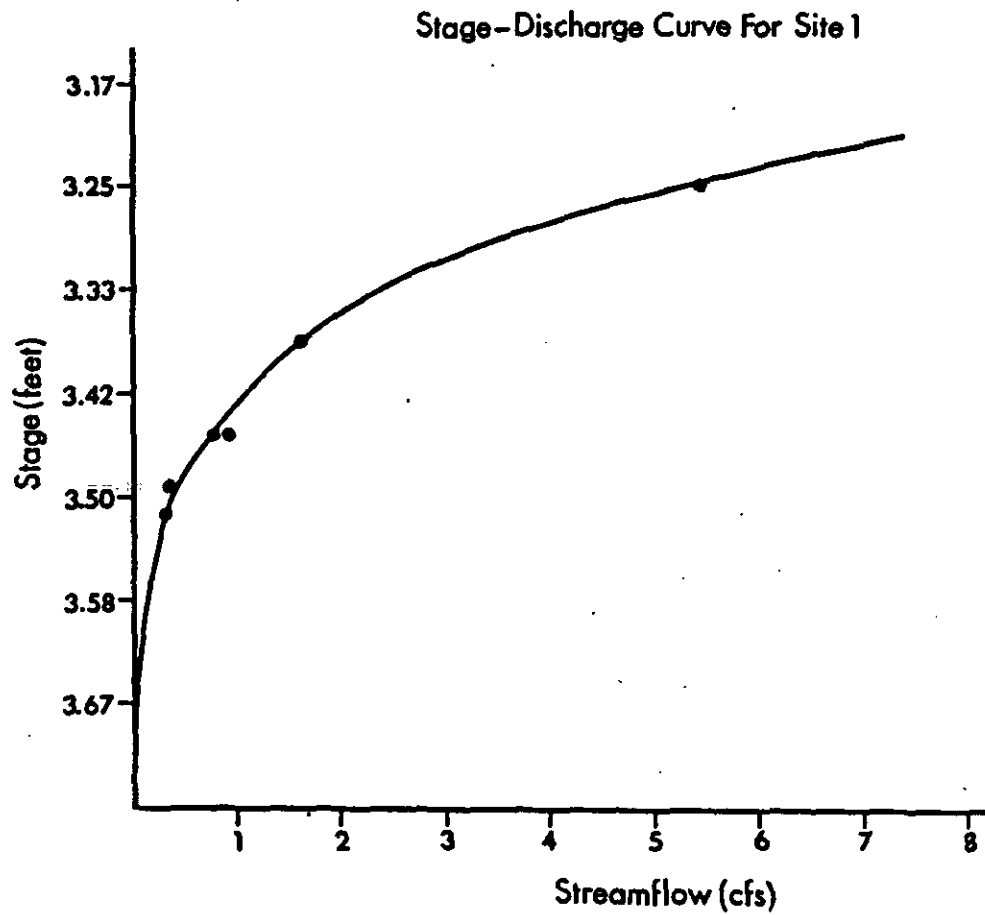


Figure 9. Stage-discharge relationship for site 1 the mountain stream site. Stage is measured in feet and streamflow is measured in cubic feet per second (cfs).

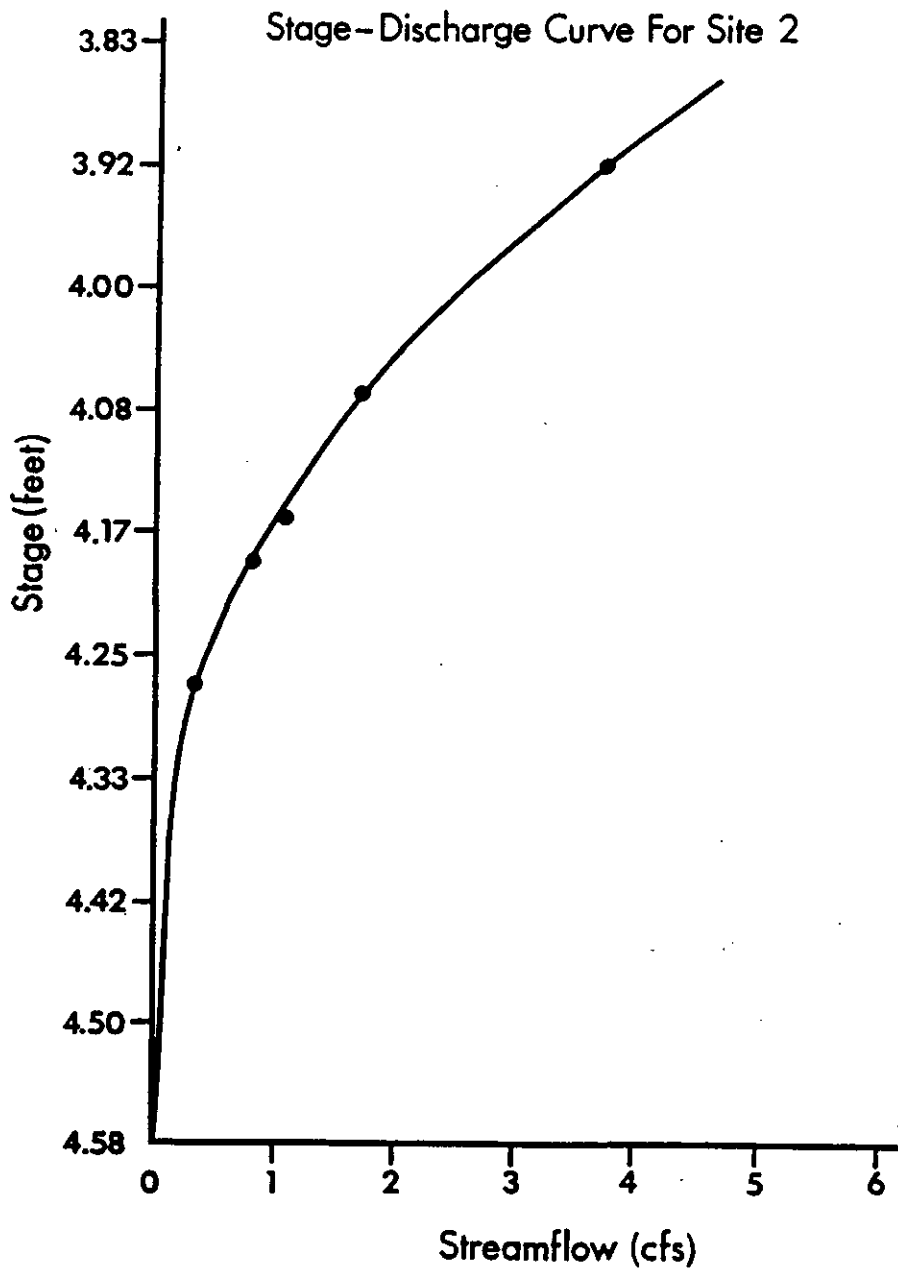


Figure 10. Stage-discharge relationship for site 2 the wetland stream site. Stage is measured in feet and streamflow is measured in cubic feet per second (cfs).

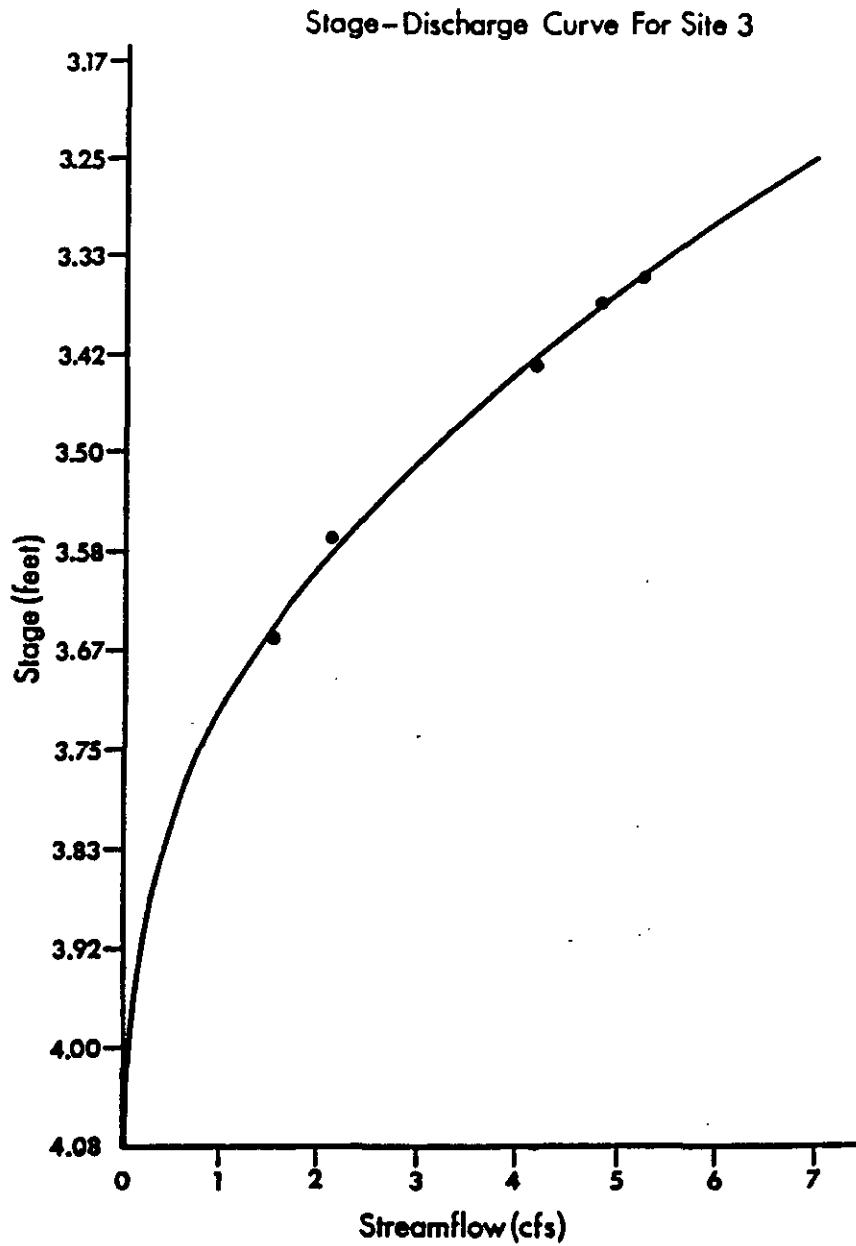


Figure 11. Stage-discharge relationship for site 3 the downstream site. Stage is measured in feet and streamflow is measured in cubic feet per second (cfs).

Soil

Soil samples were obtained at nine different sites within the watershed by hand digging a pit down to the fragipan layer, approximately 75 cm below the soil surface. Samples from the various soil horizons were collected in plastic bags. This procedure was assisted by Dr. John Baker and Steve Bodine from the UMASS Plant and Soil Science Department. The approximate locations of the soil sampling sites are presented in Figure 2. Core samples were also obtained so that soil moisture characteristics could be determined in the laboratory.

Laboratory Analysis

Precipitation and Streamwater Chemistry

Precipitation and streamwater samples were analyzed for several constituents with laboratory methods described below. All laboratory glassware and plasticware were acid washed with 10% hydrochloric acid and then rinsed first with distilled water at least three times and finally with deionized water at least twice before using. Special care was taken during all analyses to minimize contamination error. Samples were brought to room temperature before analysis. All analyses were performed on the same day as collected except for the major inorganic cations and anions which were determined by the Acid Rain Laboratory located on the UMASS campus. The analysis of these samples were usually

performed within a couple of months. All of the chemicals used in this study were of analytical grade quality.

Aluminum. A detailed description of the analytical procedure used for determining the various fractions of aluminum in this study may be found in a report by Scheackler (1985). Basically the analytical procedure used for determining monomeric aluminum was a slight modification of Barnes' method (1975). The main differences were that butyl acetate was used for extraction instead of methyl isobutyl ketone and a UV/VIS spectrophotometer was used instead of an atomic absorption spectrophotometer. In the procedure aluminum was first complexed with 8-hydroxyquinoline, then the pH was raised to 8.3 with ammonium hydroxide to reduce interferences, and finally extracted into butyl acetate. This procedure should be done as quickly as possible so that only the mononuclear forms of aluminum become extracted. The extracted alumino-oxinate complex was measured colorimetrically with a spectrophotometer at a wavelength of 395 nanometers.

The method used to fractionate monomeric aluminum into organic and inorganic forms was based after that of Driscoll (1980). The non-labile monomeric aluminum fraction, assumed to be organically bound aluminum, was determined by passing the sample through a strong acid cation exchange resin at a flow rate of approximately 3.4 ml/min/ml of exchanger bed volume. In principle the positively charged inorganic aluminum atoms were retained on the column while the neutrally charged organically bound aluminum pass through the column. Between each run the column was recharged by passing a NaCl eluant, which was near the pH

and ionic strength of the sample, through the column. The sample recovered from the column was then analyzed by the same procedure as for monomeric aluminum. Thus, by knowing the total monomeric aluminum and the organic monomeric aluminum the inorganic monomeric aluminum can be determined by difference. The aluminum samples were not filtered since it was determined by a comparison study of filtered and unfiltered samples that there was no significant difference between monomeric values.

Lastly, an acid reactive aluminum fraction was determined by acidifying aquatic samples to a pH of less than 2 for approximately one hour. This fraction of aluminum, that being the difference between total monomeric and acid reactive aluminum, probably consists of colloidal and/or polymeric aluminum as well as strongly bound aluminorganic complexes.

pH. Electrometric pH measurements were made using an Orion combination Ross ion selective electrode. The Ross electrode has a unique redox internal system designed to have virtually a zero temperature coefficient (Orion Research, 1982). Maintenance and storage of this electrode were in accordance with the Instruction Manual for Ross pH Electrodes (Orion Research, 1984). Potentials were measured with an Orion Model 901 ionalyzer meter. The electrode system was calibrated against a standard pH 7 phosphate buffer and a pH 4 potassium biphthalate buffer and rechecked before analyses were made. The calibration was rechecked every two hours during an analysis session. Between measurements the electrode was thoroughly rinsed with deionized

water and gently blotted dry with a soft tissue to help eliminate carryover. Both standards and samples were measured at room temperature.

To reduce residual junction potential and streaming potential errors, a low ionic strength pH 5 standard was checked before samples were analyzed. In addition, samples were stirred with a magnetic stirrer for approximately 30 seconds and let stand quiescently before measurement (McQuaker et al., 1983). pH was recorded when the system had stabilized. It was found that soaking the electrode in a sample for approximately 10 minutes before analysis helped reduce the response time.

Acid Neutralizing Capacity. Acid neutralizing capacity (ANC) was determined by using the Gran function analysis technique (Gran, 1952; Driscoll, 1980; Driscoll and Bisogni, 1984; Barnard and Bisogni, 1985). Essentially, this technique estimates the equivalence point of the titration by titrating water samples with a strong acid.

For a monoprotic acid/base system the ANC can be represented as:

$$\text{ANC} = [\text{A}^-] + [\text{OH}^-] - [\text{H}^+] \quad (3.1)$$

where:

ANC = sample acid neutralizing capacity (eq-L^{-1})

$[\text{A}^-]$ = sample weak base content (mol-L^{-1})

The equivalence point of the titration is when $[\text{H}^+] = [\text{A}^-] + [\text{OH}^-]$, and the volume of the titrant needed to reach this point is the

equivalent volume of the titrant (V_e). Knowing the titrant equivalent volume, the sample ANC can be calculated as:

$$ANC = V_e \times N_{ac} \times S \times V_o \quad (3.2)$$

where:

V_e = titrant equivalent volume (L)

N_{ac} = titrant normality (eq-L^{-1})

V_o = initial sample volume (L)

In addition, the acid neutralizing capacity of a sample at any point can be determined by:

$$ANC = (V_e - V) \times N_{ac} \times S \times (V_o + V) \quad (3.3)$$

where:

V = titrant volume (L)

Under low pH conditions, it is assumed that weak acids are protonated and thus:

$$ANC = -[H^+] \quad (3.4)$$

Equation (3.4) can be substituted into equation (3.3) and rearranged to give:

$$(V_o + V) \times [H^+] = (V - V_e) \times N_{ac} \quad (3.5)$$

thus,

$$F_1 = (V_o + V) \times 10^{-\text{pH}} = (V - V_e) \times N_{ac} \quad (3.6)$$

where:

F_1 = Gran function

The equivalent volume (V_e) can be estimated by plotting F_1 against the titrant volume (V), and extrapolating the linear portion of the plot to $F_1 = 0$. The slope should be equal to the titrant normality. A computer program, listed in Appendix A, was developed to calculate the equivalent volume (V_e) as well as the sample ANC.

Major Inorganic Cations. Chemical analysis of the major cations (i.e., calcium, magnesium, sodium, potassium, iron, and silica) was performed by the UMASS Acid Rain Laboratory using an atomic emission technique on a Perkin-Elmer ICP/6500 system. This system uses a high temperature argon plasma to dissociate and to excite sample atoms, which then emit characteristic radiations. The plasma was generated by passing a stream of argon and a sample aerosol through an RF coil, which heats the gas to about 10,000 degrees Kelvin. A computer controlled system measures the intensities of these emissions, and performs calibration and spectral correction. This technique permits direct determination of most metals in natural water samples without pretreatment.

The ICP/6500 system was optimized following manufacturer's instructions. A comparison between the intensities of a zinc ion transition and a calcium atom transition were performed to show when the nebulizer and plasma were properly set up. This procedure was followed daily to ensure that there was no problem with the system when introducing the sample into the plasma.

The system was calibrated by using a standard solution that contained all the elements of interest at a concentration of 10.00 mg/L.

The standards were prepared from commercial stock solutions and preserved with 1% HNO₃. A deionized water blank was also used in this procedure. Check samples were tested periodically to verify the linearity of the calibration curve as well as to check the accuracy of determination. If the check samples were found to be more than 10% from their true values, the analyses were repeated. Check samples were prepared from a stock solution supplied by the Environmental Protection Agency. Detection limits for this method were:

Si (251.611 nm)	0.023 mg/L
Fe (259.940 nm)	0.008 mg/L
Mg (285.213 nm)	0.006 mg/L
Ca (393.366 nm)	0.001 mg/L
Na (588.990 nm)	0.012 mg/L
K (769.900 nm)	0.069 mg/L

Major Inorganic Anions. Anion analysis (i.e., sulfate, nitrate, and chloride) of water samples were performed by the UMASS Acid Rain Laboratory using a Wescan high-pressure liquid chromatography system. This technique uses a separatory column specific for the analysis desired. The column has positively charged sites to which inorganic anions adsorb. A high pressure liquid eluant displaces the sample anions at a certain rate. The eluted anions from the column were then carried past a conductivity cell for quantitative measurement. Specific anions were determined by the specific retention time from injection until they elute past the detector. Standards were used to establish these times for each particular column-eluant-pressure configuration.

Quantification of unknowns was made by comparing peak heights with known standards.

Water samples were filtered through a 0.45 micron filter before analysis to eliminate any particulates that may potentially clog the sampling system and in turn contaminate the analytical column. A solution of 0.01 M O-hydroxybenzoic acid and 1% methanol was used as the eluant, This solution was degassed and adjusted to a pH of 8.60 with sodium hydroxide before use. The conductivity cell output was plotted on a Shimadzu integrator/recorder. Calibration was performed by measuring peak heights of standards for each desired anion.

Quality control was performed by analyzing Environmental Protection Agency unknown samples, and comparing the results to values supplied by the EPA.. The analysis of duplicate samples and the recovery of spiked samples were also performed to ensure that there were no matrix interferences during the analyses. Detection limits for this method were:

SO₄ 0.15 mg/L

NO₃ 0.30 mg/L

Cl 0.12 mg/L

Fluoride. Free and total fluoride were measured using an Orion Model 94-09 fluoride ion selective electrode and an Orion Model 90-01 single junction reference electrode. These electrodes were used in conjunction with an Orion Model 901 ionalyzer meter. Analysis and maintenance of the electrodes were in accordance with manufacturer's specification. All standards and samples were run at room temperature

In plasticware, since fluoride reacts with glass. Magnetic stirring was conducted at a constant speed throughout the procedure. Total fluoride was determined by adding TISAB (total ionic strength adjustor) to the samples at a ratio of 50:50 by volume. With special care new electrodes were able to obtain a linear standard curve down to 0.020 mg/L.

Dissolved Organic Carbon. Samples for DOC were first filtered through glass fiber filters (1.3 μm , Whatman GF/C) to remove solution particulates. DOC measurements were made by the Persulfate-Ultraviolet Oxidation Method according to Standard Methods using a Dohrmann DC-80 instrument.

The DOC analyzer was calibrated with a 10 mg/L as C potassium hydrogen phthalate (KHP) standard before each run of samples. The calibration was verified by injecting a 5 mg/L as C KHP standard before samples were run. If the standard result was not within 10%, the system was recalibrated. The calibration was rechecked after every ninth sample using the 5 mg/L as C standard. If the results were not within 10% of the mean standard value, the instrument was recalibrated and all samples reanalyzed. Each sample or standard was run in triplicate, after which a deionized water blank was injected to rinse the injection system prior to running the next sample. Samples containing 5 mg/L as DOC of USGS Reference Fulvic Acid were periodically analyzed to insure that the UV Persulfate/IR system recovers 90% or more of the DOC.

UV absorbance at 254 nm was also used as a surrogate measurement for dissolved organic carbon. The UV measurements were made on samples

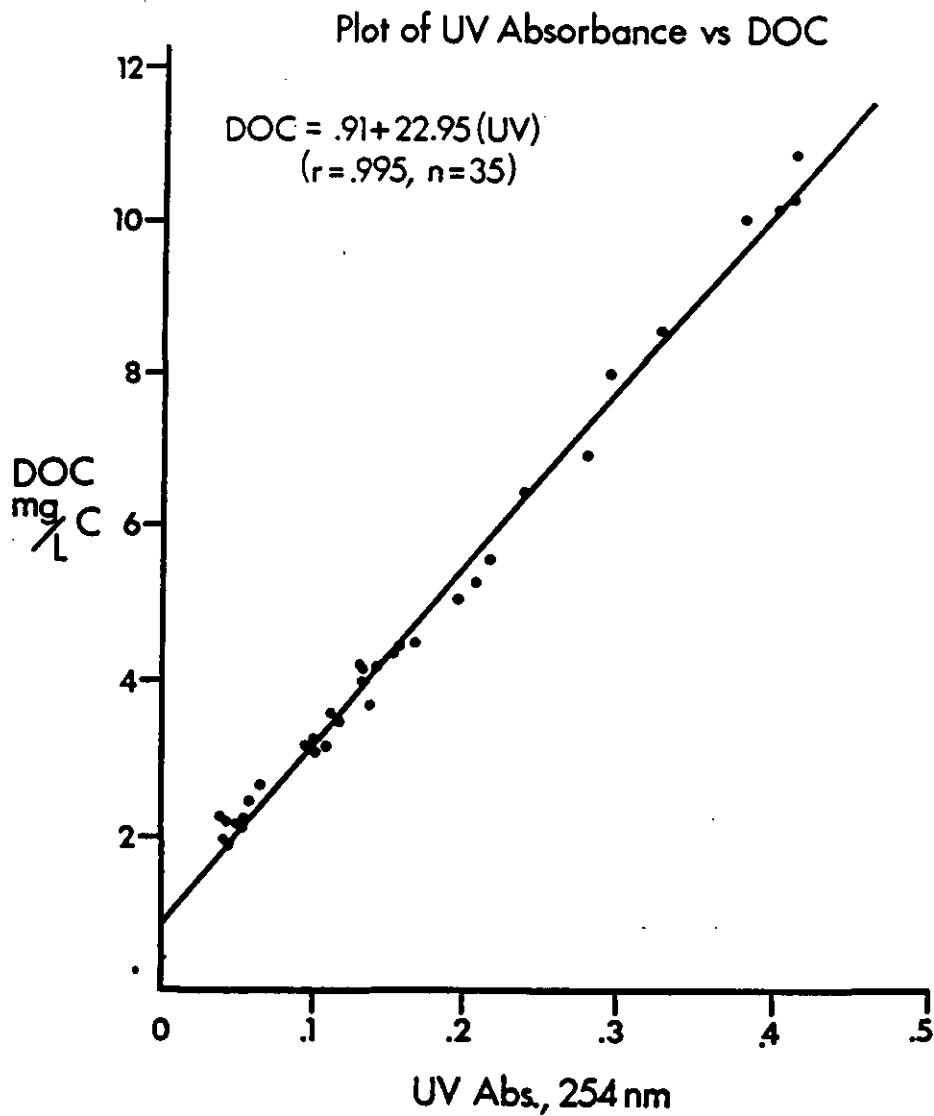


Figure 12. Plot of the surrogate variable UV absorbance (at 254 nm) against dissolved organic carbon (DOC) in milligrams per liter.

filtered through a glass fiber filter (Whatman GF/C) and then adjusted to pH 7. UV absorbance was measured at 254 nm in a 1 cm quartz cell using a Perkin Elmer Lambda 3B UV/VIS spectrophotometer. Deionized water was used as a blank. Correlation between UV absorbance and DOC may be seen in Figure 12.

Conductivity and Temperature. Streamwater conductivity and temperature were measured on site by using a Yellow Springs Instrument, YSI Model 33 Conductivity/Temperature meter. This portable meter uses a probe consisting of a plastic conductivity cell and a thermistor temperature sensor. Manufacturer's specifications were used in operating and maintaining the YSI meter. Conductivity measurements were in micromhos/centimeter with an accuracy of 3% while the temperature in degrees Celsius has an accuracy of approximately 0.2 degrees Celsius.

Soil Chemistry

Forty-two soil samples were collected from the nine different study area sampling sites (see Figure 2 for approximate locations). The soil samples were brought to the laboratory, air dried, passed through a 2-mm mesh sieve, and stored until all analyses were performed. All analyses were performed in duplicate with the methods described below.

Soil pH. Soil pH was determined by both the water and salt methods as described in the Methods of Soil Analysis (1982). Soil pH is a measure of the activity of H^+ ions in a soil-water solution. Thus, the pH of a soil depends greatly on the amount of water used in the

analysis. Soil pH also depends on the percent base saturation of the soil as base cations can replace acid cations on the soil exchange sites. Essentially, the procedure used added equal amounts, by weight, of soil and water and then mixed the solution for approximately 30 minutes so that equilibrium could be established. After letting the mixture stand for another 30 minutes, so that the solid phase separates from the liquid phase, the pH of the supernatant was measured.

Immediately after measurement, an addition of CaCl_2 was made to obtain a solution concentration of .01 M CaCl_2 . The sample was mixed again for approximately 15 minutes and then let stand quiescently for another 15 minutes before the final pH was made in the supernatant. Advantages of measuring the soil pH in a salt solution were:

1. 0.01 M CaCl_2 approximates the total salt concentration in a natural field moisture content soil solution and thus reflects more accurately the pH of field conditions.
2. The addition of the salt reduces the volume dependence as well as seasonal fluctuation effects.
3. The salt also flocculates clay particles and in turn reduces liquid junction potential errors in pH measurement.

Organic Matter Content. The organic matter content of soil samples were determined gravimetrically by loss-on-ignition (Davies, 1974 ; Ball, 1964). The procedure consists of drying the soil at 105 degrees Centigrade, weighing, then placing the sample in a muffle furnace at 430 degrees Centigrade for 24 hours, then weighing again. The organic

matter content was the difference in weight before and after the muffle furnace ignition process. A lower temperature with a longer combustion time in the muffle furnace differs from conventional organic analysis as higher temperatures may induce errors by causing additional weight loss by removing structural water from clay minerals as well as CO₂ losses from carbonates.

Exchangeable Base Cations. Exchangeable base cations were determined by the Ammonium Acetate method (Methods of Soil Analysis, 1982). Base cations were extracted from soil samples by the addition of a 1 N NH₄Ac (pH 7) solution. In principal, this solution replaces the exchangeable cations by saturating the exchange sites with ammonium ions. The soil and ammonium acetate solution was agitated on a shaker table for approximately 24 hours so that equilibrium conditions could be obtained and then filtered (using Whatman No. 42 filter paper) through a Buchner funnel to separate the solid and liquid phases. The base cations (i.e., calcium, magnesium, sodium, and potassium) were then measured by atomic absorption/atomic emission spectrophotometry (Standard Methods, 1985). Lanthanum was added to the calcium and magnesium samples while cesium was added to the sodium and potassium samples to reduce interferences with this method.

Exchangeable Acid Cations. Exchangeable acid cations or exchangeable acidity was determined by extracting acid cations from the soil samples with a 1 N potassium chloride solution. In principle, potassium replaces the acid cations (i.e., iron, aluminum, and protons) on the soil exchange sites. After a 30 minute period on a shaking table

the sample was filtered through a Buchner funnel (using a Whatman No. 42 filter) to separate the soil and liquid phases. Once brought to a known volume, a portion of the leachate was titrated with .01 N NaOH to the pink phenolphthalein endpoint, thus measuring the total extractable acidity. Hydrogen ion acidity was separated from the aluminum and iron acidity by adding 5 mL of a 1 N KF solution. Fluoride complexes the aluminum and iron in solution causing the sample to turn red. The sample was then titrated back down to a clear phenolphthalein end point with .01 N HCl. Finally, iron was separated from aluminum by measuring Fe on an atomic absorption spectrophotometer.

Cation Exchange Capacity. Mineral and organic fractions of soils possess negative charges and thus have the ability to retain cations. The amount of cations retained on the soil in an exchangeable form is known as the cation exchange capacity (CEC). In this study the cation exchange capacity was defined as the sum of exchangeable acid and base cations.

$$\text{CEC} = \text{exchangeable base cations} + \text{exchangeable acid cations}$$

Soil Moisture Characteristics. Field capacity and saturated soil moisture content were measured gravimetrically by using a Tempe Pressure Cell apparatus as specified in the Operating Instructions for the 1400 tempe pressure cell. In this procedure core samples are placed in the tempe pressure cell, then saturated and weighed to determine the soils saturated weight. Next the tempe pressure cells were placed on the

pressure apparatus and set at 1/3 bar. When equilibrium was reached, which was when the flow of moisture ceases or when the weight stabilizes, the soil was operationally defined to be at field capacity. The pressure cell was weighed again to determine the field capacity weight. Finally, the soil core was dried at 105°C for 24 hours and weighed. Knowing the dry weight of the soil, the weight at 1/3 bar, and the saturated weight, the field capacity and saturated soil moisture content can be determined.

The dry bulk density was determined as the mass of dried soil (at 105 °C) to its total core sample size volume. Typical dry bulk densities range from 1.1-1.6 gm-cm⁻³ (Hillel, 1982).

CHAPTER IV
MODEL DEVELOPMENT

Two mathematical models are presented in this chapter: a chemical equilibrium model and an aluminum transport simulation model. The chemical equilibrium model determines various inorganic aluminum species by performing chemical equilibrium calculations. The computer program presented later in this chapter is used to chemically speciate individual streamwater grab samples. The simulation model determines aluminum transport within a watershed system by incorporating soil chemistry, streamwater chemistry, and hydrologic properties. This model, whose derivation follows, is used to gain insight into the more important processes influencing aluminum transport. The following describes the mathematical basis of these two separate modeling frameworks.

Chemical Equilibrium Model

Several chemical equilibrium models exist that have the potential to perform aluminum speciation calculations. Some of these are WATEQ (Truesdell and Jones, 1974), WATSPEC (Wigley, 1977), and MINEQL (Westall et al., 1976), which are designed for large scale problems requiring a main frame computer. In addition, ALCHEMI (Driscoll and Schecher, 1984) was developed specifically for aluminum equilibria problems and runs on a personal computer.

Another chemical equilibrium model, EQUAL, was developed for the specific needs of this project. The major benefit of EQUAL was its compatibility with the data base management system used for this particular project. In addition, chemical equilibrium calculations were needed in the simulation model, thus the framework of EQUAL was also utilized in the simulation program.

EQUAL calculates the equilibrium distribution of inorganic aluminum by utilizing mass-action equilibrium and mass balance equations. Thermodynamic stability constants are used for hydroxyl, fluoride, and sulfate ligand complexes. Temperature corrections and ionic strength adjustments are also included.

Mass-Action Equilibrium Equations

A general form of an equilibrium reaction is expressed as,



where the lowercase letters are the stoichiometric coefficients to their corresponding chemical species. The mass-action equation for this general reaction is,

$$K = \frac{\{C\}^c \{D\}^d}{\{A\}^a \{B\}^b} \quad (4.2)$$

where K is the equilibrium constant and the brackets represent species activities.

The equilibrium reactions used in EQUAL follow the same form as equations (4.1) and (4.2) and are listed below.



The mass-action equations for these reactions are in Table 4, and the thermodynamic equilibrium information used for EQUAL, i.e., equilibrium constants and enthalpy data, are in Appendix B. The equilibrium constants in Appendix B are based on infinite dilution at 25 degrees Centigrade. Therefore, ionic strength and temperature corrections for these variations are made by the formulations presented below.

Temperature Correction. Equilibrium constant can be estimated at any temperature by knowing the enthalpy of the reaction. Assuming the change in enthalpy, ΔH^0 , is independent of temperature, the

Table 4

Equations Used In EQUAL Computer Program

Equilibrium Equations

$$\frac{\{\text{AlOH}^{2+}\}\{\text{H}^+\}}{\{\text{Al}^{3+}\}} = K_{1\text{OH}}$$

$$\frac{\{\text{H}^+\}\{\text{F}^-\}}{\{\text{HF}\}} = K_{\text{HF}}$$

$$\frac{\{\text{Al}(\text{OH})_2^+\}\{\text{H}^+\}^2}{\{\text{Al}^{3+}\}} = K_{2\text{OH}}$$

$$\frac{\{\text{AlF}^{2+}\}}{\{\text{Al}^{3+}\}\{\text{F}^-\}} = K_{1\text{F}}$$

$$\frac{\{\text{Al}(\text{OH})_4^-\}\{\text{H}^+\}^4}{\{\text{Al}^{3+}\}} = K_{4\text{OH}}$$

$$\frac{\{\text{AlF}_2^+\}}{\{\text{Al}^{3+}\}\{\text{F}^-\}^2} = K_{2\text{F}}$$

$$\frac{\{\text{AlSO}_4^+\}}{\{\text{Al}^{3+}\}\{\text{SO}_4^{2-}\}} = K_{1\text{SO}_4}$$

$$\frac{\{\text{AlF}_3\}}{\{\text{Al}^{3+}\}\{\text{F}^-\}^3} = K_{3\text{F}}$$

$$\frac{\{\text{Al}(\text{SO}_4)^-\}}{\{\text{Al}^{3+}\}\{\text{SO}_4^{2-}\}^2} = K_{2\text{SO}_4}$$

$$\frac{\{\text{AlF}_4^-\}}{\{\text{Al}^{3+}\}\{\text{F}^-\}^4} = K_{4\text{F}}$$

$$\frac{\{\text{AlF}_5^{2-}\}}{\{\text{Al}^{3+}\}\{\text{F}^-\}^5} = K_{5\text{F}}$$

Table 4 (continued)

Fluoride Mass Balance

$$TF = \frac{\{HF\}}{f_0} + \frac{\{F^-\}}{f_1} + \frac{\{AlF^{2+}\}}{f_2} + 2 \frac{\{AlF_2^+\}}{f_1} + 3 \frac{\{AlF_3\}}{f_0} + 4 \frac{\{AlF_4^-\}}{f_1} + 5 \frac{\{AlF_5^{2-}\}}{f_2}$$

Sulfate Mass Balance

$$TSO_4 = \frac{\{SO_4^{2-}\}}{f_2} + \frac{\{AlSO_4^+\}}{f_1} + \frac{\{Al(SO_4)_2^-\}}{f_1}$$

Aluminum Mass Balance

$$TAL = \frac{\{Al^{3+}\}}{f_3} + \frac{\{AlOH^{2+}\}}{f_2} + \frac{\{Al(OH)_2^+\}}{f_1} + \frac{\{Al(OH)_4^-\}}{f_1} + \frac{\{AlF^{2+}\}}{f_2} + \frac{\{AlF_2^+\}}{f_1} \\ + \frac{\{AlF_3\}}{f_0} + \frac{\{AlF_4^-\}}{f_1} + \frac{\{AlF_5^{2-}\}}{f_2} + \frac{\{AlSO_4^+\}}{f_1} + \frac{\{Al(SO_4)_2^-\}}{f_1}$$

Van't Hoff relationship (Stumm and Morgan, 1981) can be used to correct for temperature differences:

$$\log K = \log K_{25} - \Delta H^{\circ}(1/T - 1/T_{25})/(2.303 \times R) \quad (4.14)$$

where:

- K = equilibrium constant at any temperature
- K₂₅ = equilibrium constant at 25 degrees Centigrade
- ΔH^o = change in enthalpy (cal-mol⁻¹)
- R = gas constant (cal-deg⁻¹-mol⁻¹)
- T = absolute temperature
- T₂₅ = 25 degrees (degrees Kelvin)

Enthalpy data has not been determined for all reactions, so when values are lacking, the 25 degree Centigrade equilibrium constants are used.

Ionic Strength Adjustment. Ions in solution can alter the apparent concentration of species involved in equilibrium reactions. This effect can be accounted for by including activity coefficients in the analytical analysis. An activity coefficient is essentially the ratio of the activity of the species to its molar concentration. Thus, the activity can be represented as:

$$\{X\} = f \times [X] \quad (4.15)$$

where:

{ χ } = activity of species χ

[χ] = molar concentration of species χ

f = activity coefficient

For charged species the activity coefficient is less than 1, thus having an apparent concentration less than the actual. The activity coefficient of charged species is estimated in the program by the Gutlberg approximation (Stumm and Morgan, 1981):

$$\log f = -A \times z^2 \times I^{.5} + (1 + I^{.5}) \quad (4.16)$$

where:

I = ionic strength = $0.5 \times C \times z^2$

z = ionic charge

C = ion molar concentration

$A = 1.82 \times 10^6 \times (E \times T)^{-1.5}$

E = dielectric constant = 78.54 (Butler, 1964)

T = absolute temperature

Uncharged species typically have activity coefficients greater than 1, and can be approximated as (Drever, 1982):

$$\log f = 0.1 \times I \quad (4.17)$$

Mass Balance Equations

The driving force of EQUAL is its mass balance equations. Total mass for inorganic monomeric aluminum (TAL), fluoride (TF), and sulfate (TSO_4) are each assumed to be conserved. Therefore, the three conservation of mass equations are:

$$\begin{aligned} \text{TAL} = & [\text{Al}^{3+}] + \Sigma[\text{Al-OH species}] + \Sigma[\text{Al-F species}] \\ & + \Sigma[\text{Al-SO}_4 \text{ species}] \end{aligned} \quad (4.18)$$

$$\text{TF} = [\text{HF}] + [\text{F}^-] + \Sigma[\text{Al-F species}] \quad (4.19)$$

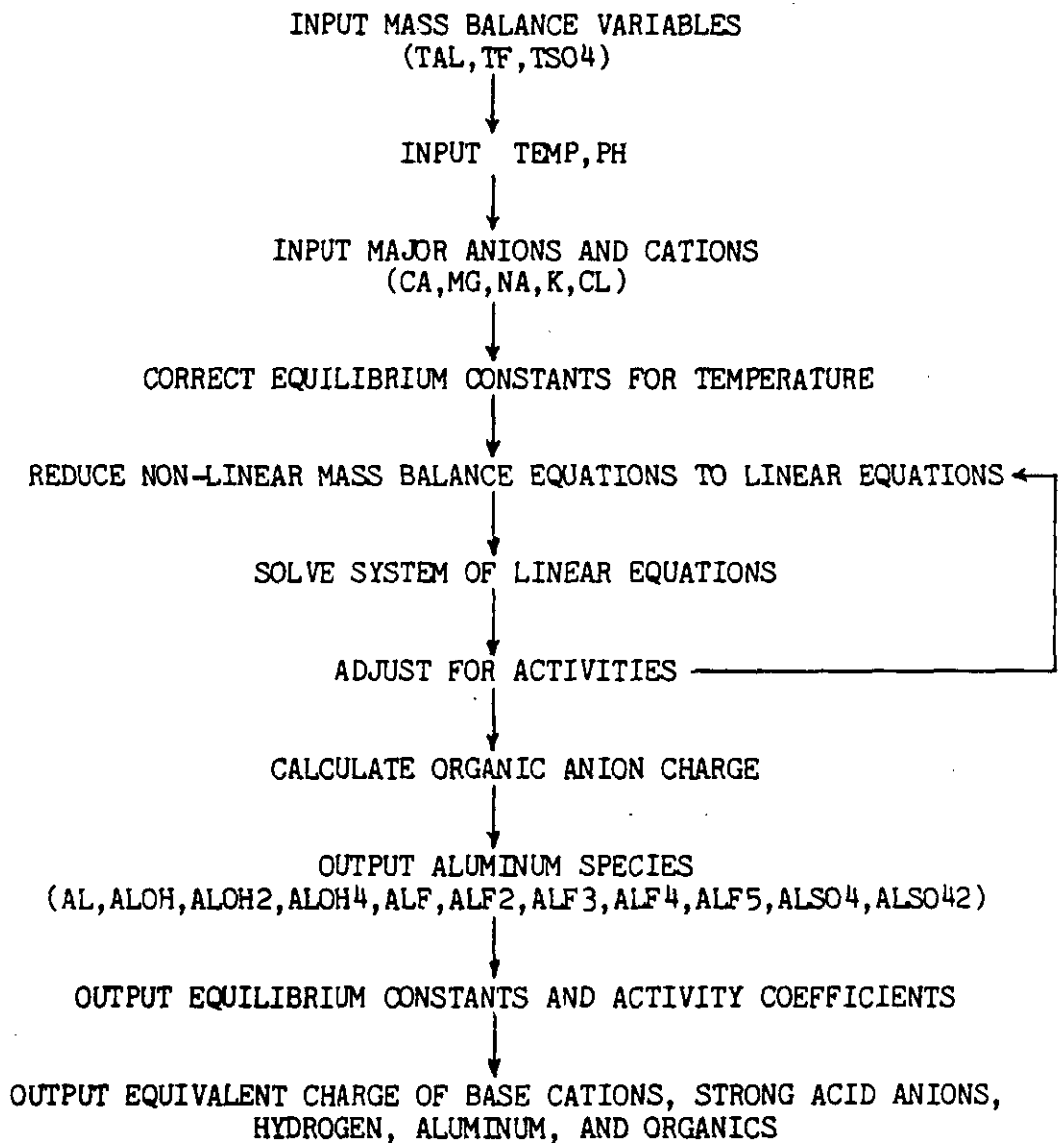
$$\text{TSO}_4 = [\text{SO}_4^{2-}] + \Sigma[\text{Al-SO}_4 \text{ species}] \quad (4.20)$$

These three non-linear equations are solved simultaneously when determining the concentrations of the aluminum species.

Solution Technique

EQUAL calculates various inorganic aluminum species in an aqueous sample knowing the total concentrations of inorganic monomeric aluminum, fluoride, and sulfate. In addition, pH is needed for determining hydroxyl complexes. Inputs of temperature for equilibrium constant corrections and major ions for ionic strength adjustment are also needed. Mass-action equations in Table 4 are substituted into the mass balance equations (4.7-4.9) to give three non-linear equations with three unknowns (i.e., $\{\text{Al}^{3+}\}$, $\{\text{F}^-\}$, and $\{\text{SO}_4^{2-}\}$). These three non-linear equations are reduced to a system of linear equations by using Newton's method and then solved by Gaussian elimination. A flowchart of

Figure 13. Flow Chart for EQUAL



the computer program is presented in Figure 13 with the computer program listing presented in Appendix C.

The solution uses an iterative technique and is started by making an initial guess for each of the three unknowns. Total concentrations of each of the mass balance variables are calculated and checked against their measured input values. If the relative error is not within .01%, the initial guesses are revised and the mass balance equations resolved. Iterations proceed until the error criterion is met. Newton's method converges quadratically and if a reasonable guess is made the solution technique converges within 10 iterations. The method can diverge, thus the initial guess of the three unknown variables is critical. To eliminate problems with divergence, the unknown free species were initially set at half the measured input total element levels.

A subroutine that estimates the organic anion charge is also included in the computer program. The organic anion charge is determined by taking the difference between the positive and negative inorganic charges. Results from this subroutine are utilized in the next chapter.

Transport Simulation Model

The objective of the simulation model is to describe quantitatively streamwater chemistry, particularly the movement of aluminum, during a short-term runoff period. The model is used to gain insight into the various hydrochemical processes occurring within the watershed.

Intensive sampling, for the purpose of obtaining model testing data, as well as general short-term water quality information, was conducted during the first two weeks of May and November, 1985. These time periods also allow for the following assumptions to be made which simplify the model development process and minimize data collection.

1. Conducting the study during periods with no snowpack eliminates the need to simulate snow hydrology. Incorporating snow hydrology into the modeling framework would complicate data gathering and model calibration.
2. During these time periods the atmospheric temperatures are generally cool causing biological activity to be reduced, and thus is ignored.
3. Deciduous trees are bare of leaves during these periods, thus canopy reactions and interception losses would be at a minimum and are ignored.

The aluminum transport model consists of three distinct submodels: a hydrologic submodel, a soil chemistry submodel, and a stream chemistry submodel. The hydrologic and soil chemistry submodels presented below are similar to those used in the Birkenes model (Christophersen et al., 1982). The similarities are that a simple linear reservoir model is used to route flow through the soil compartment and a mobile anion concept is used to drive the soil chemistry submodel. The stream chemistry submodel is like the MAGIC model (Cosby et al., 1985b) in which chemical equilibrium equations are used to determine aluminum, pH, and ANC levels. Conceptually the model can be thought of as a series of

two completely mixed batch reactors consisting of a soil compartment and a streamwater compartment. The model was tested on a segment of the West Wachusett brook, between the confluence of the two upstream branches and a distance of about a kilometer downstream (see map of study area, Figure 2). A physical configuration of the conceptual model for this stream segment is given in Figure 14. Mass transfer within the system is governed by the flow rates through the compartments. The simulation model is driven by the hydrologic submodel, then followed by the chemical submodels. The hydrologic submodel and the soil and stream chemistry submodels are conceptually depicted in Figures 15 and 16, respectively. The current version of the model does not simulate the dashed line pathways.

Hydrologic Submodel

The hydrologic submodel determines the amount of water flowing into and out of each compartment, thus controlling mass transport through the system during each time step. Volumes of water in the compartments are then determined and used to calculate the various chemical constituents in the two chemical submodels. The hydrologic submodel can be used separately or in combination with the soil and stream chemistry submodels.

The following assumptions are used in developing the hydrologic submodel. Evapotranspiration is assumed to be negligible during short-term runoff periods and is ignored. It is also assumed that the soil compartment consist mostly of quickflow (i.e., mainly in contact with

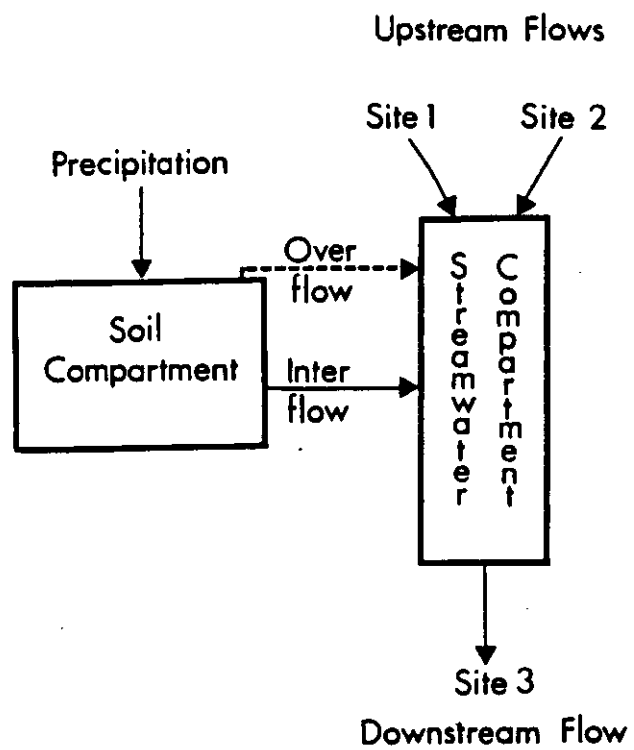


Figure 14. Physical configuration and flowpaths for the transport simulation model.

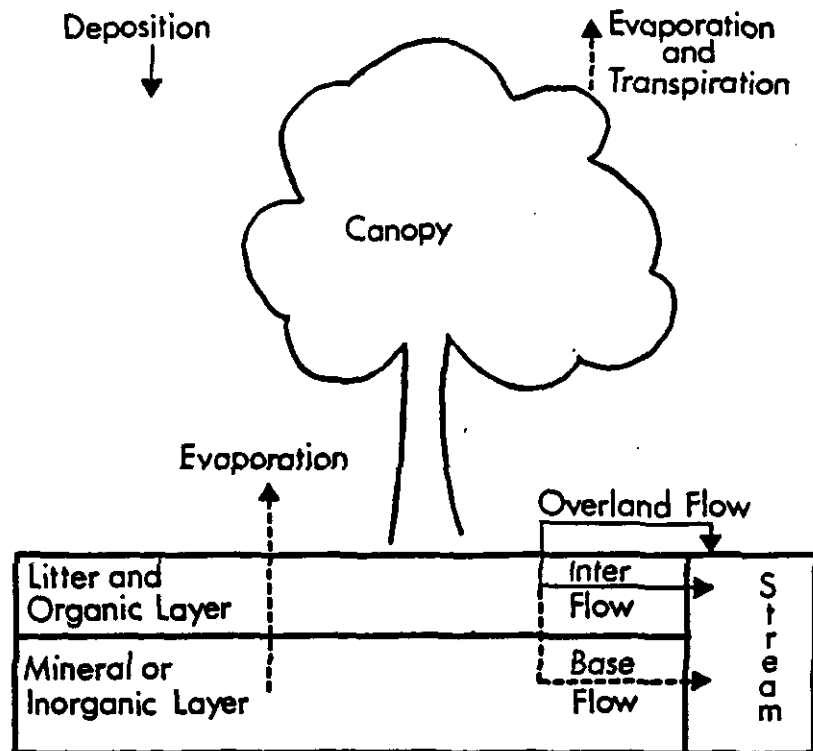


Figure 15. Conceptual depiction of the hydrologic submodel.

Conceptual Diagram of Chemistry Submodels

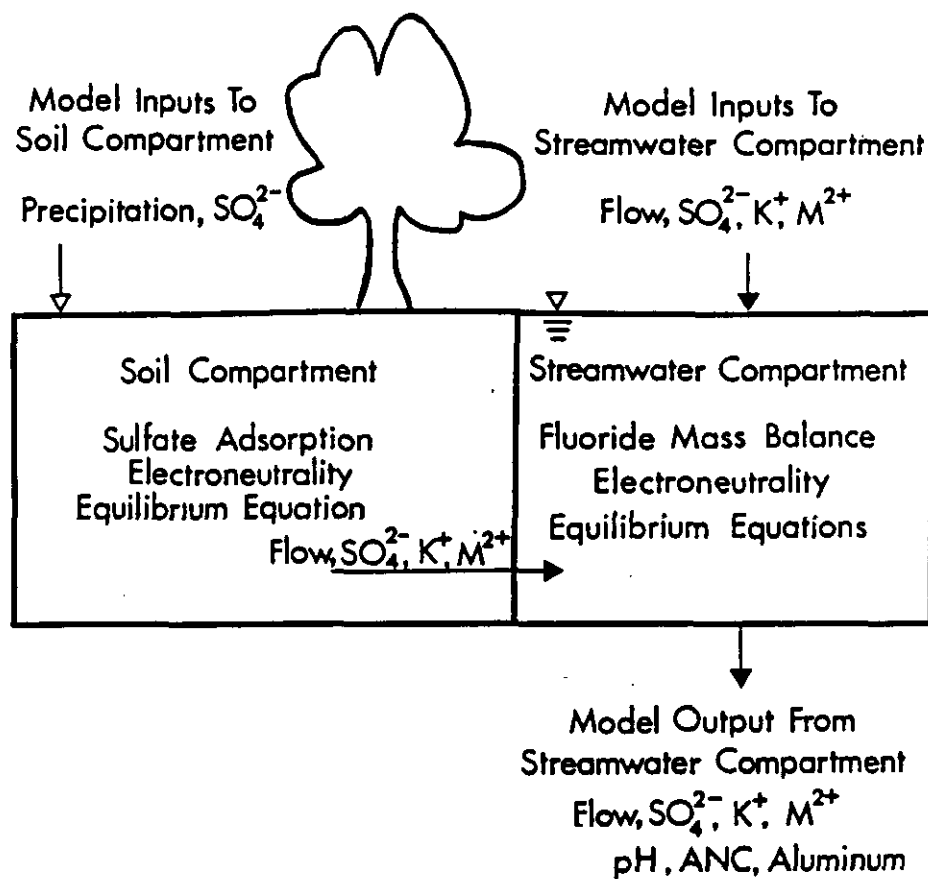


Figure 16. Conceptual depiction of the soil and stream compartment submodels.

the upper soil horizons) during high runoff periods and therefore only one soil compartment is modeled. Lastly, it is assumed that the difference between the two upstream flows and the downstream flow at any particular time-step is due to groundwater input.

Soil Compartment. The soil compartment is modeled as a simple linear reservoir. Precipitation is assumed to infiltrate instantaneously into the soil compartment with overland flow occurring only when the box is full. The precipitation flowrate into the soil compartment is calculated as:

$$Q_p = P \times A \quad (4.21)$$

where:

Q_p = precipitation flowrate, (L^3/T)

P = rainfall intensity, (L/T)

A = drainage basin surface area, (L^2)

The minimum volume in which water does not flow out of the soil compartment is set as the field capacity soil moisture content. By definition, the field capacity of a soil is that amount of water retained after gravitational draining (Linsley et al., 1975). The soil compartment's maximum volume occurs at the saturated soil moisture content. When the soil compartment is full the excess water is routed directly to the stream compartment. The saturated moisture content of a soil is also equal to its porosity. The moisture content at any time in

the soil compartment is the volume of water divided by the total compartment volume.

The soil compartment is modeled as one completely mixed box. Performing a water balance around the soil compartment leads to the following equation,

$$\frac{dV}{dt} = Q_p - L \quad (4.22)$$

where:

V = volume of water in soil compartment, (L^3)

L = lateral flow from soil compartment, (L^3-T^{-1})

t = time, (T)

with accumulation of water in the box equal to the inputs minus the outputs. This equation is applicable when the soil compartment volume is between field capacity and saturated levels. Lateral flow is assumed to follow a first order release rate from zero at field capacity to a maximum at saturation. Hydrograph analysis (Linsley et al., 1975) of data from the West Wachusett Brook shows two separate linear first order portions of the recession curve (see Figure 17). Presumably these represent interflow and base flow. This analysis supports the assumption of modeling interflow as a first order function. The linear release model is:

$$L = R_r \times (V - V_{\min}) \quad (4.23)$$

SEMI-LOG PLOT OF FLOW VS TIME

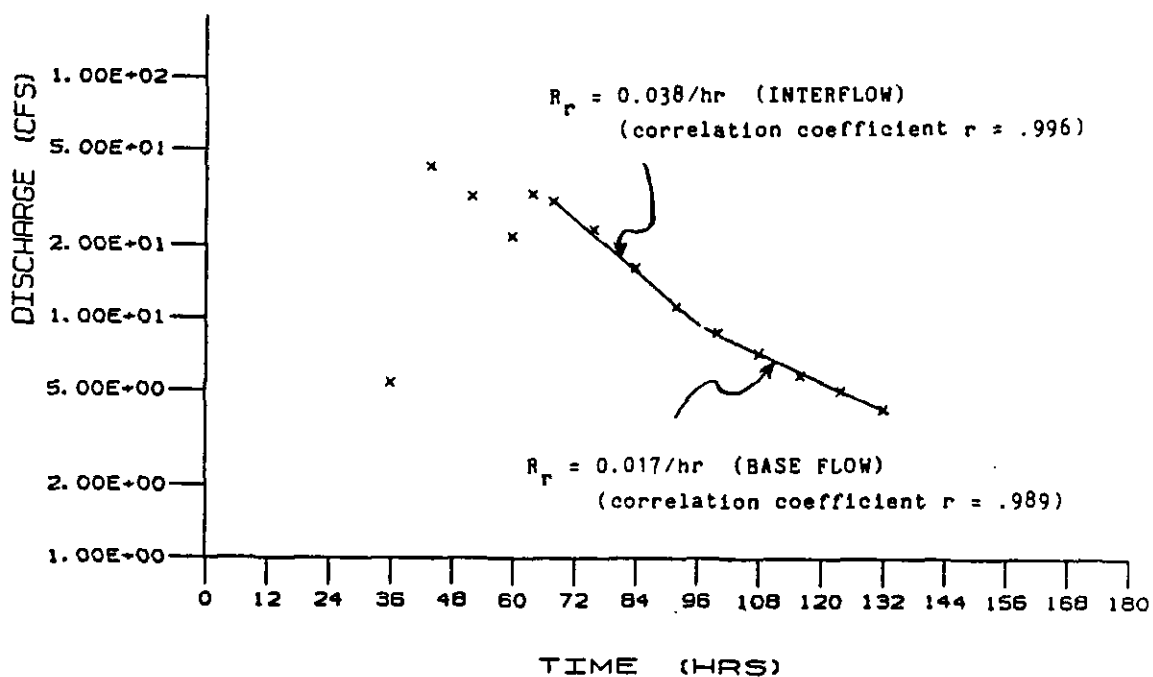


Figure 17. Semi-log plot of streamflow verses time for the November storm. The recession curve has two first order release rates, presumably interflow and base flow.

where:

R_r = release rate from soil compartment, (T^{-1})

V_{min} = volume at field capacity moisture content, (L^3)

Substituting equation (4.23) into equation (4.22) gives,

$$\frac{dV}{dt} = Qp - R_r \times (V - V_{min}) \quad (4.24)$$

which is a linear, first order ordinary differential equation and can be solved quite easily. A fourth order Runge-Kutta numerical solution technique is used to solve this equation with a time step of one hour. Precipitation flowrates (Qp) are assumed constant over the one hour time step, but may vary from time step to time step. The release rate (R_r) and the field capacity volume (V_{min}) are assumed to be constant throughout the entire simulation.

If the soil compartment volume ever falls below the field capacity volume (V_{min}) the lateral flow (L) is set to zero and equation (4.22) resolved. Likewise, if the soil compartment volume ever exceeds the maximum saturated volume, the volume of water in the soil compartment (V) is set at the maximum saturated soil volume. In addition, the volume of water that exceeds the maximum is routed directly into the stream compartment as overflow.

Stream Compartment. The stream compartment is modeled on continuity principles. For assumed steady flows over the one hour time

step, the flow out of the stream compartment is set equal to the total flow of water flowing into the compartment. This is analogous to a completely mixed batch reactor. Direct precipitation to the streamwater compartment is assumed to be negligible since the surface area of the drainage basin is significantly larger than the surface area of the stream. Thus, the downstream flow is equal to the sum of the upstream flows and is represented as:

$$Q_3 = Q_1 + Q_2 + Q_L + Q_j \quad (4.25)$$

where:

$$Q_3 = \text{stream flow at site 3, (L}^3\text{/T)}$$

$$Q_1 = \text{stream flow at site 1, (L}^3\text{/T)}$$

$$Q_2 = \text{stream flow at site 2, (L}^3\text{/T)}$$

$$Q_L = \text{lateral flow from soil compartment, (L}^3\text{/T)}$$

$$Q_j = \text{overflow rate, (L}^3\text{/T)}$$

Since the stream compartment is assumed to be a completely mixed batch reactor, the volume at any time step can be calculated as:

$$V_t = Q_{3,t} \times \Delta t \quad (4.26)$$

where:

V_t = stream volume at time t , (L^3)

$Q_{3,t}$ = stream flow at time t , (L^3-T^{-1})

Δt = time step, (T)

Soil Chemistry Submodel

Soil chemistry has a profound effect on streamwater quality, thus the inclusion of the soil chemistry submodel is crucial in understanding aluminum transport and watershed acidification processes. The objective of this submodel is to simulate the major soil-water ions that contribute to the aluminum transport process. Several simplifying assumptions are invoked to reduce the number of simulated ions in the soil chemical submodel.

1. It is assumed that Na^+ and Cl^- travel through the soil horizons at similar levels and balance each other ionically. In addition, these ions do not influence other ions in solution and thus are ignored.
2. The ions NH_4^+ and NO_3^- are assumed to be negligible because of their low streamwater levels (Hemond and Eshleman, 1984), particularly during non-winter months.
3. The organic anion charge in the soil water is not simulated because of the complexity, but levels are calculated by taking a difference between upstream and downstream concentrations.

4. Fluoride is ignored because of its low concentration.
5. Bicarbonate concentrations are assumed to be controlled by carbon dioxide equilibrium.

These assumptions leave only sulfate as the major mobile anion to be simulated.

Sulfate is the driving force of the soil chemistry submodel and may enter the watershed system by either wet or dry deposition. Since the model is designed for short-term rainfall events it is assumed that wet deposition is significantly greater than dry deposition and, therefore, dry deposition is assumed to be insignificant. A mobile anion concept is used to model sulfate in the soil compartment with adsorption/desorption assumed to control its transport. On a microscale sulfate may actually be involved with precipitation/dissolution reactions but for modeling purposes these two processes (i.e., sorption and solubility) are essentially indistinguishable.

Soil sulfate is modeled by taking a mass balance around the soil compartment. A schematic of the soil sulfate model is presented in Figure 18. The mass balance equation is represented as:

$$\frac{d \text{SO}_4(\text{tot})}{dt} = P \times A \times \text{SO}_4(\text{precip}) - L \times \text{SO}_4(\text{sol}) \quad (4.27)$$

where:

$\text{SO}_4(\text{tot})$ = total sulfate in soil compartment, (M)

Schematic of Soil Sulfate Model

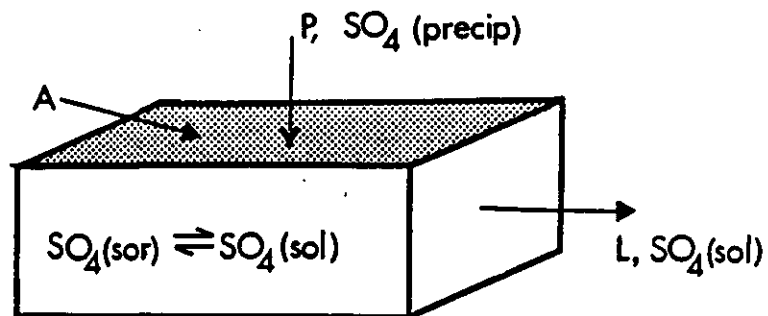


Figure 18. Schematic of soil sulfate model. P is precipitation volume flux (L-T^{-1}), A is drainage area (L^2), $\text{SO}_4(\text{precip})$ is precipitation sulfate concentration (M-L^{-3}), $\text{SO}_4(\text{sol})$ is soil solution sulfate concentration (M-L^{-3}), $\text{SO}_4(\text{sor})$ is soil sorbed sulfate concentration (M-M^{-1}), L is lateral flow ($\text{L}^3\text{-T}^{-1}$).

$SO_4(\text{precip})$ = precipitation sulfate concentration, $(M-L^{-3})$

$SO_4(\text{sol})$ = soil solution sulfate concentration, $(M-L^{-3})$

The total sulfate in the soil compartment is the sum of the solution and the sorbed phases.

$$SO_4(\text{tot}) = SO_4(\text{sol}) \times BDEN \times V_T + SO_4(\text{sol}) \times MOIST \times V_T \quad (4.28)$$

where:

$BDEN$ = soil bulk density, (M/L^3)

$MOIST$ = soil moisture content = V/V_T

$SO_4(\text{sol})$ = solid phase sorbed sulfate, (M/M)

For small changes in soil sulfate concentrations it is assumed that a linear portion of the adsorption isotherm controls the soil solution sulfate concentration, thus the following equation holds.

$$SO_4(\text{sol}) = Kp \times SO_4(\text{sol}) \quad (4.29)$$

where:

Kp = partitioning coefficient, $(M/M)/(M/L^3)$

Substituting equation (4.29) into equation (4.28) and rearranging gives the following equation:

$$SO_{4(sol)} = SO_{4(tot)} + (V_T \times (K_p \times BDEN + MOIST)) \quad (4.30)$$

Finally, substituting equation (4.30) back into the mass balance equation (4.27) gives a linear, first order ordinary differential equation in terms of total sulfate:

$$\frac{dSO_{4(tot)}}{dt} + LxSO_{4(tot)} / (V_T \times (K_p \times BDEN + MOIST)) = PxAxSO_{4(precip)} \quad (4.31)$$

The watershed's soil properties of bulk density (BDEN), drainage basin area (A), compartment depth (D), and sulfate partitioning coefficient (Kp) are assumed as constant parameters through out the entire simulation. During each time step lateral flow (L), soil moisture content (MOIST), rainfall intensity (P), and precipitation sulfate concentration ($SO_{4(precip)}$) are assumed to be constant.

Equation (4.31) is solved by a fourth order Runge-Kutta numerical technique. Once the total sulfate in the compartment is known, the solution and sorbed sulfate concentrations can be determined by using equations (4.30) and (4.29), respectively.

By simulating sulfate, setting the organic anion concentration, and assuming that the bicarbonate anion is determined by carbon dioxide equilibrium, the major anionic charges in the soil water are known. The major cations K^+ , Ca^{2+} , Mg^{2+} , and Al^{3+} are assumed to ionically balance these anions. The cations are determined by solving a set of equilibrium equations describing the soil processes and by using

electroneutrality as a constraint. Furthermore, to simplify the modeling effort it is assumed that the divalent cations calcium and magnesium behave similarly (e.g., both are involved in cation exchange and weathering reactions within the soil horizons) and thus are added together as M^{2+} . All cations are modeled with cation exchange reactions. It is assumed that aluminum exchanges with the divalent cations and the divalent cations exchanges with potassium as presented below.



where:

Al^{3+} , M^{2+} , and K^+ = soil solution cations

AlX_3 , MX_2 , and KX = solid phase adsorbed cations

Sodium was assumed to be in balance with chlorine and was ignored. Iron concentrations were low and therefore it was also ignored. The above cation exchange reactions are modeled using the Gaines-Thomas selectivity coefficient expression (Gaines and Thomas, 1953) with their equations presented in Table 5. The exchangeable fractions of these cations, i.e., the equivalence of each cation to the total cation

Table 5

Equations Used In Soil Chemistry Submodel

Charge Balance

$$\frac{\{H^+\}}{f_1} + \frac{\{K^+\}}{f_1} + 2\frac{\{M^{2+}\}}{f_2} + 3\frac{\{Al^{3+}\}}{f_3} - \frac{\{HCO_3^-\}}{f_1} = 2[SO_4^{2-}] + [Org^-]$$

Gibbsite Solubility

$$\frac{\{Al^{3+}\}}{\{H^+\}^3} = K_{SO}$$

Cation Exchange Reactions

$$\frac{\{K^+\}^2}{\{M^{2+}\}} = S_{KM} \frac{E_K^2}{E_M}$$

$$\frac{\{M^{2+}\}^3}{\{Al^{3+}\}^2} = S_{MAL} \frac{E_M^3}{E_{AL}^2}$$

Carbon Dioxide Equilibrium

$$\{H^+\}\{HCO_3^-\} = K_1 K_{H^+} P_{CO_2}$$

exchange capacity, is represented by E_i in Table 5 (where the subscript i represents the exchangeable cation). It is assumed that the exchangeable fractions are constant during the short-term (i.e., less than seven days) simulation runs. The sum of the exchangeable fractions must equal 1.0, with the percent base saturation equal to the sum of the exchangeable base cation fractions. The selectivity coefficients are also assumed constant during the short-term simulations.

Mineral phase solubility with gibbsite ($\text{Al}(\text{OH})_3$) is assumed to control aluminum in the soil horizons and is represented as:



The mass-action equilibrium equation for this reaction is presented in Table 5, where K_{so} is the solubility constant for this reaction.

Inorganic aluminum complexes are assumed to be insignificant with respect to the charge balance because soil pH levels are typically quite low (<4.5), and thus are ignored.

The dissolution of CO_2 and its subsequent dissociation to bicarbonate is assumed to control inorganic carbon in the soil water. Utilizing Henry's law constant and Dalton's law of partial pressure, aqueous carbon dioxide can be determined as:



where Henry's law constant (K_H) and the partial pressure of carbon dioxide (P_{CO_2}) is assumed to be constant throughout the entire simulation. Assuming that $CO_2(aq)$ is equal to $H_2CO_3^*$, the first dissociation reaction is:



The mass-action equilibrium expression for inorganic carbon in Table 5 can be determined by combining equations (4.35) and (4.36).

Lastly, positive and negative charges in the soil water must be ionically balanced. Thus, given the previous assumptions that Na and Cl are balanced, and that NH_4 , Fe, and NO_3 have low concentrations, the electroneutrality constraint for the soil chemistry submodel is:

$$[H^+] + [K^+] + 2[M^{2+}] + 3[Al^{3+}] = 2[SO_4^{2-}] + [HCO_3^-] + [ORG^-] \quad (4.37)$$

where the major cations on the left hand side balance the major anions on the right hand side.

Sequentially, the soil chemistry submodel determines the major cations and anions in the soil water by first calculating the soil solution sulfate concentration. Since the organic anion charge is set for each particular time step the mathematics reduce to five non-linear

equations and five unknowns. Substituting the chemical equilibrium equations (Table 5) into the charge balance equation (4.37) further reduces the problem to one non-linear equation and one unknown. This equation is then solved by Newton-Raphson's numerical technique for finding roots of a non-linear equation. It is assumed that the kinetics of the reactions in the soil chemistry submodel are faster than the hydrologic time step. This assumption seems reasonable since only fast reactions are considered (e.g., cation exchange adsorption/desorption, and equilibrium solubility).

In summary, the overall sequence of the soil chemical submodel is to first determine the solution sulfate concentration and, after setting the organic anion charge and the carbon dioxide partial pressure, determine the cations by utilizing equilibrium and electroneutrality relationships.

Stream Chemistry Submodel

The streamwater compartment for the West Wachusett brook has inputs from two upstream sources as well as the soil compartment. Input variables to the streamwater compartment consist of the base cations K^+ and M^{2+} , and the strong acid anion SO_4^{2-} , all of which are assumed to be conservative constituents. The concentrations of these conservative streamwater compartment ions are determined by the principle of conservation of mass as:

$$Q_3 \times \text{VAR}_{3,i} = Q_1 \times \text{VAR}_{1,i} + Q_2 \times \text{VAR}_{2,i} + L \times \text{VAR}_{L,i} \quad (4.38)$$

where Q_1 , Q_2 , Q_3 , and L are the flow rates at the stream sites 1, 2, 3, and the groundwater contribution, respectively (see Figure 2 for site locations). $\text{VAR}_{j,i}$ represents the conservative elements K^+ ($i=1$), M^{2+} ($i=2$), and SO_4^{2-} ($i=3$) from the various contributing sources (represented by subscript j). Thus, the mass of each of the conservative constituents at the downstream site is equal to the sum of their masses from the upstream sources. Direct atmospheric inputs to the stream segment are assumed insignificant.

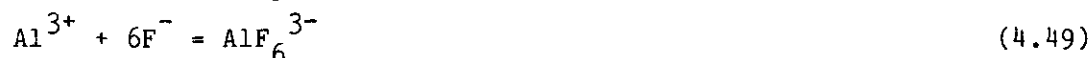
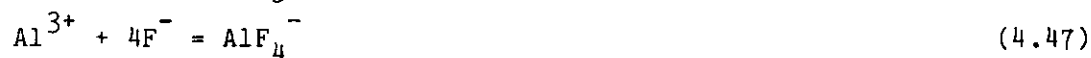
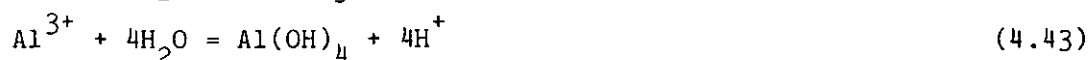
In addition to the conservative elements mentioned above, total fluoride and DOC are direct inputs to the streamwater compartment. These elements are not simulated because of their complexity, but are set at the downstream site's measured values. The inclusion of these two variables in the streamwater compartment is necessary because of their importance in regard to the fate of aluminum through complexation reactions as well as the charge balance.

Aluminum is assumed to be regulated by solubility equilibrium with the solid phase aluminum trihydroxide ($\text{Al}(\text{OH})_3$). The governing reaction,



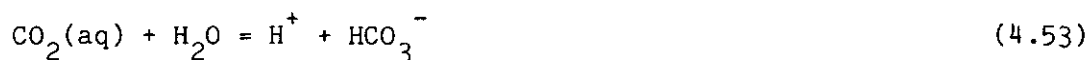
is assumed to be instantaneous and reversible with the mass-action equilibrium equation for this reaction presented in Table 6.

In order to characterize quantitatively the movement of aluminum and therefore assess its toxicity, speciation must be considered. The various forms of aluminum in the model are determined by the chemical equilibrium relationships described earlier in this chapter. Aluminum hydrolysis as well as complexation reactions with SO_4^{2-} , F^- , and organic anions are considered. The inorganic aluminum complexation reactions included in the model are:



with their mass-action equilibrium equations summarized in Table 6. Thermodynamic constants for these reactions are temperature dependent, with corrections made by equation (4.14).

It is also assumed that the streamwater is in equilibrium with atmospheric carbon dioxide. Thus, inorganic carbon is regulated by the dissolution of CO_2 and the subsequent dissociation to bicarbonate and carbonate anions:



The equilibrium expressions of these reactions are also in Table 6.

The organic anion charge is modeled empirically by regressing the organic anion on DOC. The organic anion charge is assumed to be the difference between positive and negative inorganic charges and is estimated by EQUAL. The regression equation for the November data at site 3, the downstream site, is:

$$Y = 7.05X + .83 \quad (4.55)$$

Table 6

Equations Used In Stream Chemistry Submodel

Equilibrium Equations

$$\frac{\{\text{AlOH}^{2+}\}\{\text{H}^+\}}{\{\text{Al}^{3+}\}} = K_{1\text{OH}}$$

$$\frac{\{\text{Al}(\text{OH})_2^+\}\{\text{H}^+\}^2}{\{\text{Al}^{3+}\}} = K_{2\text{OH}}$$

$$\frac{\{\text{Al}(\text{OH})_3(\text{aq})\}\{\text{H}^+\}^3}{\{\text{Al}^{3+}\}} = K_{3\text{OH}}$$

$$\frac{\{\text{Al}(\text{OH})_4^-\}\{\text{H}^+\}^4}{\{\text{Al}^{3+}\}} = K_{4\text{OH}}$$

$$\frac{\{\text{AlSO}_4^+\}}{\{\text{Al}^{3+}\}f_2[\text{SO}_4^{2-}]} = K_{1\text{SO}_4}$$

$$\frac{\{\text{Al}(\text{SO}_4)_2^-\}}{\{\text{Al}^{3+}\}f_2^2[\text{SO}_4^{2-}]^2} = K_{2\text{SO}_4}$$

$$\frac{\{\text{AlF}^{2+}\}}{\{\text{Al}^{3+}\}\{\text{F}^-\}} = K_{1\text{F}}$$

$$\frac{\{\text{AlF}_2^+\}}{\{\text{Al}^{3+}\}\{\text{F}^-\}^2} = K_{2\text{F}}$$

$$\frac{\{\text{AlF}_3\}}{\{\text{Al}^{3+}\}\{\text{F}^-\}^3} = K_{3\text{F}}$$

$$\frac{\{\text{AlF}_4^-\}}{\{\text{Al}^{3+}\}\{\text{F}^-\}^4} = K_{4\text{F}}$$

$$\frac{\{\text{AlF}_5^{2-}\}}{\{\text{Al}^{3+}\}\{\text{F}^-\}^5} = K_{5\text{F}}$$

$$\frac{\{\text{AlF}_6^{3-}\}}{\{\text{Al}^{3+}\}\{\text{F}^-\}^6} = K_{6\text{F}}$$

Table 6 (continued)

Equilibrium Equations

$$\frac{\{H^+\}\{HCO_3^-\}}{\{H_2CO_3^*\}} = K_1$$

$$\frac{\{H^+\}\{F^-\}}{\{HF\}} = K_{HF}$$

$$\frac{\{H^+\}\{CO_3^{2-}\}}{\{HCO_3^-\}} = K_2$$

$$\{H^+\}\{OH^-\} = K_w$$

$$\{H_2CO_3^*\} = K_H P_{CO_2}$$

Gibbsite Solubility

$$\frac{\{Al^{3+}\}}{\{H^+\}^3} = K_{so}$$

Fluoride Mass Balance

$$TF = \frac{\{HF\}}{f_0} + \frac{\{F^-\}}{f_1} + \frac{\{AlF^{2+}\}}{f_2} + 2\frac{\{AlF_2^+\}}{f_1} + 3\frac{\{AlF_3\}}{f_0} + 4\frac{\{AlF_4^-\}}{f_1} + 5\frac{\{AlF_5^{2-}\}}{f_2} + 6\frac{\{AlF_6^{3-}\}}{f_3}$$

Table 6 (continued)

Electroneutrality

$$\begin{aligned}
 & \frac{\{H^+\}}{f_1} + [K^+] + 2[M^{2+}] + 3\frac{\{Al^{3+}\}}{f_3} + 2\frac{\{Al(OH)^{2+}\}}{f_2} + \frac{\{Al(OH)_2^+\}}{f_1} + 2\frac{\{AlF^{2+}\}}{f_2} \\
 & + \frac{\{AlF_2^+\}}{f_1} + \frac{\{AlSO_4^+\}}{f_1} = 2[SO_4^{2-}] + \frac{\{HCO_3^-\}}{f_1} + 2\frac{\{CO_3^{2-}\}}{f_2} + \frac{\{Al(OH)_4^-\}}{f_1} \\
 & + \frac{\{AlF_4^-\}}{f_1} + 2\frac{\{AlF_5^{2-}\}}{f_2} + 3\frac{\{AlF_6^{3-}\}}{f_3} + \frac{\{F^-\}}{f_1} + \frac{\{Al(SO_4)_2^-\}}{f_1} + \frac{\{OH^-\}}{f_1} + [Org^-]
 \end{aligned}$$

where:

Y = organic anion ($\mu\text{eq/L}$)

X = DOC (mg/L)

(n = 95, correlation coefficient r = .73)

The slope of the regression line is an estimate of the amount of organic negative charge per mass of DOC.

An independent study from the West Wachusett brook watershed (Eshleman and Hemond, 1985), using a titration analysis technique, showed surface and groundwater samples to have approximately 7.5 μeq of carboxylic groups per mg of DOC. This corresponds quite well with the regression analysis.

The equilibrium equations (4.39-4.54) are constrained by electroneutrality as well as by conservation of mass with fluoride. These two constraining equations are presented in Table 6 and summarized as:

$$\Sigma \text{ positive charges} = \Sigma \text{ negative charges} \quad (4.56)$$

$$\text{TF} = [\text{F}^-] + [\text{HF}] + \Sigma[\text{Al-F species}] \quad (4.57)$$

The solution sequence of the streamwater chemical submodel is to first determine the concentrations of the base cations K^+ and M^{2+} , and the acid anion SO_4^{2-} by conservation of mass principles. Substituting the equilibrium equations into the fluoride mass balance and the charge

balance equations (Table 6) gives two non-linear equations and two unknowns (i.e., $\{H^+\}$ and $\{F^-\}$). These two non-linear equations are reduced to a linear form using Newton's method, and then solved by Gaussian elimination. This solution technique is an iterative process with the initial guess of the unknowns critical for the solution to converge.

Once all the above mentioned variables are solved, the following state variables can be determined:

$$pH = -\log\{H^+\} \quad (4.58)$$

$$ANC = [OH^-] + [Al(OH)^{2+}] + 2[Al(OH)_2^+] + 3[Al(OH)_3] \\ + 4[Al(OH)_4^-] - [H^+] \quad (4.59)$$

$$\text{inorganic Al} = [Al^{3+}] + \Sigma[Al-OH] \text{ complexes} + \Sigma[Al-F] \text{ complexes} \\ + \Sigma[Al-SO_4] \text{ complexes} \quad (4.60)$$

$$\text{organic Al} = K_{PDOC} \times DOC^n \times Al_{in}^m \quad (4.61)$$

$$Al_{tot} = Al_{in} + Al_{org} \quad (4.62)$$

The model for organically bound aluminum is an empirical formulation that relates organic aluminum to inorganic aluminum and DOC. This model is semi-analogous to sorption partitioning isotherm analysis. One can determine the coefficient in equation (4.61) by taking the logarithm of both sides and regressing:

$$\log Al_{org} = \log K_{PDOC} + n \log DOC + m \log Al_{in} \quad (4.63)$$

Regressing the November data for site 3 gave the following coefficients.

$$K_{PDOC} = 23.46$$

$$n = 1.08 \quad (\text{student } t = 12.2)$$

$$m = 0.02 \quad (\text{student } t = 0.62)$$

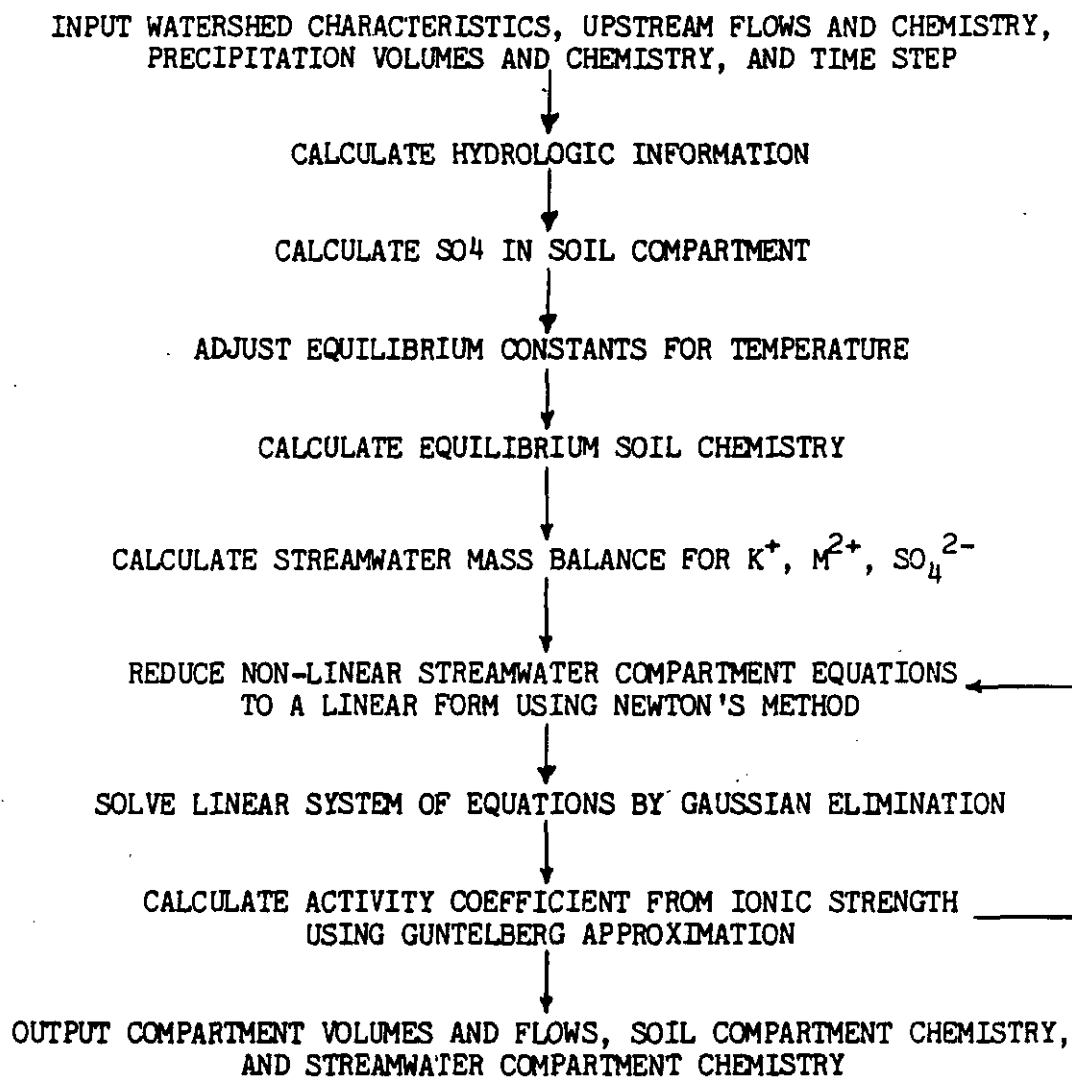
It can be seen from the regression results that organically bound aluminum depends mostly on the DOC level.

Summary of Simulation Model

The simulation model is first driven by the hydrologic submodel, then followed by the soil and stream chemistry submodels. Inputs to the hydrologic submodel are precipitation in the soil compartment and the two upstream flows in the stream compartment. A simple linear reservoir model is used to route flow through the soil compartment with continuity principals controlling flow in the stream compartment. Once flows into and out of each compartment are known for each time step, compartment volumes can be determined. These flows and volumes are used in the chemistry submodels to calculate chemical compositions. The overall sequence of the soil chemistry submodel is to first determine the solution sulfate concentration, and after setting the organic anion charge and the carbon dioxide partial pressure, determine the cations by utilizing equilibrium and electroneutrality relationships. The solution

sequence of the stream chemistry submodel is to first determine the concentrations of the base cations K^+ and M^{2+} , and the acid anion SO_4^{2-} by conservation of mass principals. Once these conservative constituents are known, and after setting the total fluoride and DOC concentrations to the downstream site's measured values, the various ions are determined using equilibrium, mass balance, and charge balance equations. A flow chart of the computer program for this model is presented in Figure 19 with the program listing presented in Appendix D.

Figure 19. Flow Chart for Simulation Model



CHAPTER V
RESULTS AND DISCUSSION

This chapter addresses spatial and temporal changes in streamwater chemistry for the West Wachusett Brook catchment. Seasonal trends as well as episodic events will be discussed. Because of its importance to streamwater quality, a soil survey will also be presented. Lastly, the simulation modeling results will be presented with a discussion of the important aluminum transport processes. Raw data for this study can be found in Appendix E.

Seasonal Streamwater Chemistry

Studying one-year seasonal trends of streamwater quality is important because it may reveal the most critical times of the year for streamwater toxicity. Long-term monitoring may also lend insight into the various mechanisms that control aluminum transport and streamwater acidification on a seasonal basis. For example, winter may have a different streamwater response to runoff as compared to summer conditions. Thus, the following section discusses spatial and temporal seasonal trends for the West Wachusett Brook, Massachusetts.

Three stream sites were sampled on a monthly basis from March 1985 to January 1986 in this small Massachusetts catchment. The locations of these sampling sites are presented in Figure 2 (see Chapter I). The stream contributing to site 1 originates from Mt. Wachusett and is

characterized as being steeply sloped with a shallow bedrock. This site from now on will be called the "mountain stream". The stream contributing to sampling site 2 originates from a smaller peak, but passes through a wetland before combining with the mountain stream. Site 2 will be known as the "wetland stream". Approximately one kilometer downstream from the confluence of the mountain and wetland streams is the monitoring site 3. This site will be referred to as the "downstream" site. The downstream site exhibits streamwater quality after the two upstreams have mixed.

Stream flows, measured at each of the three sites during the monthly grab survey, are presented in Figure 20. Flows during the winter months were not measured because of ice cover. Stream flows are generally higher in the spring and fall with their lowest levels occurring during the summer months. During low-flow periods the mountain and wetland streams are approximately the same in magnitude and together make up about 85% of the the downstream flow.

Streamwater temperatures vary from approximately zero degrees Centigrade during the winter months to a maximum of around 20 degrees Centigrade in August (Figure 21). Transitional periods occur during April and October.

pH is generally used as the master variable for assessing overall streamwater quality (Stumm and Morgan, 1981). Seasonal pH levels for the three stream sites are presented in Figure 22. These results show that the wetland stream has a relatively constant pH of around 5.2 throughout the year, whereas the mountain stream and downstream sites

STREAM FLOW

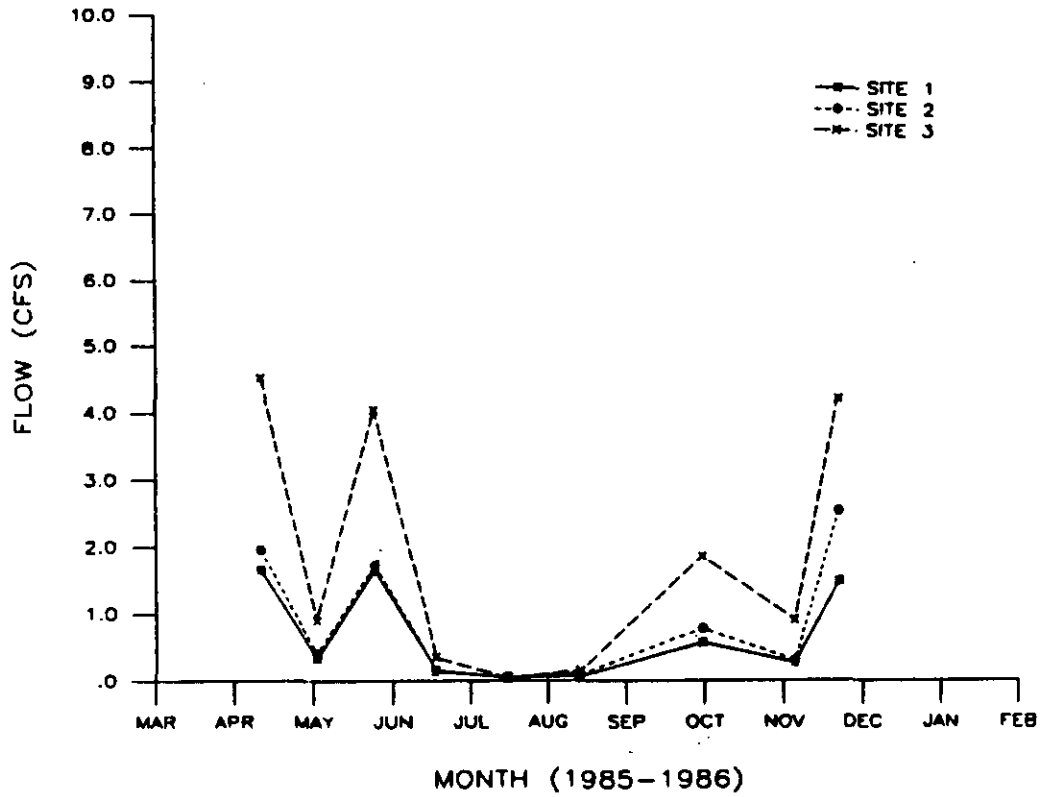


Figure 20. Stream flows, in cubic feet per second (cfs), for site 1 the mountain stream site, site 2 the wetland stream site, and site 3 the downstream site, measured at the time of data collection.

STREAMWATER TEMPERATURE

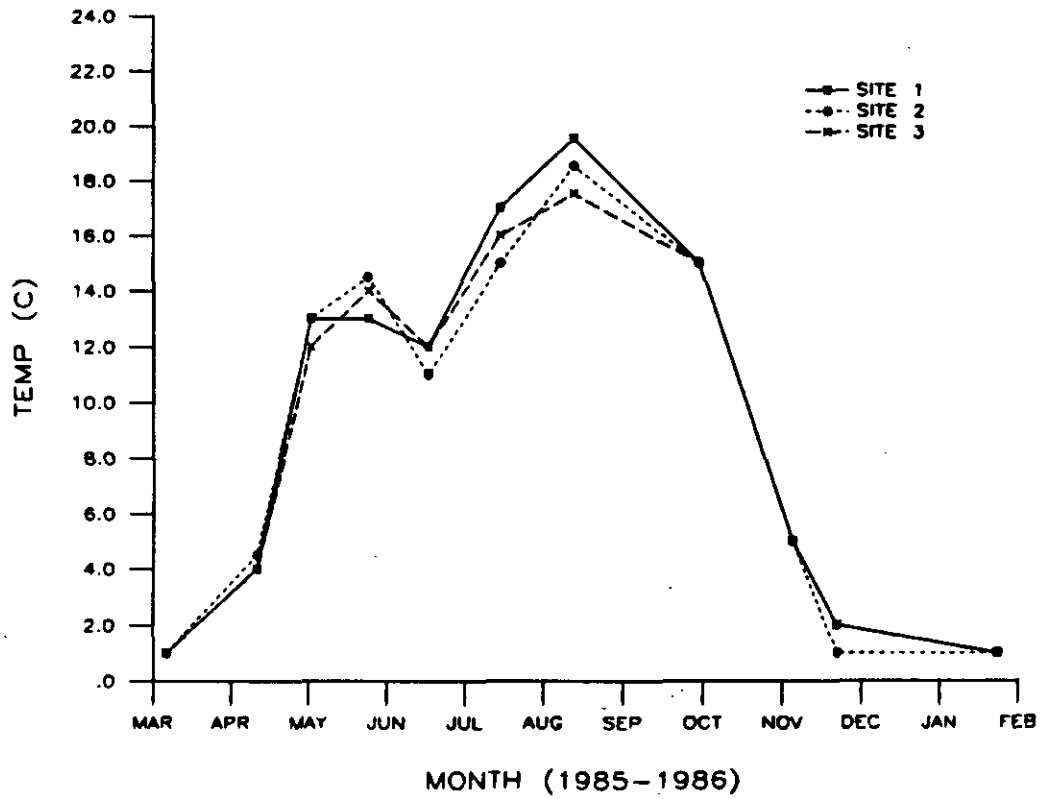


Figure 21. Streamwater temperatures, in degrees Centigrade, for site 1 the mountain stream site, site 2 the wetland stream site, and site 3 the downstream site.

STREAMWATER PH VALUES

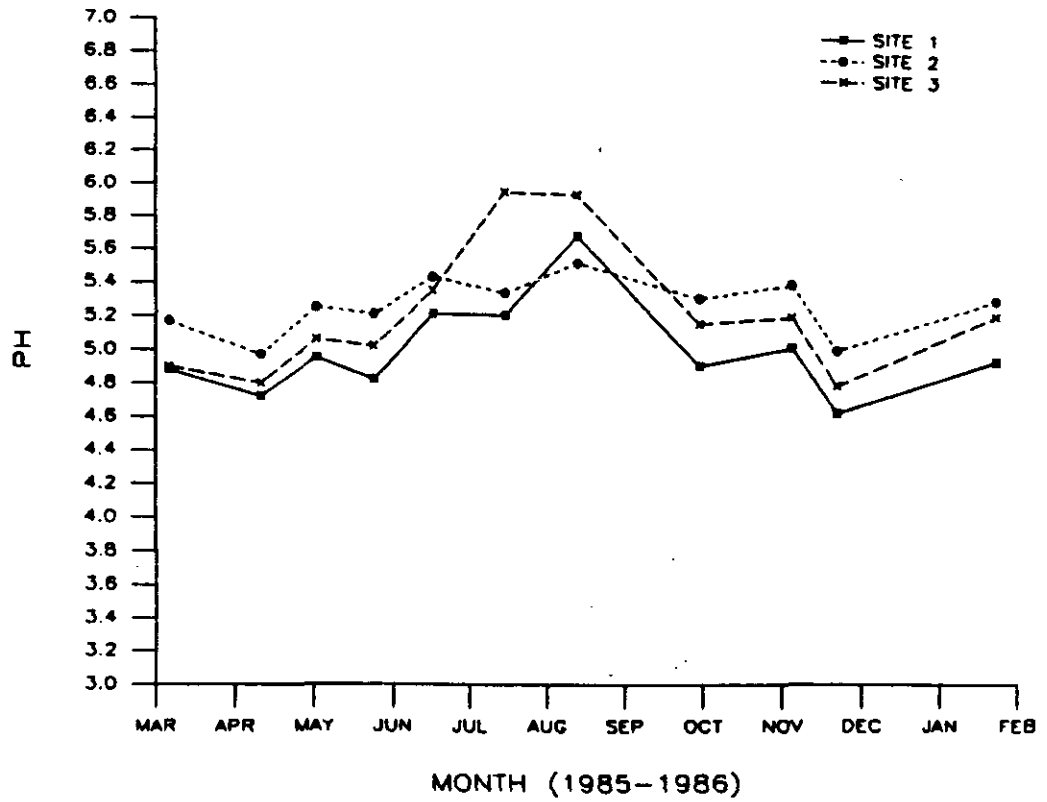


Figure 22. Streamwater pH values, for site 1 the mountain stream site, site 2 the wetland stream site, and site 3 the downstream site.

vary significantly, with pH's ranging from 4.6 to 5.6 and 4.8 to 5.9 respectively. Higher pH levels during the low-flow summer months could be due to the predominance of groundwater as compared to overland flow, and the fact that it would have a longer contact time with the soil and bedrock. Johnson et al. (1981) reported this phenomenon in which a decrease in down stream acidity along a small New England stream was thought to be due to an increase in contact time with the silicate minerals in the soil horizons. In addition, these higher pH levels in the wetland stream could be caused by biological activity generating alkalinity. Eshleman (1985) concluded that the wetlands' most significant acid-base role in the Bickford Pond watershed, of which the West Wachusett Brook is a part, is the generation of alkalinity by sulfate and nitrate reduction and the subsequent production of organic acids.

Another important constituent in assessing streamwater acidification is acid neutralizing capacity (ANC). The greater the ANC the better the system is at buffering changes in pH. Typically the ANC or alkalinity of low ionic strength systems, like the West Wachusett Brook, consists primarily of aluminum and organic acids. Driscoll (1980) found this to be true in Adirondack surface waters. Bloom et al. (1979) also concluded that the hydrolysis of organically bound aluminum over the pH range of 4.0 to 5.0 is a major source of buffering capacity. As seen in Figure 23 the ANC of the mountain stream never exceeds zero and becomes quite negative during high runoff periods. The wetland stream and the downstream sites have positive values for ANC during the

STREAMWATER ACID NEUTRALIZING CAPACITY

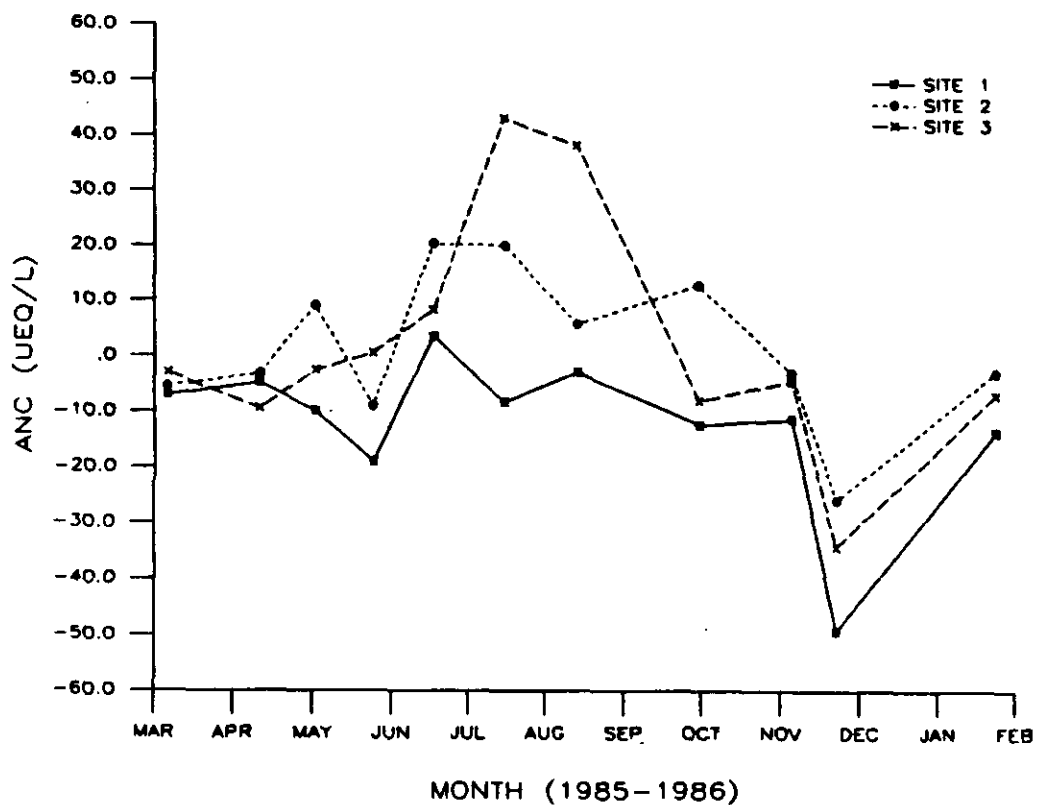


Figure 23. Streamwater acid neutralizing capacity (ANC) levels, in micro-equivalents per liter, for site 1 the mountain stream site, site 2 the wetland stream site, and site 3 the downstream site.

summer months, but remain negative during the rest of the year. As with pH, the increase in ANC during the summer months is probably attributed to longer contact times with the soil environment, as well as alkalinity generated from biological activity. Even during the summer months the ANC of this stream is quite low, making this an acid-sensitive stream. Organic acids in the wetland stream appear to buffer and regulate its quality.

Organic compounds in streamwaters are also important in terms of aluminum transport, as aluminum forms strong complexes with natural organic substances (Hem, 1968). Dissolved organic carbon (DOC) is typically used as a surrogate parameter for assessing the effects of organic substances in natural water systems. Figure 24 presents the DOC concentrations for the three sampling sites. The mountain stream's DOC levels remain relatively low and constant throughout the year whereas that for the wetland stream is quite variable, especially during high runoff periods. Eshleman and Hemond (1985) believe that the source of DOC in the Bickford Pond watershed is largely derived from the canopy, the organic soil horizons, and the stream channel wetlands. The extremely high DOC values recorded in the fall are probably attributed to a washout of the summer's biological activity. The production of organic acids in the organic soil horizons represents a significant acid source (Eshleman and Hemond, 1985).

Electroneutrality is another important consideration when assessing aluminum mobility and acidification in a streamwater system. Simply stated, electroneutrality means that the positive charges equal the

negative charges in an aquatic solution. The charge balance of an aquatic solution lends insight into the importance of acid and base cations. In particular, the ratio of base cations to strong acid anions is important in controlling aluminum transport. If the base cations do not balance the strong acid anions the difference must be made up with acid cations like aluminum and hydrogen ion. Electroneutrality for the three sampling sites is plotted in Figures 25-27, with the imbalance of negative charge assumed to represent the organic anion contribution.

For the mountain stream (Figure 25) the base cations equal or exceed the strong acid anions during the summer months and in turn the aluminum fraction is small. In contrast, during the high runoff periods the strong acid anions exceed the base cations, and thus the aluminum fraction increases. Strong acid anions, in particular SO_4^{2-} , decrease during the summer months whereas the base cations generally increase. This reduction in sulfate could be attributed to biological uptake or sulfate reduction in the soils. The increase in base cations could be due to increased weathering because of longer contact times in the soil environment.

The base cations always exceeded the strong acid anions in the wetland stream (Figure 26), and thus the aluminum fraction remains quite small. Both the strong acid anions and the base cations generally decrease during the summer months whereas the organic anion contribution increases. Furthermore, the overall ion level is greater in the wetland than in the mountain stream. This is presumably due to the increase of biological activity in the wetland.

STREAMWATER DOC CONCENTRATIONS

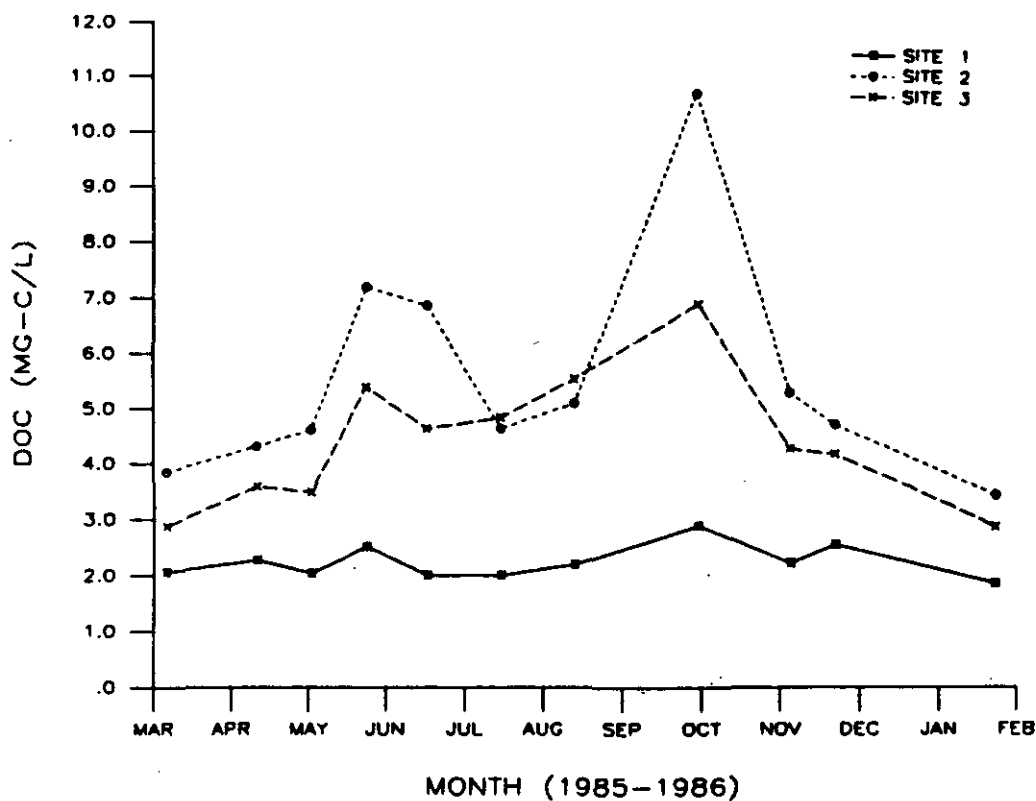


Figure 24. Streamwater dissolved organic carbon (DOC) concentrations, in milligrams per liter, for site 1 the mountain stream site, site 2 the wetland stream site, and site 3 the downstream site.

ELECTRONEUTRALITY FOR SITE 1

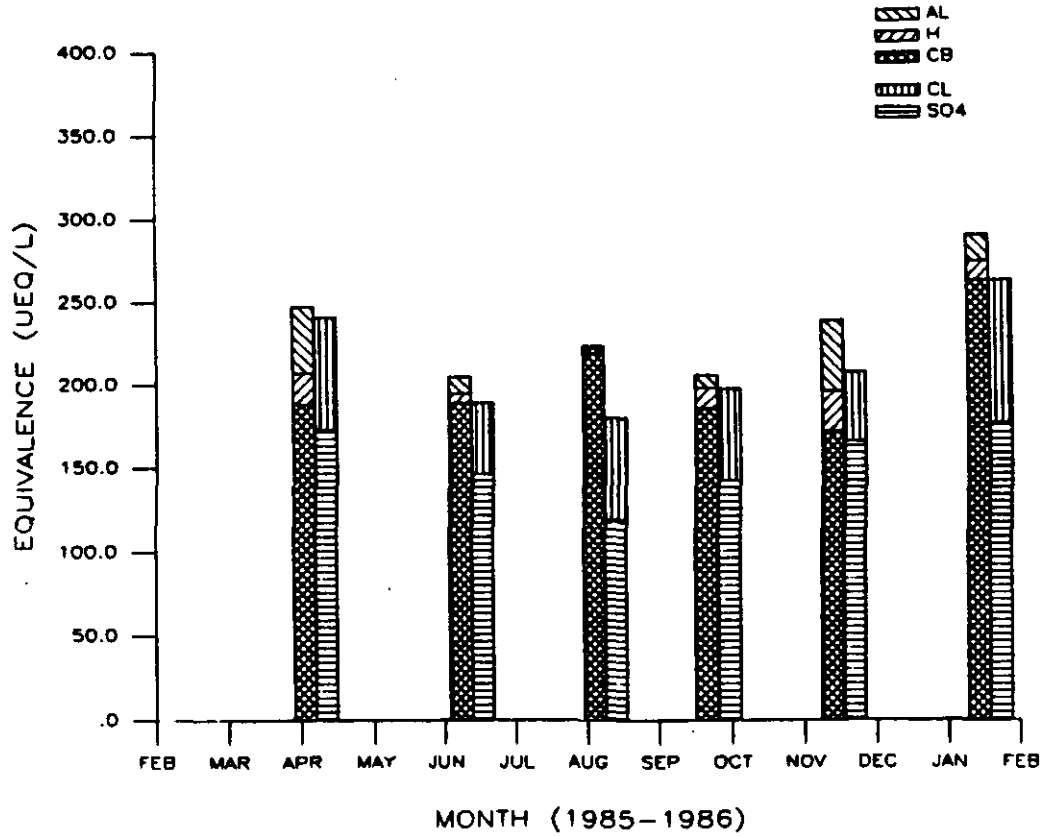


Figure 25. Electroneutrality plot for site 1 the mountain stream site. AL equals the total inorganic monomeric aluminum equivalence charge, H equals the hydrogen ion equivalence charge, CB equals the base cations (Ca, Mg, Na, K) equivalence charge, CL equals the chloride ion equivalence charge, SO₄ equals the sulfate ion equivalence charge.

ELECTRONEUTRALITY FOR SITE 2

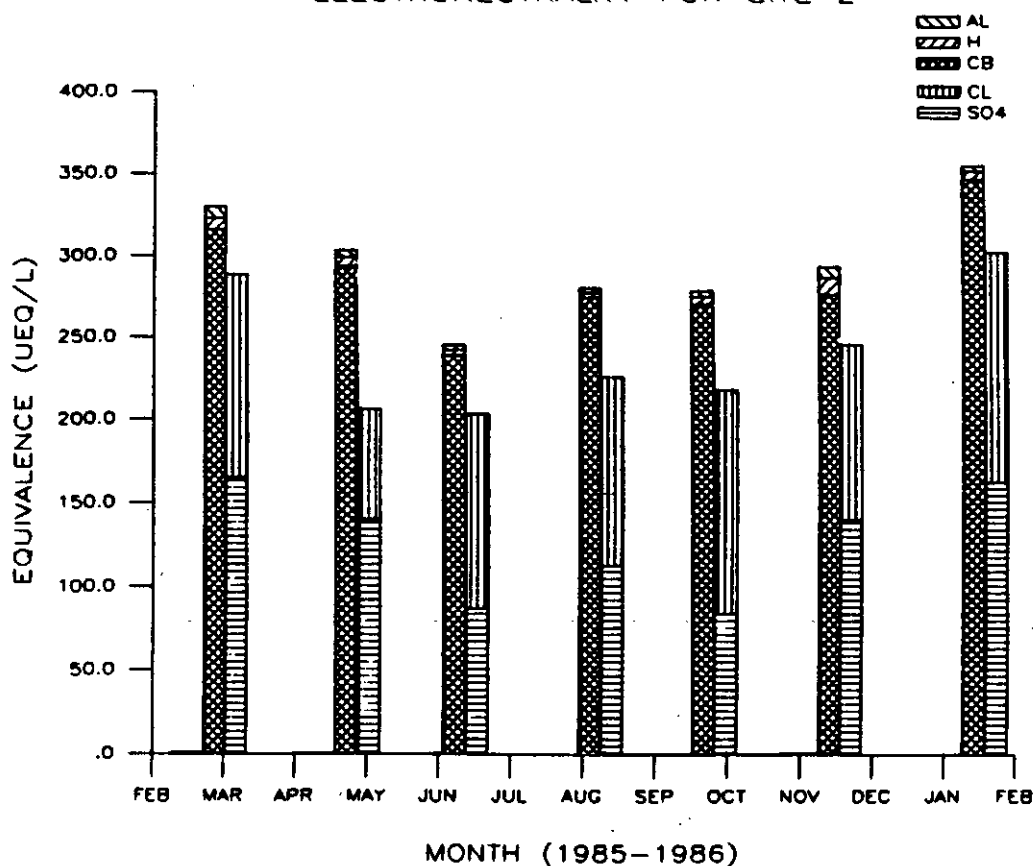


Figure 26. Electroneutrality plot for site 2 the wetland stream site. AL equals the total inorganic monomeric aluminum equivalence charge, H equals the hydrogen ion equivalence charge, CB equals the base cations (Ca, Mg, Na, K) equivalence charge, CL equals the chloride ion equivalence charge, SO₄ equals the sulfate ion equivalence charge.

ELECTRONEUTRALITY FOR SITE 3

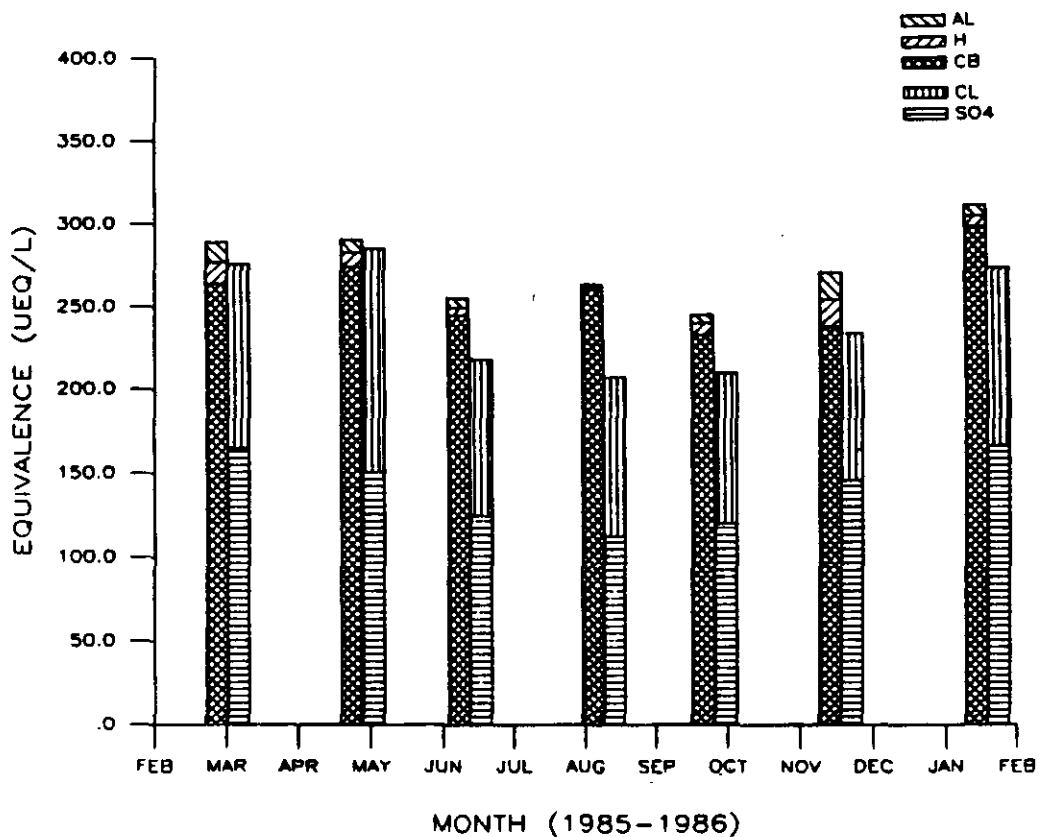


Figure 27. Electroneutrality plot for site 3 the downstream site. AL equals the total inorganic monomeric aluminum equivalence charge, H equals the hydrogen ion equivalence charge, CB equals the base cations (Ca, Mg, Na, K) equivalence charge, CL equals the chloride ion equivalence charge, SO₄ equals the sulfate ion equivalence charge.

The electroneutrality plot for the downstream site (Figure 27) shows the base cations to be greater than the strong acid anions, except during high runoff periods. This charge discrepancy causes the aluminum fraction to be quite small during the summer low-flow period and at moderate levels during the high-flow spring and fall periods. The organic anion fraction is greatest during the summer months when biological activity is at its greatest. Overall ion levels remain relatively constant throughout the year.

Figures 25-27 illustrate the importance of base cations to the aquatic system. If the base cations exceed the strong acid anions and the organic anion contribution is small, the amount of acidity (or acid cations) present in the stream is small. Base cations ultimately come from the weathering of parent materials in the soil horizons. Therefore, the rate at which the base cations are resupplied to the soil by weathering is crucial in mitigating acidification effects. The release of base cations in the soil zone not only influences the base saturation of soil and in turn its short-term buffering capacity, but also affects the streamwater acidity as well.

Aluminum levels for the three stream sites are presented in Figures 28-30. The analytical techniques used to measure aluminum are described in Chapter III. Basically, monomeric aluminum is a measure of the mononuclear aluminum species. Monomeric aluminum has been fractionated into inorganic and organic forms. Total aluminum is actually a measure of the acid soluble fraction and is presumably made up of polymeric, colloidal, and strongly bound organic fractions of aluminum.

STREAMWATER ALUMINUM FRACTIONS FOR SITE 1

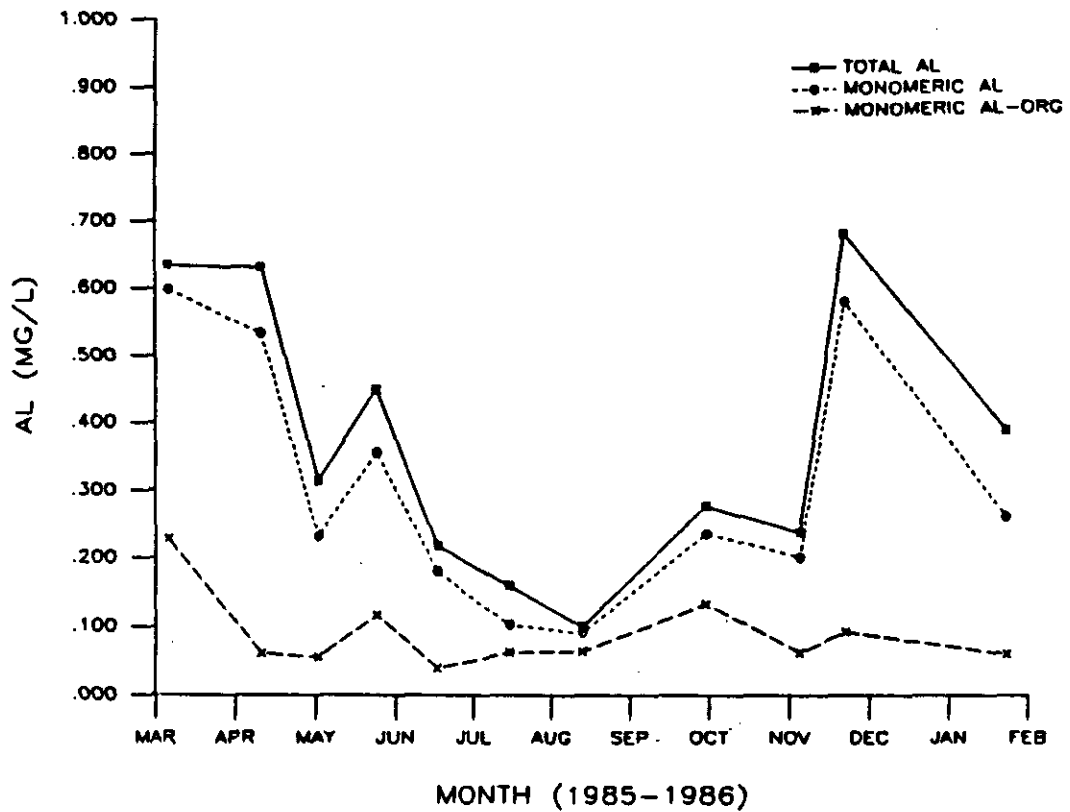


Figure 28. Measured streamwater aluminum fractions, in milligrams per liter, for site 1 the mountain stream site.

STREAMWATER ALUMINUM FRACTIONS FOR SITE 2

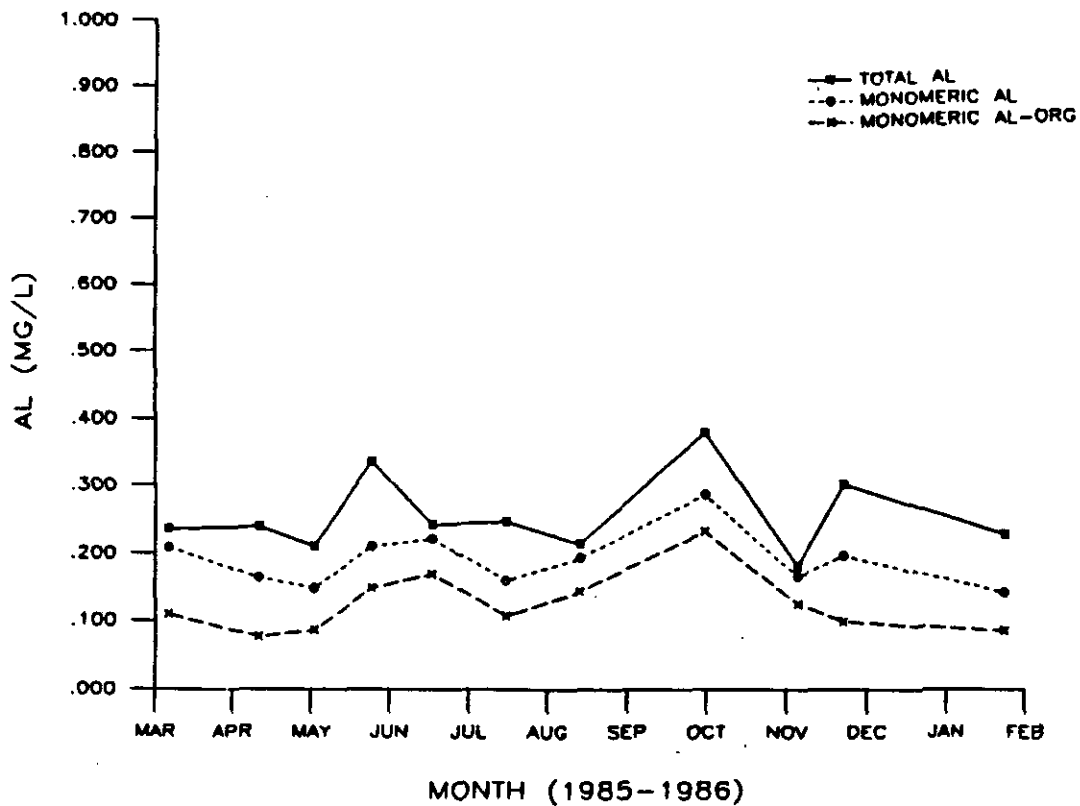


Figure 29. Measured streamwater aluminum fractions, in milligrams per liter, for site 2 the wetland stream site.

STREAMWATER ALUMINUM FRACTIONS FOR SITE 3

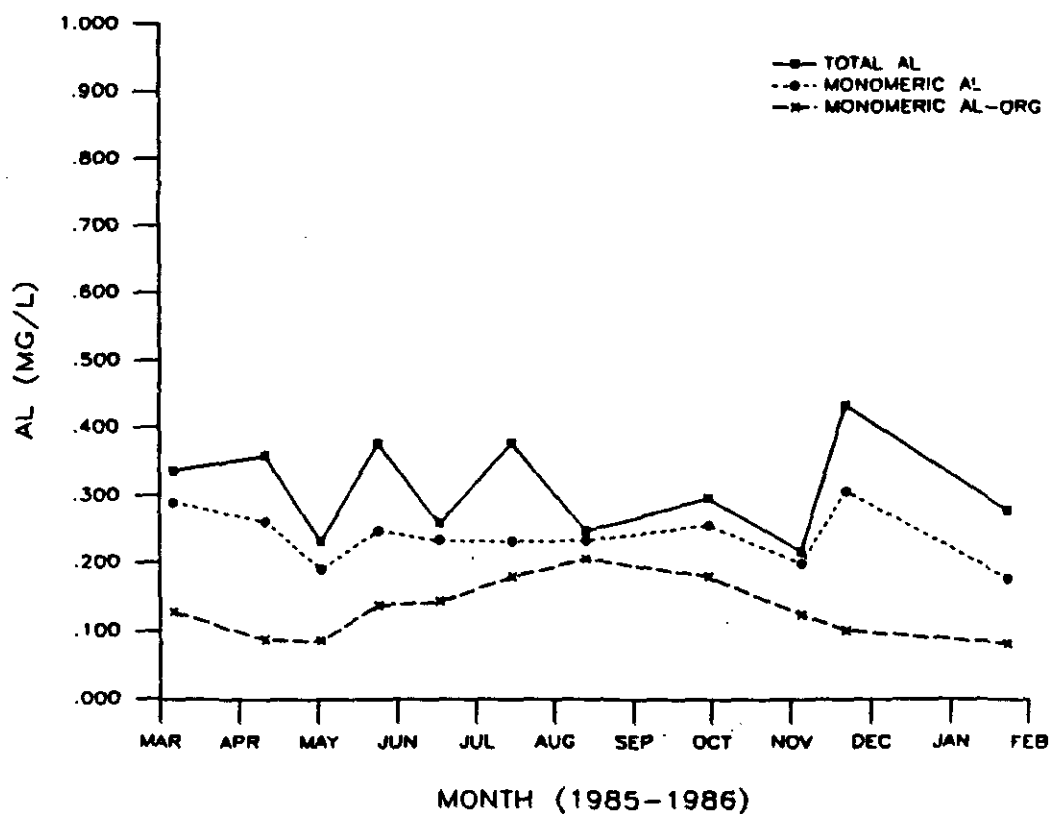


Figure 30. Measured streamwater aluminum fractions, in milligrams per liter, for site 3 the downstream site.

As seen in Figure 28, the mountain stream had high aluminum levels during the spring and fall runoff periods, as would be expected when considering electroneutrality. The organic monomeric and the acid soluble fractions at this site remain relatively constant throughout the year. The increase of aluminum during high runoff periods is mostly in the inorganic monomeric form. pH levels during these high flow periods are correspondingly low, thus suggesting that the increase of aluminum could be due to the solubility with an aluminum trihydroxide mineral phase. Other researchers have also suggested that surface water aluminum levels may be controlled by an aluminum trihydroxide phase (Johnson et al., 1981; Driscoll et al., 1982).

The wetland stream's (Figure 29) aluminum concentration is relatively constant throughout the year. This corresponds to the relatively constant pH levels throughout the year, further supporting the idea that streamwater aluminum is controlled by a mineral phase. The organic monomeric fraction and the acid soluble fraction, which is probably composed mostly of strongly bound organic aluminum, makes up the majority of the streamwater aluminum. Levels of aluminum in the wetland stream are considerably lower than the mountain stream during the spring and fall high-runoff months, but can be higher during the summer period.

The downstream site (Figure 30) illustrates the mixing effect of the two tributary streams. Monomeric aluminum at the downstream site varies somewhat throughout the year, but the organic and inorganic portions making up the total vary much more.. Organically bound

aluminum increases considerably during the summer months, with aluminum levels in August being almost entirely in the organic form.

Knowing the total streamwater aluminum concentration is not sufficient when assessing the potential toxicological effects on aquatic organisms. Speciation of a metal is extremely important when looking at toxicity. As discussed in Chapter II the most toxic form of aluminum appears to be the free (aquo) aluminum, followed by inorganic complexes and lastly organic complexes. In this study the acid soluble fraction is assumed to be fairly inert and thus non-toxic to aquatic organism.

To evaluate potential toxicity, the monthly grab samples were fractionated into the various aluminum species by using the EQUAL program described in Chapter IV. Results of the fractionation procedure are presented in Figures 31-33. The most toxic form of aluminum is shown on the bottom of the bar graph with a decrease in toxicity as one moves up. Recalling from the literature review chapter, monomeric aluminum values, free plus hydroxyl complexes, as low as 0.2 mg/L (7.5 $\mu\text{mol/L}$) are thought to have detrimental effects on fish (Muniz and Leivestad, 1980; Schofield and Trojnar, 1980; and Baker and Schofield, 1982). While this value will be used as a bench mark when assessing streamwater toxicity, other factors such as pH, calcium and temperature should also be considered.

Using this criteria, Figure 31 shows the mountain stream to be potentially toxic during spring and fall runoff periods. Free-aqueous plus hydroxide-bound monomeric aluminum ranges from 10-14 $\mu\text{mol/L}$, which

SEASONAL ALUMINUM CONCENTRATIONS FOR SITE 1

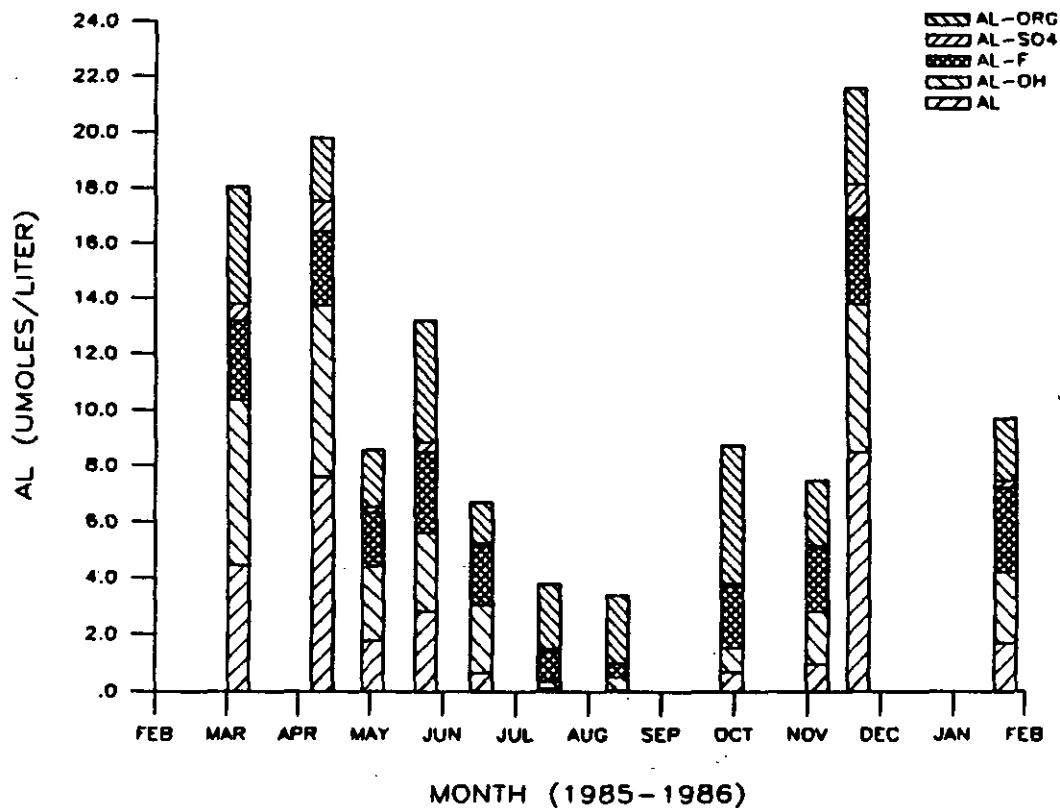


Figure 31. Monomeric aluminum fractions, in micro-moles per liter, as estimated from the EQUAL program for site 1 the mountain stream site.

SEASONAL ALUMINUM CONCENTRATIONS FOR SITE 2

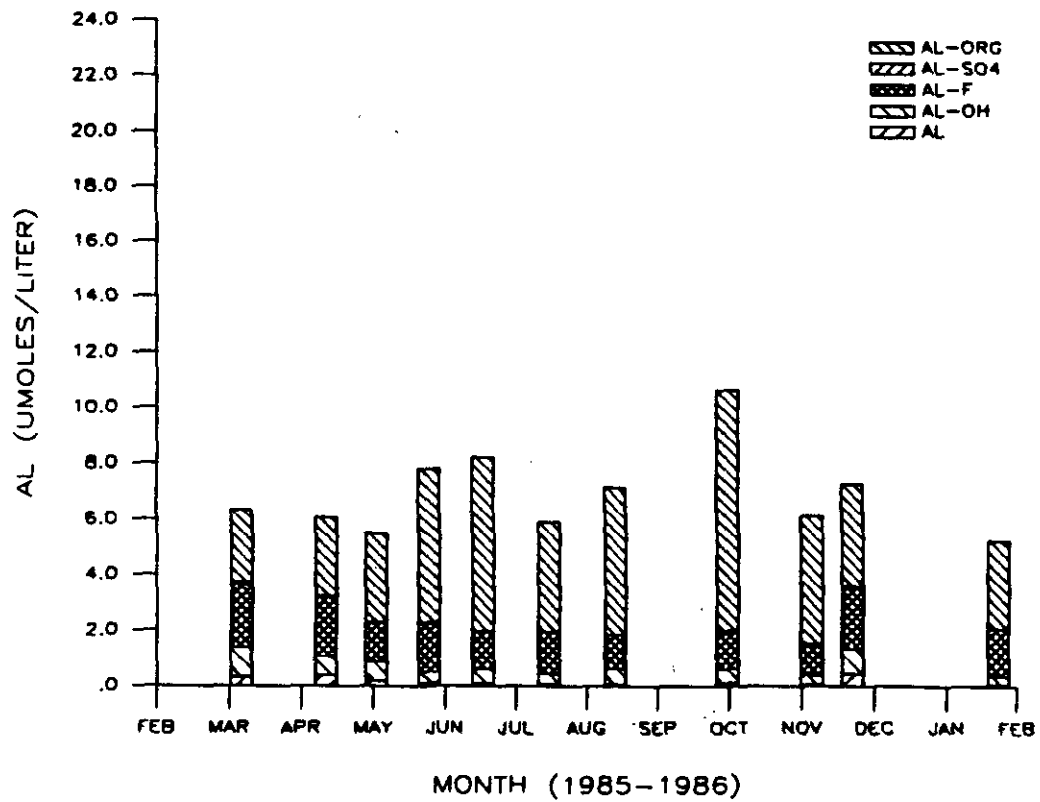


Figure 32. Monomeric aluminum fractions, in micro-moles per liter, as estimated from the EQUAL program for site 2 the wetland stream site.

SEASONAL ALUMINUM CONCENTRATIONS FOR SITE 3

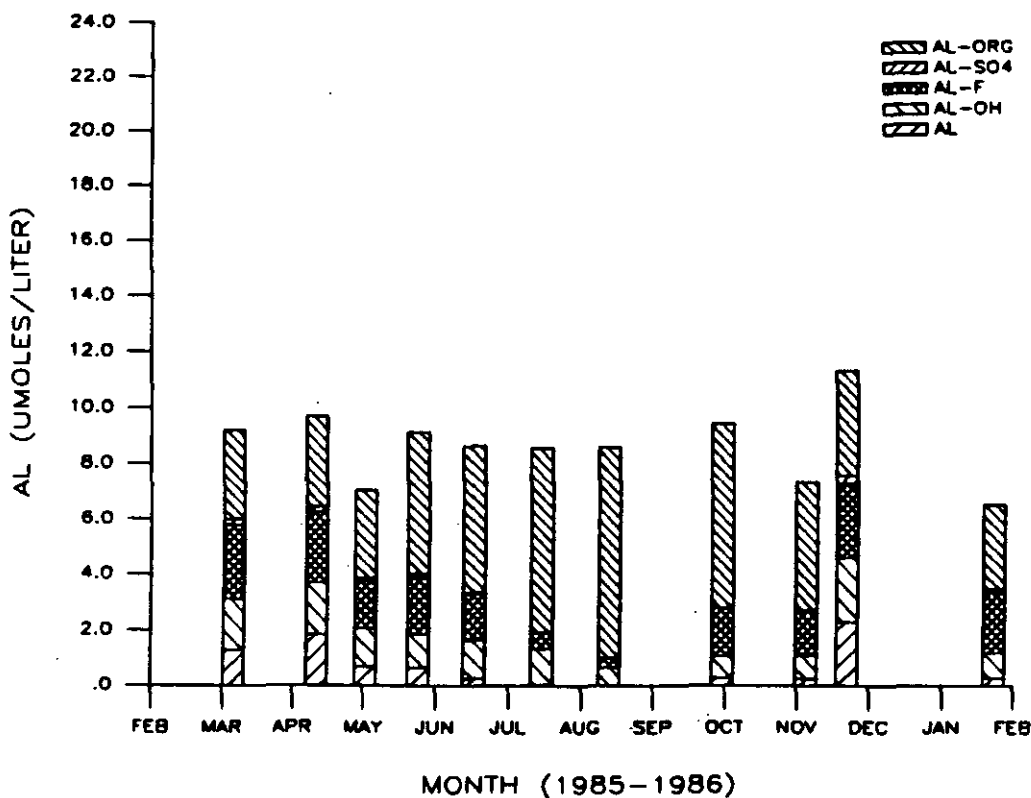


Figure 33. Monomeric aluminum fractions, in micro-moles per liter, as estimated from the EQUAL program for site 3 the downstream site.

is almost twice as much as the laboratory bench mark. pH levels during these time periods were also quite low, ranging from 4.2-4.8. During the summer months, though, total monomeric aluminum levels are less than the critical value of 7.5 $\mu\text{mol/L}$. Inorganic aluminum fractions dominate during high-flow periods whereas during the low-flow summer months the organic fraction dominates.

The wetland stream has the majority of its aluminum in the organic fraction throughout the year (Figure 32). Its inorganic fraction is composed mostly of fluoride complexes. Total monomeric levels hardly ever exceed the toxicity threshold and are predominately in a chelated or complexed form. These factors minimize toxicity in the wetland stream.

The downstream site (Figure 33) also shows a minimal potential for toxicity. Total monomeric aluminum levels are relatively constant, around 8-9 $\mu\text{mol/L}$, with more than half the total complexed with organic or fluoride ligands. Free aluminum levels never exceeded 2 $\mu\text{mol/L}$. The organic fraction is significant throughout the year and dominates the system during the summer months.

In conclusion, there is a significant difference in streamwater chemistry between the adjacent mountain and wetland streams. These differences are due in part to their different hydrologic flowpaths. The mountain stream has greater variability in pH and aluminum levels whereas the wetland stream varies more in DOC. Base cations as well as organic anions play an important role in aluminum mobility. If the total charge of the base cations are less than the total charge of the

strong acid anions this charge discrepancy must be made up with acid cations, thus increasing aluminum and decreasing pH. Organic acids are important in terms of buffering the system, and also in chelating and transporting aluminum. This was demonstrated in the wetland stream with organically bound aluminum increasing with DOC during high run off periods and pH values not decreasing as much as the adjacent mountain stream. Solubility with a mineral phase like aluminum trihydroxide seems to control aluminum in the mountain stream whereas organic anions appear to regulate aluminum in the wetland. Only the mountain stream, during high runoff periods, exhibits aluminum toxicity.

Intensive Surveys

Two intensive field surveys were conducted during the first two weeks of May and of November, 1985. These time periods were chosen because of their typical high runoff responses. Experimental design and sampling procedures used during these surveys are presented in Chapters I and III, respectfully. The stream sites were the same as those used for the monthly grab investigation.

May, 1985

May, 1985 started with two light-to-moderate rainfall events. For approximately a month prior to these storms very little precipitation had fallen. Rainfall intensities along with stream flow response for this particular time period are presented in Figures 34 and

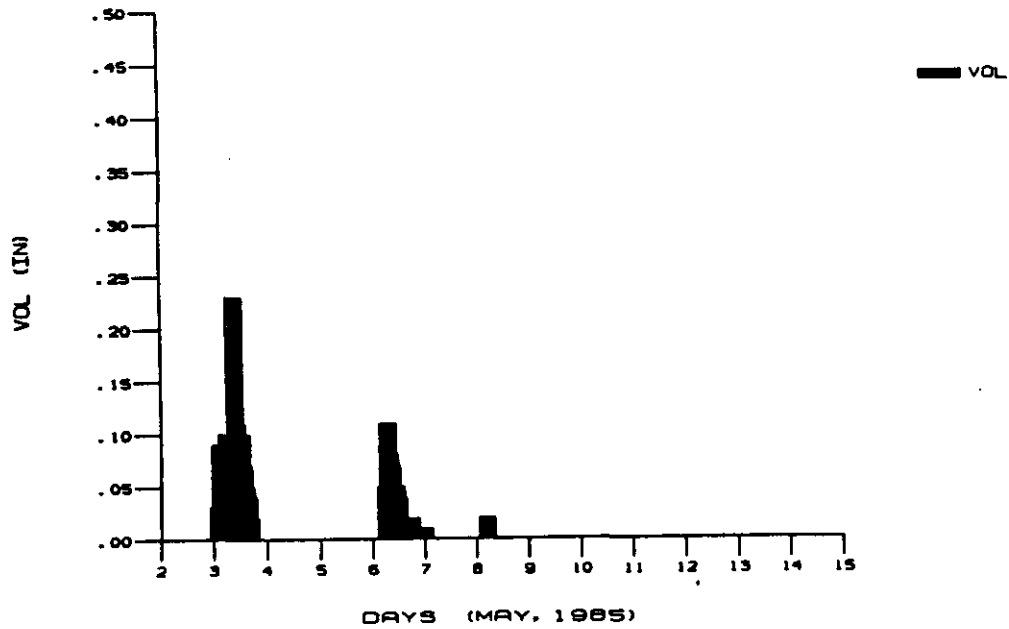


Figure 34. Rainfall intensity recorded at the Worcester Municipal Airport during May 1985.

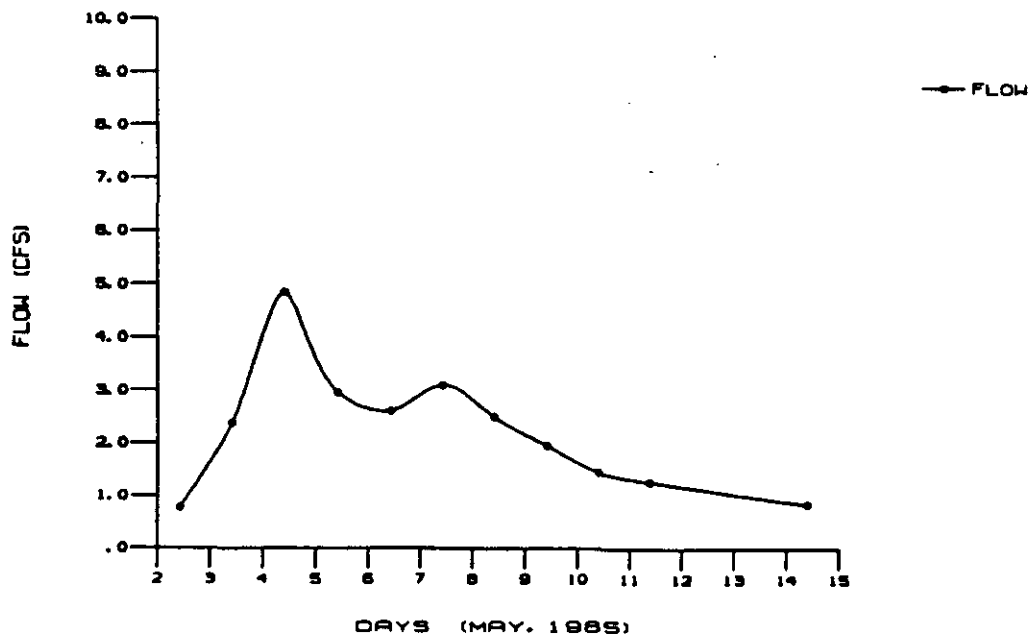


Figure 35. Streamflow at the downstream site, in cubic feet per second (cfs), during May 1985.

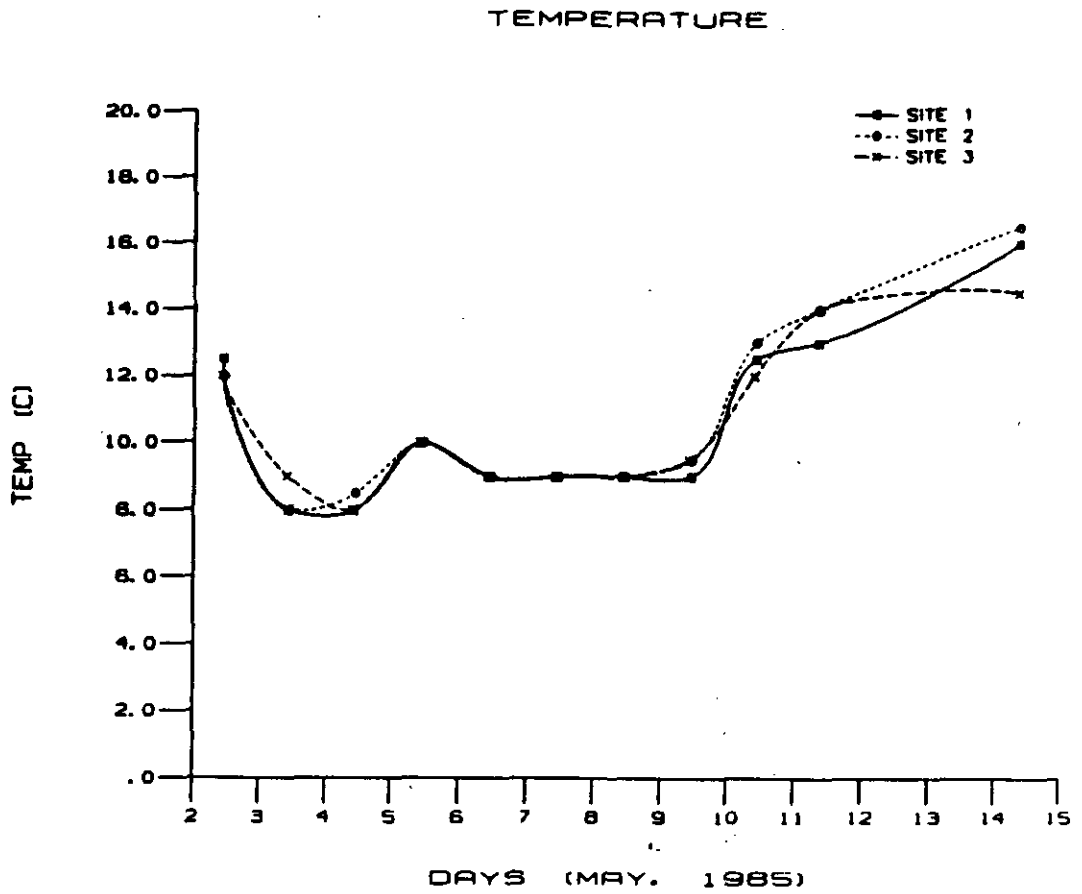


Figure 36. Streamwater temperature, in degrees Centigrade, during May 1985 for site 1 the mountain stream site, site 2 the wetland stream site, and site 3 the downstream site.

35. A total rainfall volume measured at the study site of 2.6 cm fell during the study period with a maximum recorded stream flow of 5 cfs. pH levels of the rain averaged 4.1 and ranged from 3.89 to 4.32 during this period. Streamwater temperatures ranged from 8-16 degrees Centigrade (Figure 36).

Streamwater pH dropped approximately 0.3 units during the storm at all three of the monitoring sites and slowly recovered to their original levels by the end of the two week study period (Figure 37). The mountain stream dropped to a pH of 4.8 and the wetland stream to 5.1 during the peak of the storm.

The decrease in the mountain stream's pH from 5.1 to 4.8 between May 2 and 3 had a significant effect on the streamwater aluminum level. This response is depicted in Figure 38 where total monomeric aluminum nearly doubled from 8 to 15 $\mu\text{mol/L}$ with free plus hydroxide-bound aluminum increasing from 4 to 9 $\mu\text{mol/L}$ during the peak of the storm. These levels are potentially toxic as based on the 7.5 $\mu\text{mol/L}$ criterion presented previously. The increase in aluminum is mostly associated with the free form, thus supporting the contention that aluminum is controlled by solubility with an aluminum trihydroxide mineral phase.

The wetland stream (Figure 39) provides a contrast as the rise in aluminum concentration during the peak of the storm is approximately

STREAMWATER PH

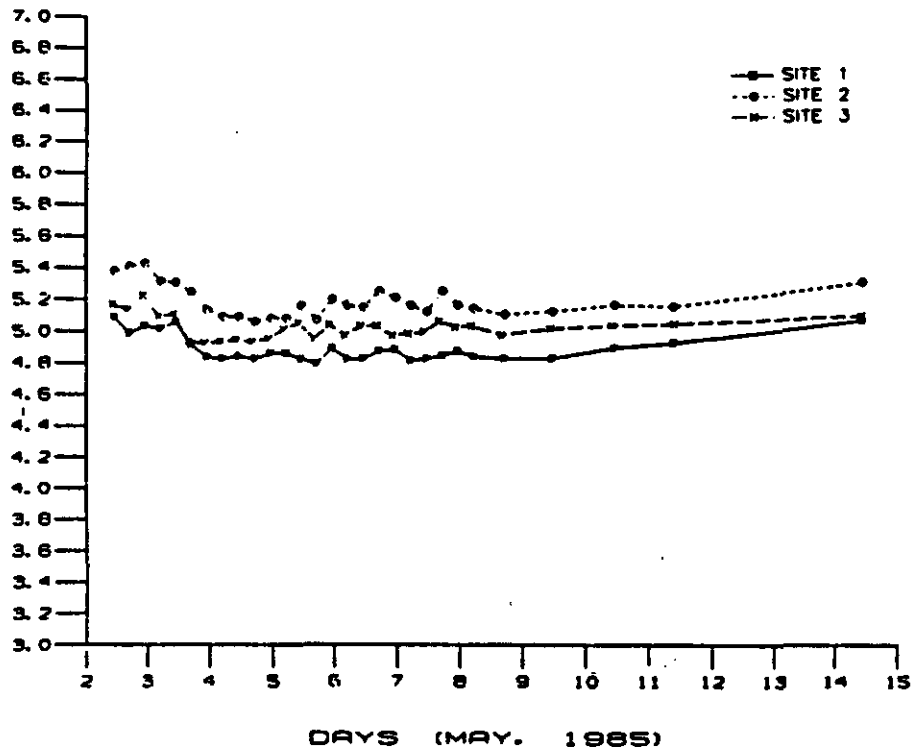


Figure 37. Streamwater pH response during May 1985 for site 1 the mountain stream site, site 2 the wetland stream site, and site 3 the downstream site.

ALUMINUM FRACTIONS FOR SITE 1

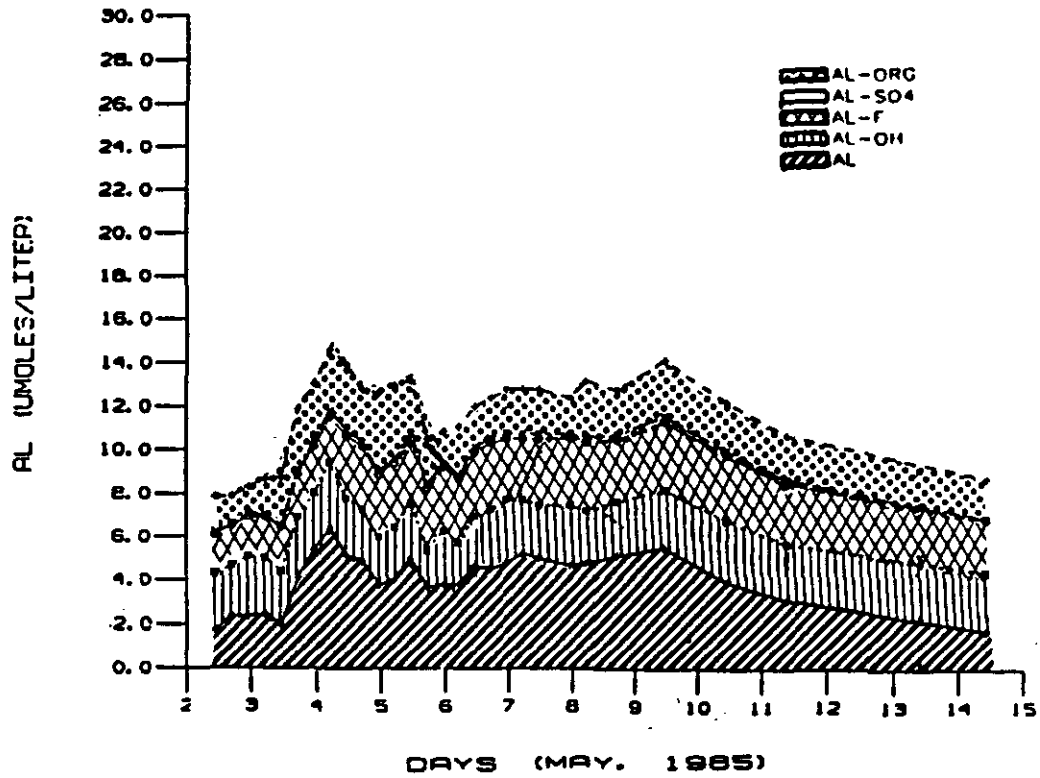


Figure 38. Monomeric aluminum fractions, in micro-moles per liter, as estimated from EQUAL during May 1985 for site 1 the mountain stream site.

ALUMINUM FRACTIONS FOR SITE 2

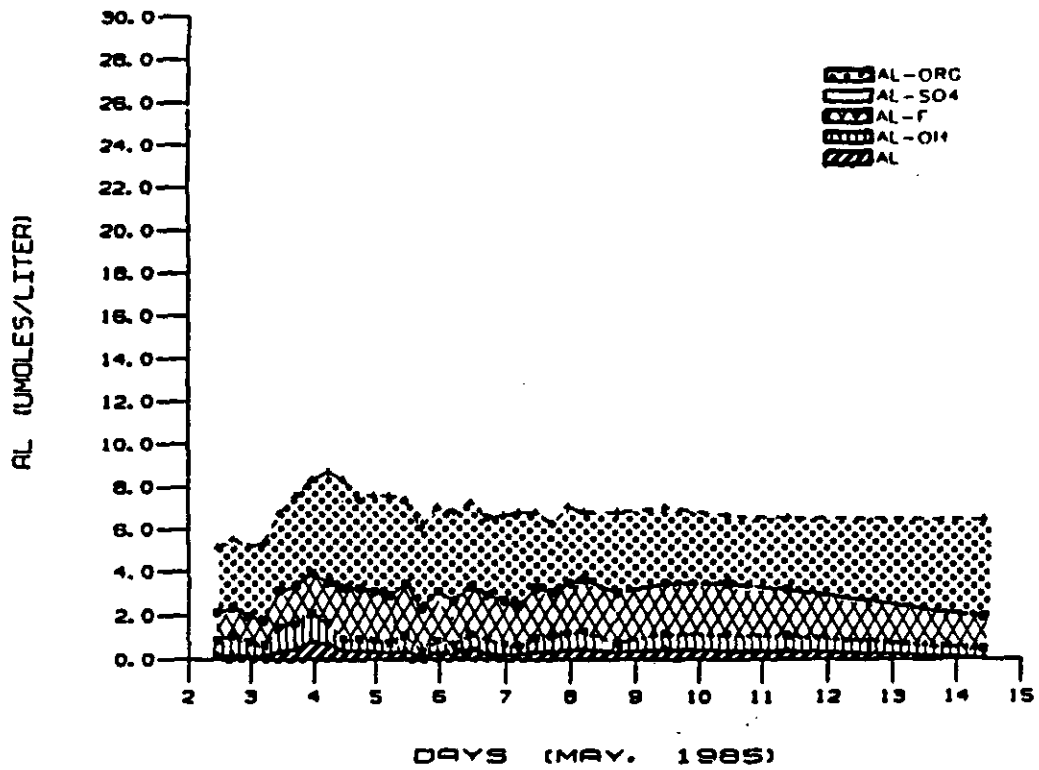


Figure 39. Monomeric aluminum fractions, in micro-moles per liter, as estimated from EQUAL during May 1985 for site 2 the wetland stream site.

equal between all fractions. Total monomeric aluminum is at a maximum around 8 $\mu\text{mol/L}$ during the peak of the storm with free plus hydroxide-complexed aluminum peaking at 2 $\mu\text{mol/L}$. These levels are well below the potentially toxic range.

The downstream site (Figure 40) appears to be greatly influenced by the organic acids present, as approximately half of the monomeric aluminum is in an organic form. Toxic levels of aluminum are at a minimum as free and hydroxide-bound aluminum only reach a maximum value of 3 $\mu\text{mol/L}$.

DOC levels at the three monitoring sites (Figure 41) illustrate the importance that organic substances have on the magnitude of the organo-aluminum fraction. The increase in DOC in the wetland stream and the downstream sites during the rainfall event corresponded with an increase in the aluminum organic fraction at these sites. On the other hand, the mountain stream's DOC and organo-aluminum fraction hardly changed. This effect seems to be due to the lowland areas having a larger organic substance pool which is flushed out during major episodic events.

As pointed out in the previous section, the equivalent charge of the major ions greatly affect aluminum mobility. Charge balance plots for the base cations and the strong acid anions for each of the three sampling sites are presented in Figures 42, 43, and 44. Before the storm the mountain stream is nearly balanced in positive and negative inorganic charges, but during the storm a cation deficit occurs. This allows for the excess negative charge to be balanced by the acid cations

ALUMINUM FRACTIONS FOR SITE 3

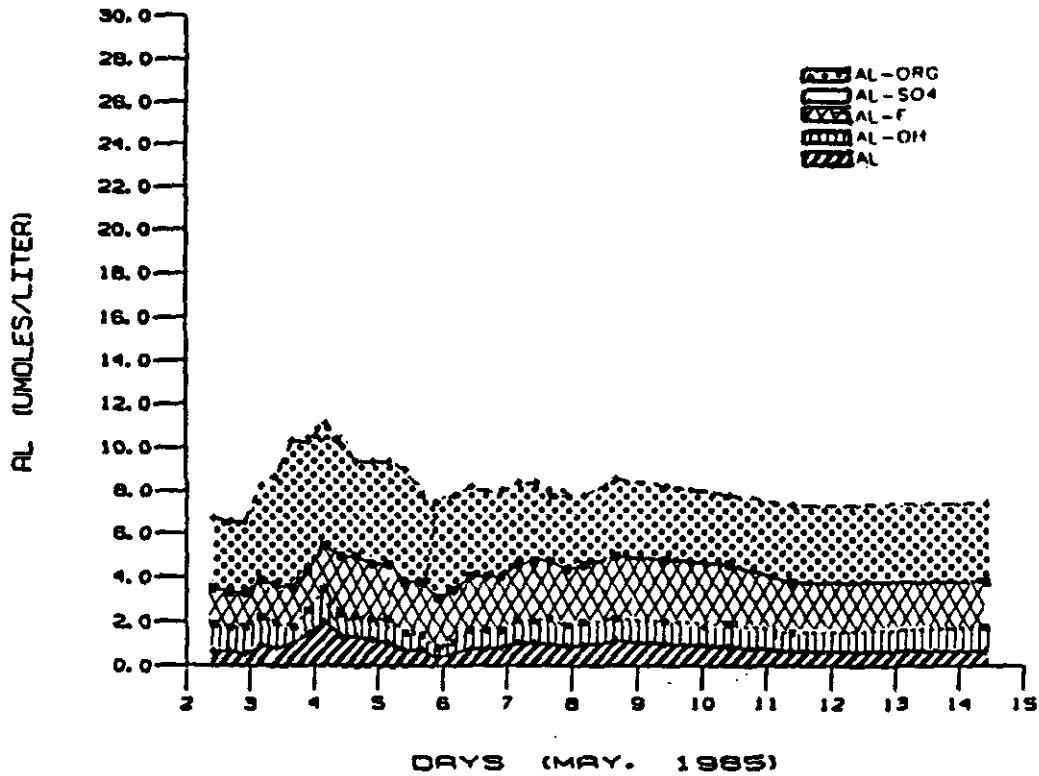


Figure 40. Monomeric aluminum fractions, in micro-moles per liter, as estimated from EQUAL during May 1985 for site 3 the downstream site.

DISSOLVED ORGANIC CARBON

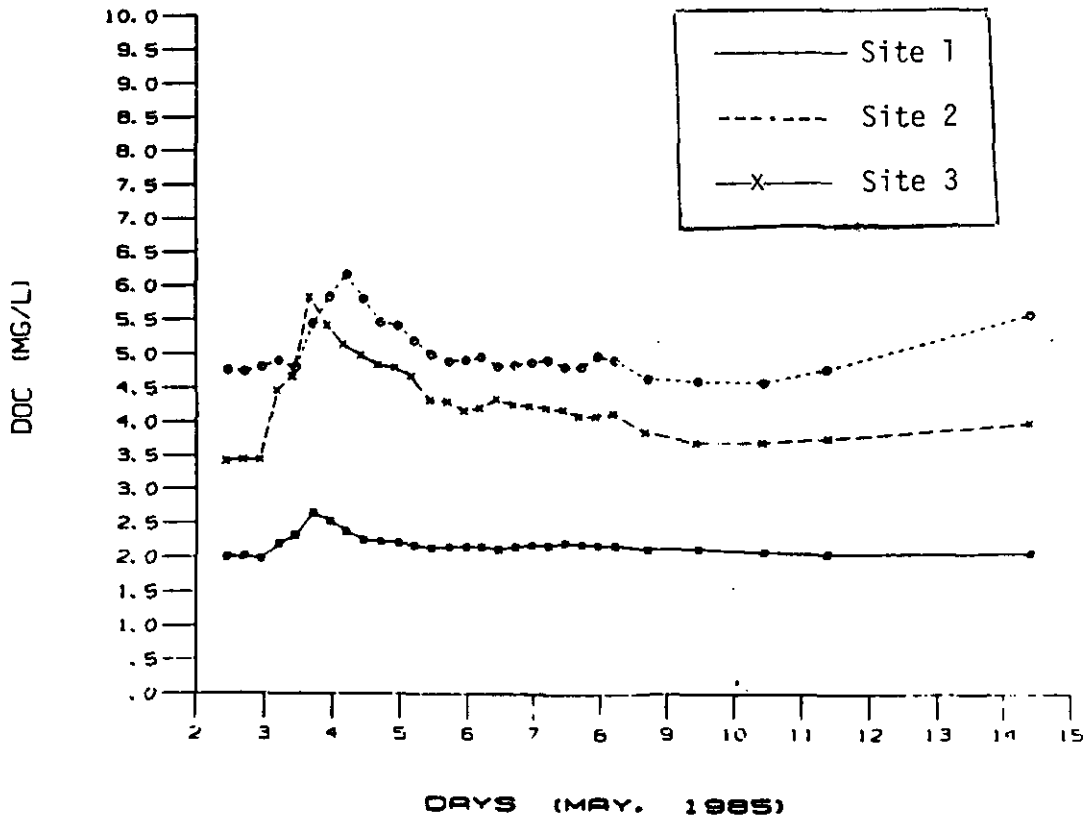


Figure 41. Dissolved organic carbon (DOC), in milli-grams per liter, during May 1985 for site 1 the mountain stream site, site 2 the wetland stream site, and site 3 the downstream site.

CHARGE EQUIVALENCE FOR SITE 1

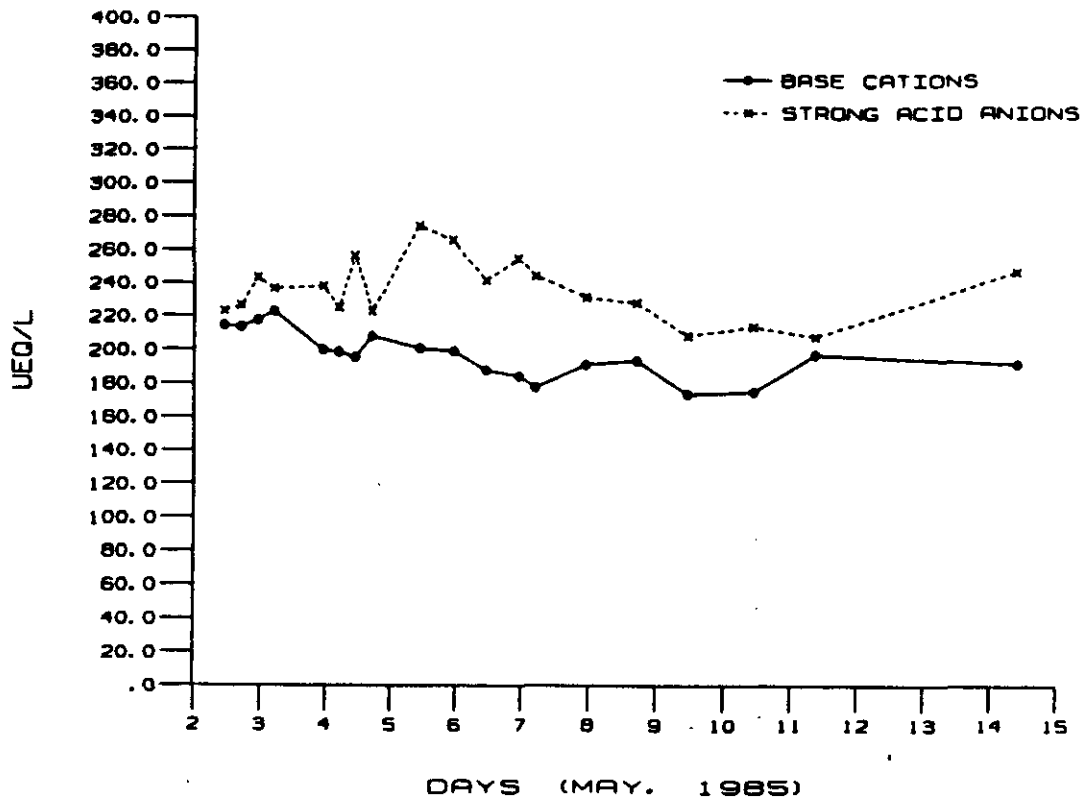


Figure 42. Charge equivalence, in micro-equivalence per liter, of base cations to strong acid anions for site 1 the mountain stream.

CHARGE EQUIVALENCE FOR SITE 2

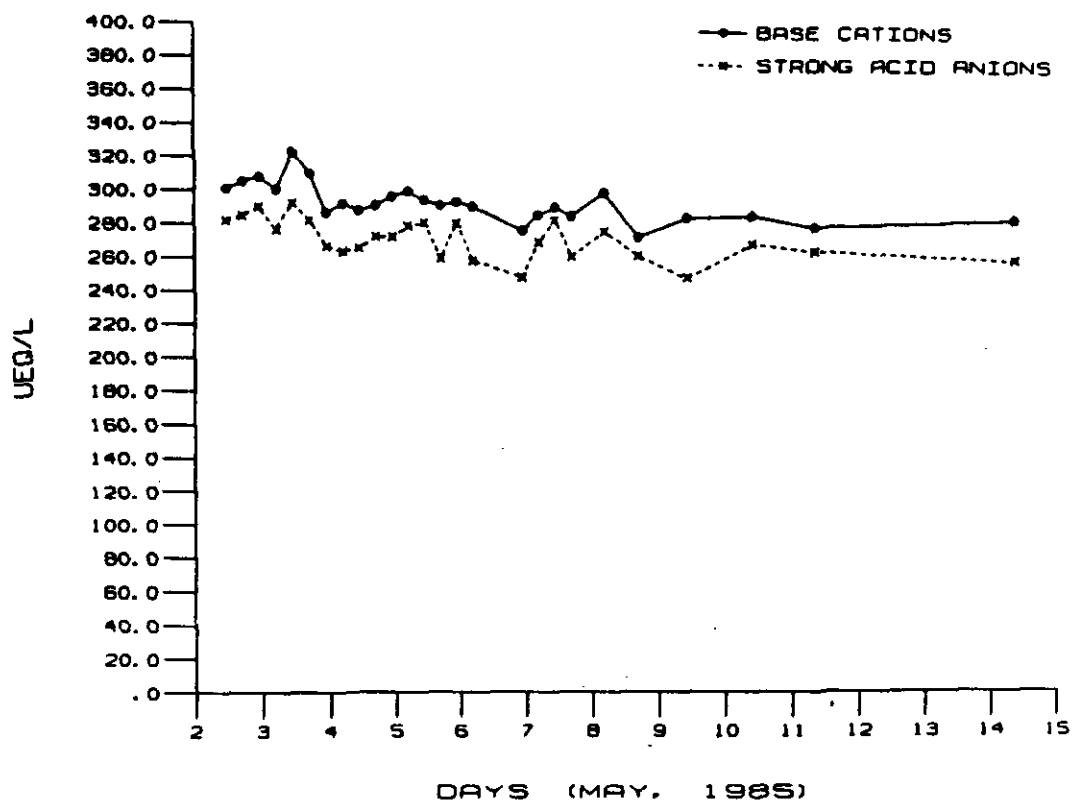


Figure 43. Charge equivalence, in micro-equivalence per liter, of base cations to strong acid anions for site 2 the wetland stream.

CHARGE EQUIVALENCE FOR SITE 3

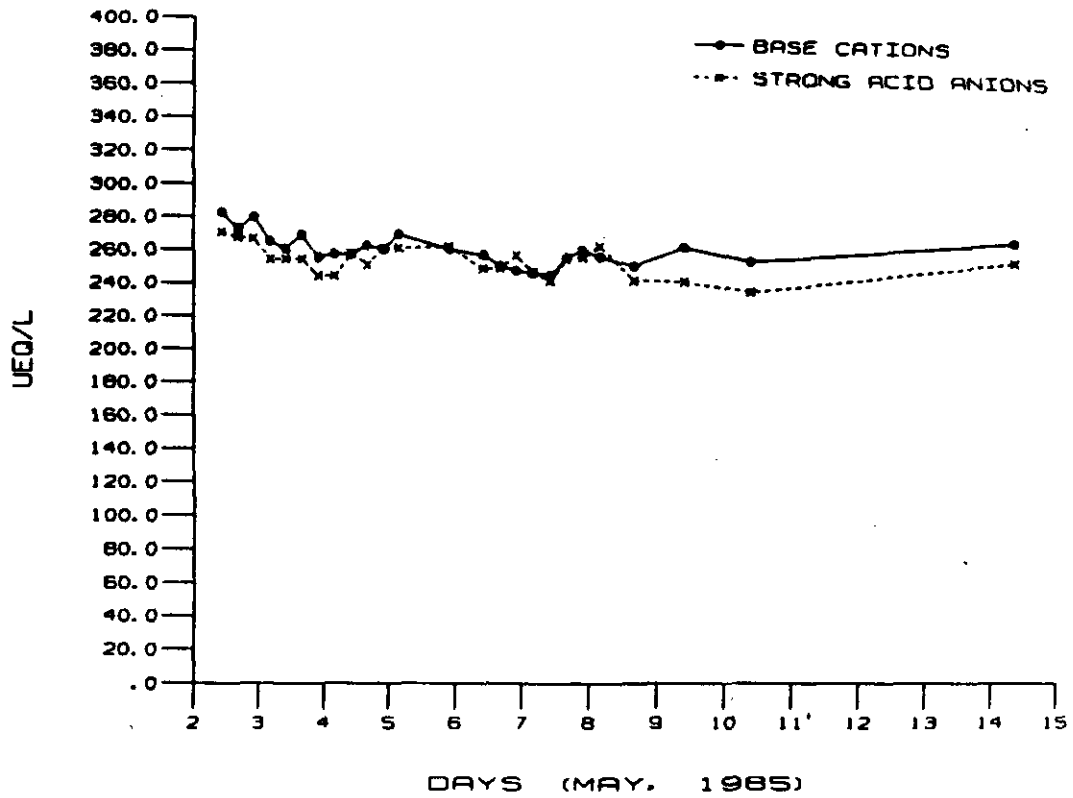


Figure 44. Charge equivalence, in micro-equivalence per liter, of base cations to strong acid anions for site 3 the downstream site.

intensities as well as the stream flow response are presented in Figures 45 and 46. A peak stream flow of 42 cfs at the downstream site is considerably greater than the peak of 5 cfs observed during the May study. Streamwater temperatures ranged from 9.0 to 1.0 degrees Centigrade (Figure 47).

Figure 48 shows the streamwater's pH response to the November storm events. As seen from this figure a dramatic change in pH occurred with the mountain stream dropping 0.9 of a units (5.1-4.2) and the wetland stream dropping 0.7 of a units (5.4-4.7) during the peak of the storm. This response raises an interesting question of why did the streamwater pH drop considerably lower than the rainwater pH. Hydrologic flow paths through the soil environment along with soil chemical reactions seem to regulate this response. The following analysis and the simulation modeling effort will focus on this particular time period to gain a better understanding of the processes controlling this response.

The monomeric aluminum fractions for the three sampling sites, as calculated by the EQUAL program, are plotted in Figures 49-51. As would be expected from mineral phase solubility, an aluminum increase corresponds to the drop in streamwater pH.

A closer look at the aluminum fractions reveals that the increase in aluminum for the mountain stream is primarily in the free form, with the organic fraction having the next largest increase. Furthermore, after the onset of the storm the free aluminum concentration for the

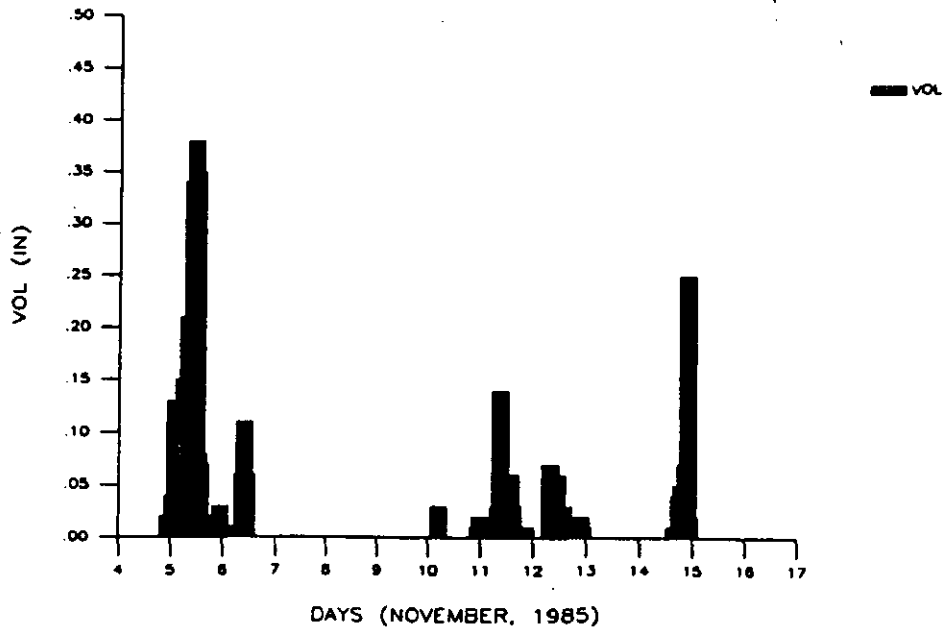


Figure 45. Rainfall intensity recorded at the Worcester Municipal Airport during November 1985.

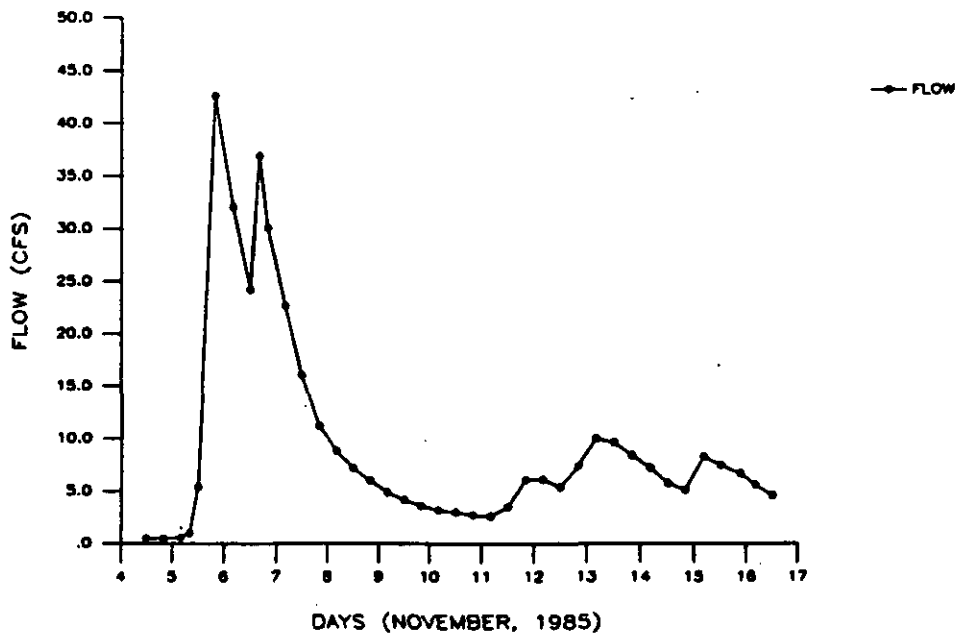


Figure 46. Streamflow at site 3 the downstream site, in cubic feet per second (cfs).

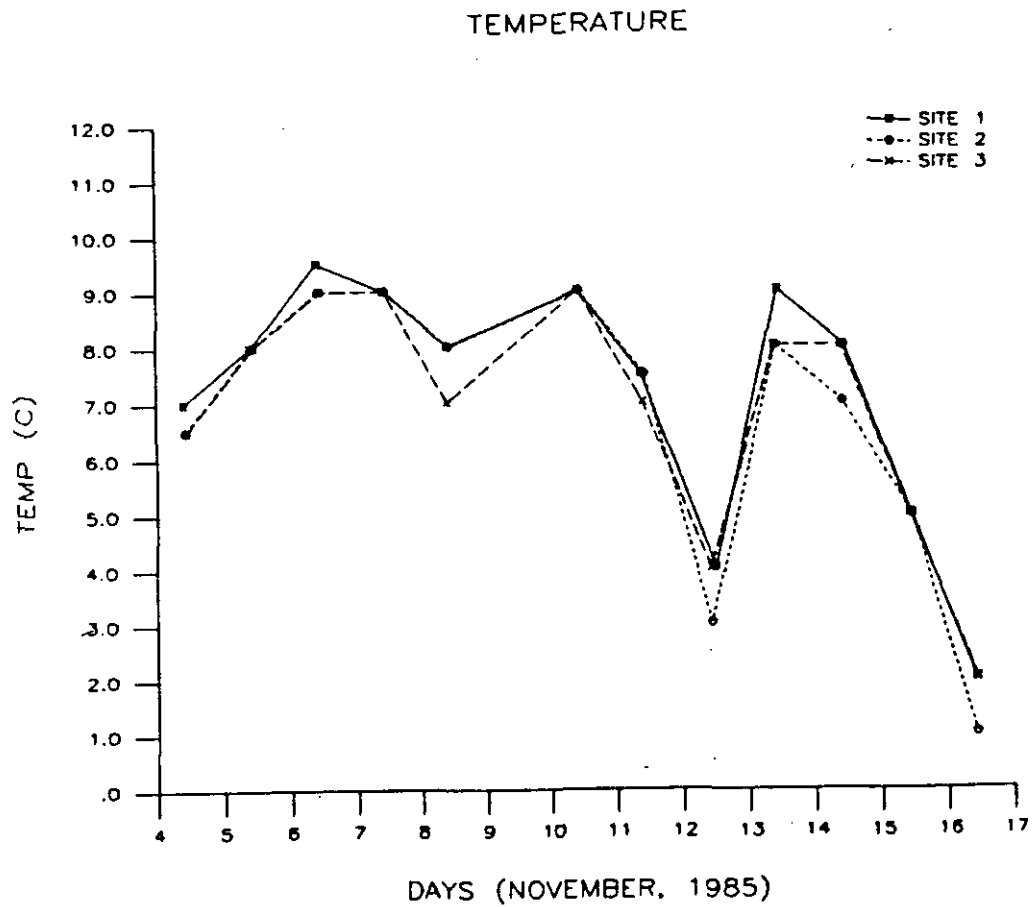


Figure 47. Streamwater temperature, in degrees Centigrade, during November 1985 for site 1 the mountain stream site, site 2 the wetland stream site, and site 3 the downstream site.

STREAMWATER PH

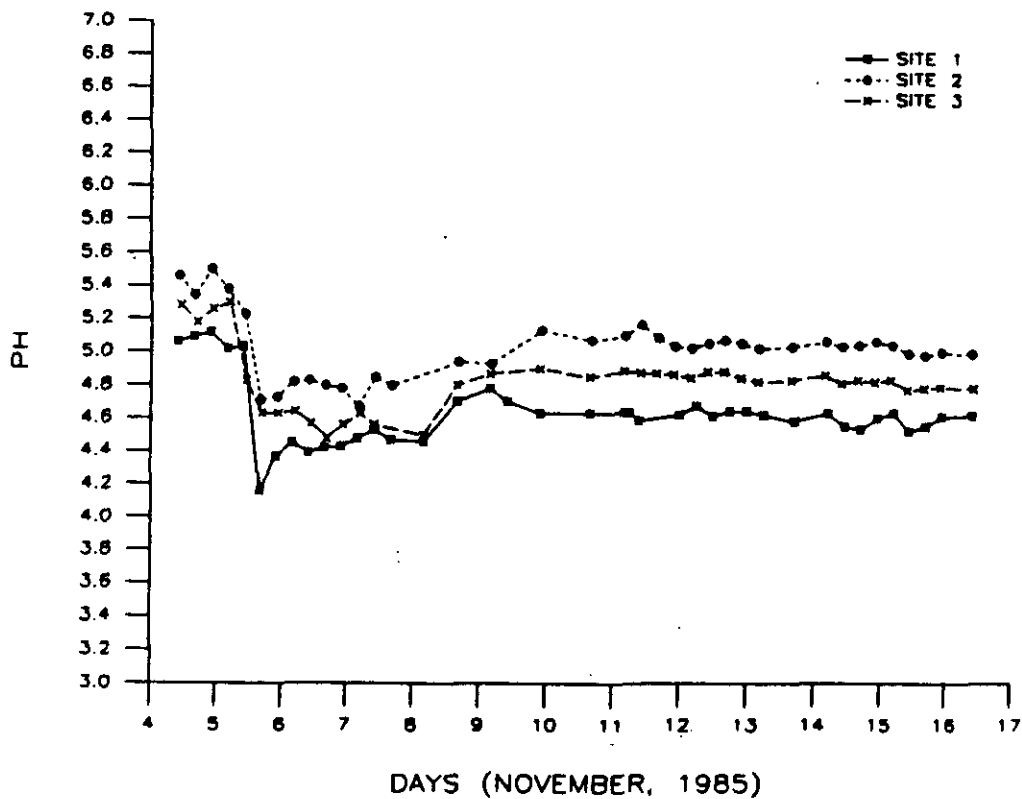


Figure 48. Streamwater pH response during November 1985 for site 1 the mountain stream site, site 2 the wetland stream site, and site 3 the downstream site.

ALUMINUM FRACTIONS FOR SITE 1

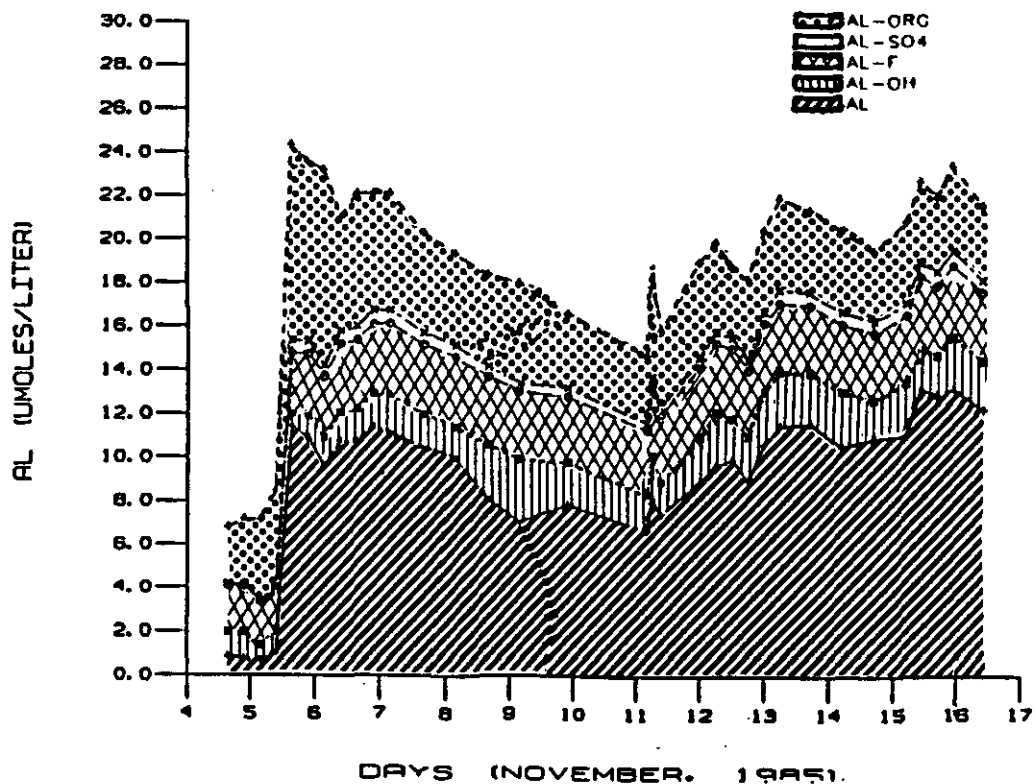


Figure 49. Monomeric aluminum fractions, in micro-moles per liter, as estimated from EQUAL during November 1985 for site 1 the mountain stream site.

ALUMINUM FRACTIONS FOR SITE 2

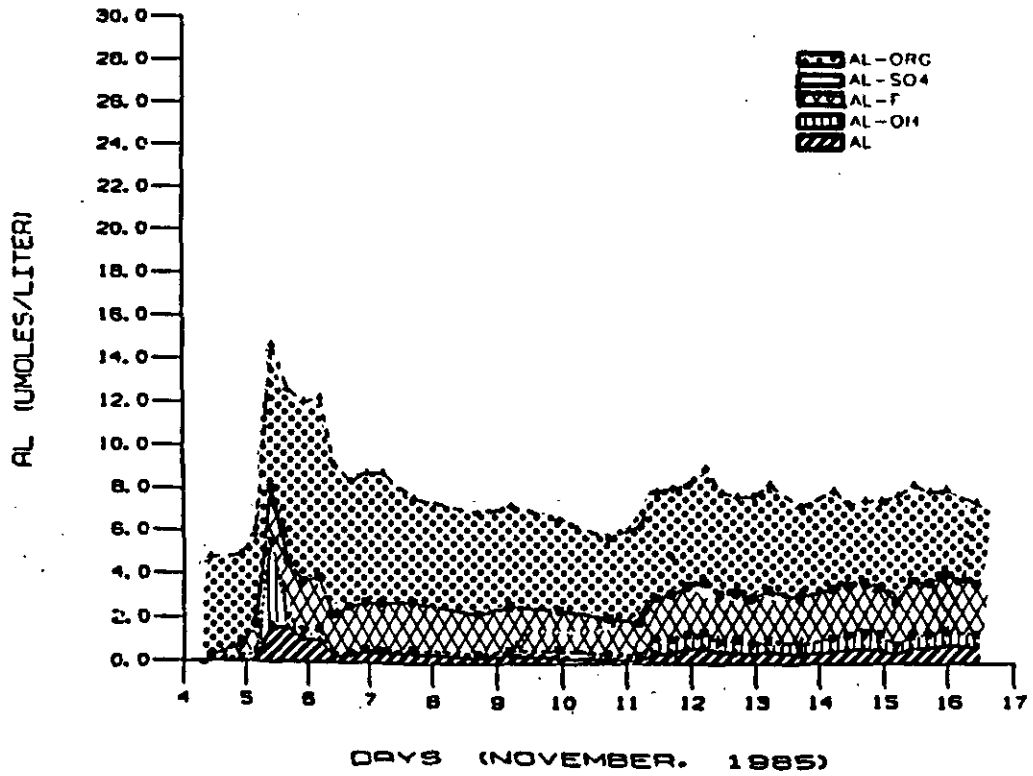


Figure 50. Monomeric aluminum fractions, in micro-moles per liter, as estimated from EQUAL during November 1985 for site 2 the wetland stream site.

ALUMINUM FRACTIONS FOR SITE 3

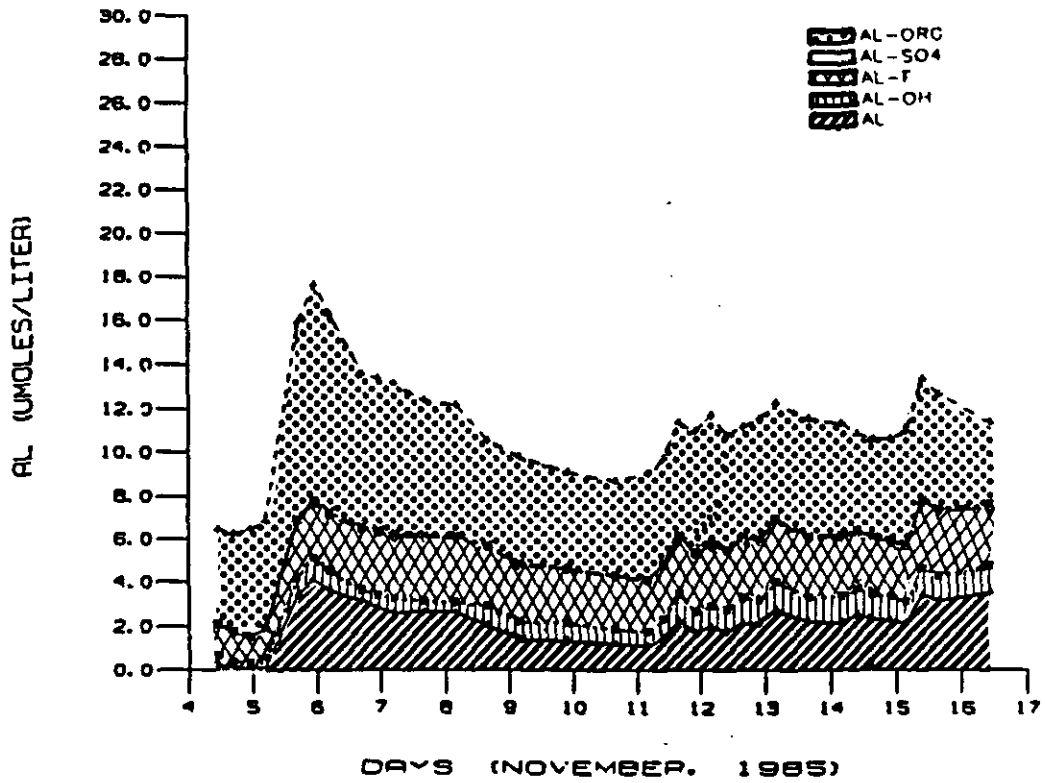


Figure 51. Monomeric aluminum fractions, in micro-moles per liter, as estimated from EQUAL during November 1985 for site 3 the downstream site.

mountain stream is higher than the toxicity criterion of 7.5 $\mu\text{mol/L}$. This portion of the stream exhibits the potential for aluminum toxicity over a duration of at least 10 days.

For the wetland stream, the inorganic aluminum fractions increased during the storm whereas the organic fraction remained relatively constant. Before the storm, monomeric aluminum was predominantly in an organic form, whereas at the peak of the storm it is reduced to approximately 50% of the total. Free plus hydroxide-bound aluminum does not reach toxic levels in the wetland stream.

The downstream site shows an increase in free, as well as fluoride and organically complexed aluminum. Inorganic monomeric aluminum levels, though, never exceed 7.5 $\mu\text{mol/L}$ and thus appear not to be toxic.

The organic aluminum fraction increased at all sampling sites and is strongly correlated with the increase in DOC levels. Figure 52 shows the DOC response in the stream during the November storms. The large DOC flush is due in part to the dry period that proceeded the storm event, as the later storms did not show this response. The high runoff rate may also have contributed to this flushing. Thus, large storms that occur after a dry warm period have the potential to flush high levels of organic substances from the ecosystem and in turn transport aluminum.

For the acid cations Al^{3+} and H^+ to increase during a storm, either the anions must increase and/or the base cations must decrease to maintain electroneutrality. The response of the base cations and strong

DISSOLVED ORGANIC CARBON

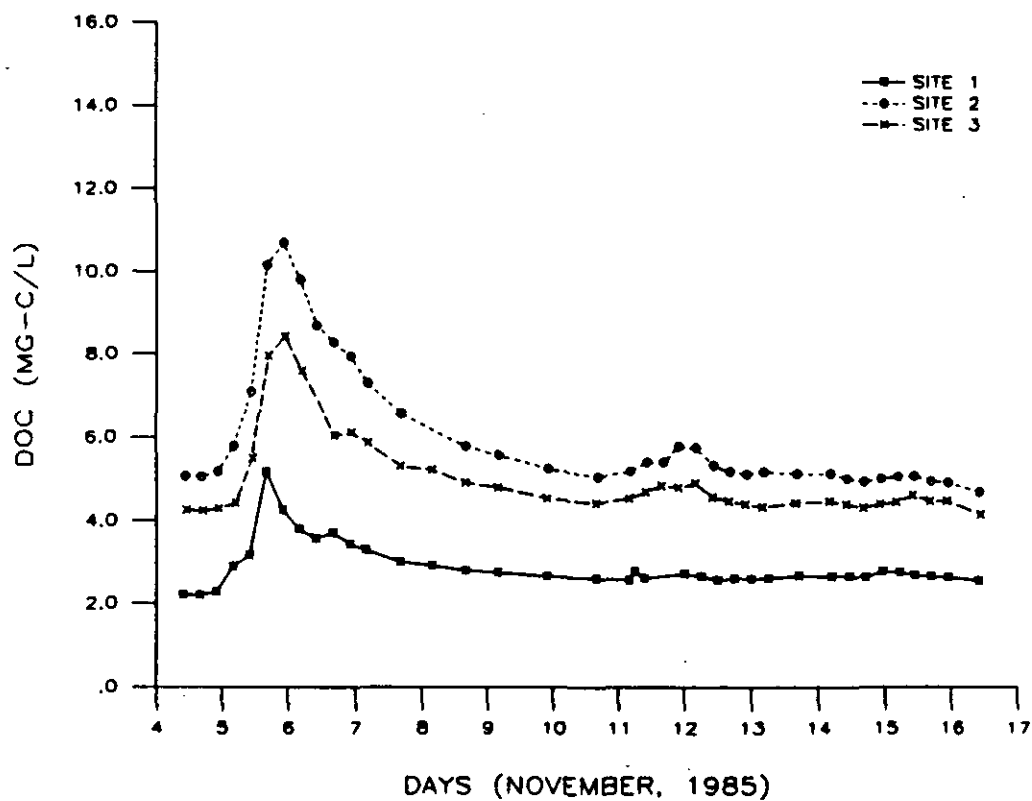


Figure 52. Dissolved organic carbon (DOC), in milli-grams per liter, during November 1985 for site 1 the mountain stream site, site 2 the wetland stream site, and site 3 the downstream site.

acid anions are presented in Figures 53-55. Plots of the individual ions may be found in an accompanying document. This storm's response is similar to that in May. Initially the mountain stream's base cations and strong acid anions are in balance, but during the storm the base cations decrease, leaving a charge imbalance that must be made up by acid cations. In contrast, the wetland stream always has more base cations than strong acid anions and thus the increase in aluminum must be balanced by an increase in organic anions. The wetland itself has an affect on streamwater quality, especially if one assumes that the stream feeding the wetland has a chemical composition similar to the mountain stream. If true, a drastic change in streamwater chemistry takes place in the wetland's organic acids buffering pH and chelating aluminum. The downstream site is in balance among the base cations and the strong acid anions during the study period. Thus, for this site the organic anion charge controls the aluminum concentration.

In conclusion, the intensive surveys conducting during May and November contributed significantly to the understanding of the streamwater processes that control aluminum transport in a watershed system. Organic substances play an important role in terms of the charge balance as well as complexing and mobilizing aluminum along the stream system. In addition, the primary source of streamwater aluminum appears to be from the soil environment. Due to the apparent equilibrium with an aluminum trihydroxide mineral phase stream water aluminum may also be resolubilized from the stream sediment. With regard to toxicity, it appears that the mountain stream is potentially

CHARGE EQUIVALENCE FOR SITE 1

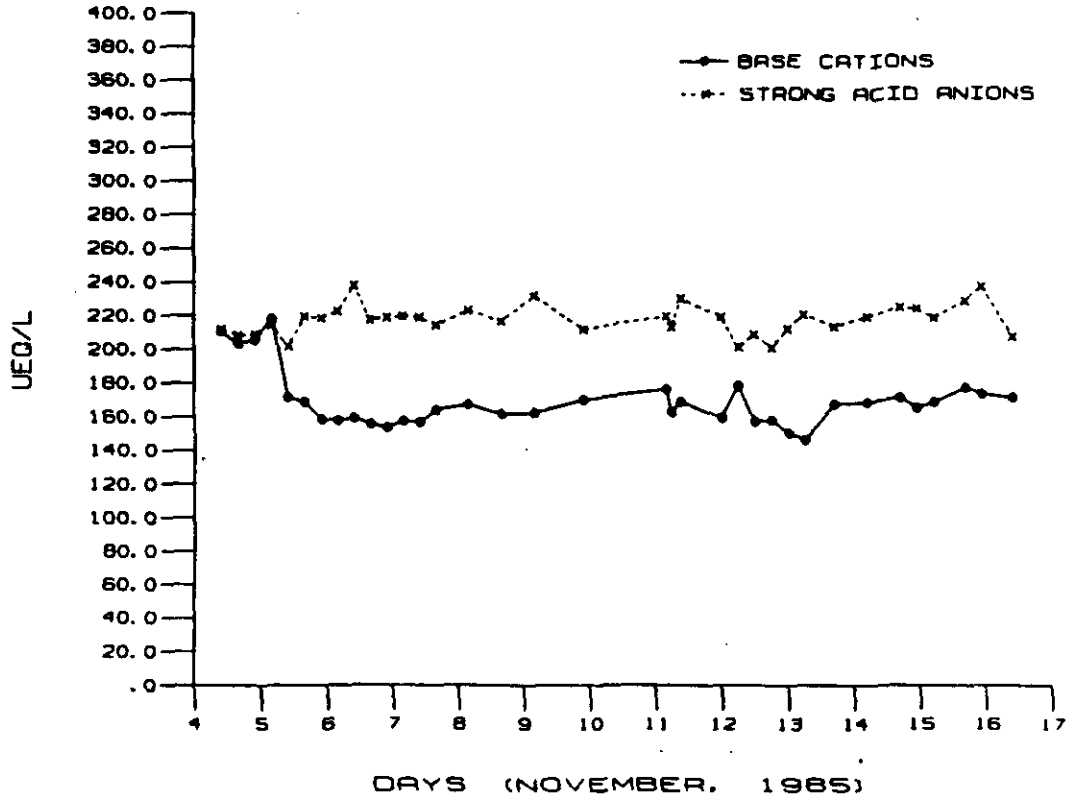


Figure 53. Charge equivalence, in micro-equivalence per liter, of base cations to strong acid anions for site 1 the mountain stream site.

CHARGE EQUIVALENCE FOR SITE 2

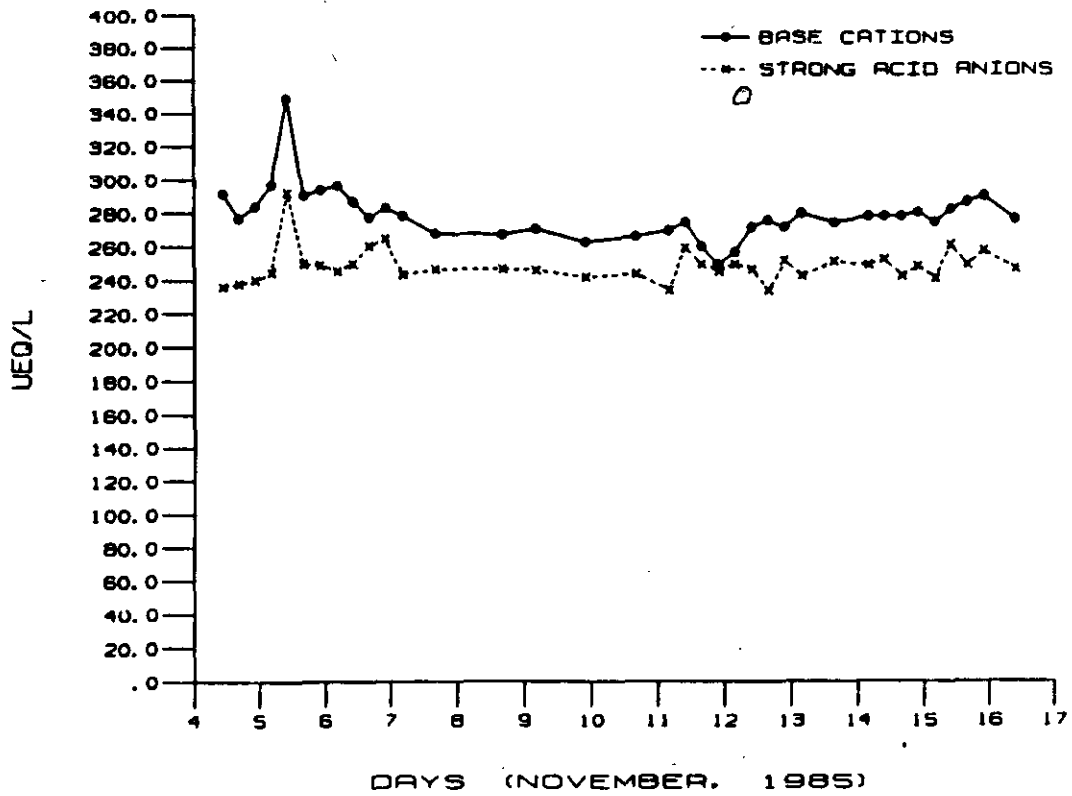


Figure 54. Charge equivalence, in micro-equivalence per liter, of base cations to strong acid anions for site 2 the wetland stream site.

CHARGE EQUIVALENCE FOR SITE 3

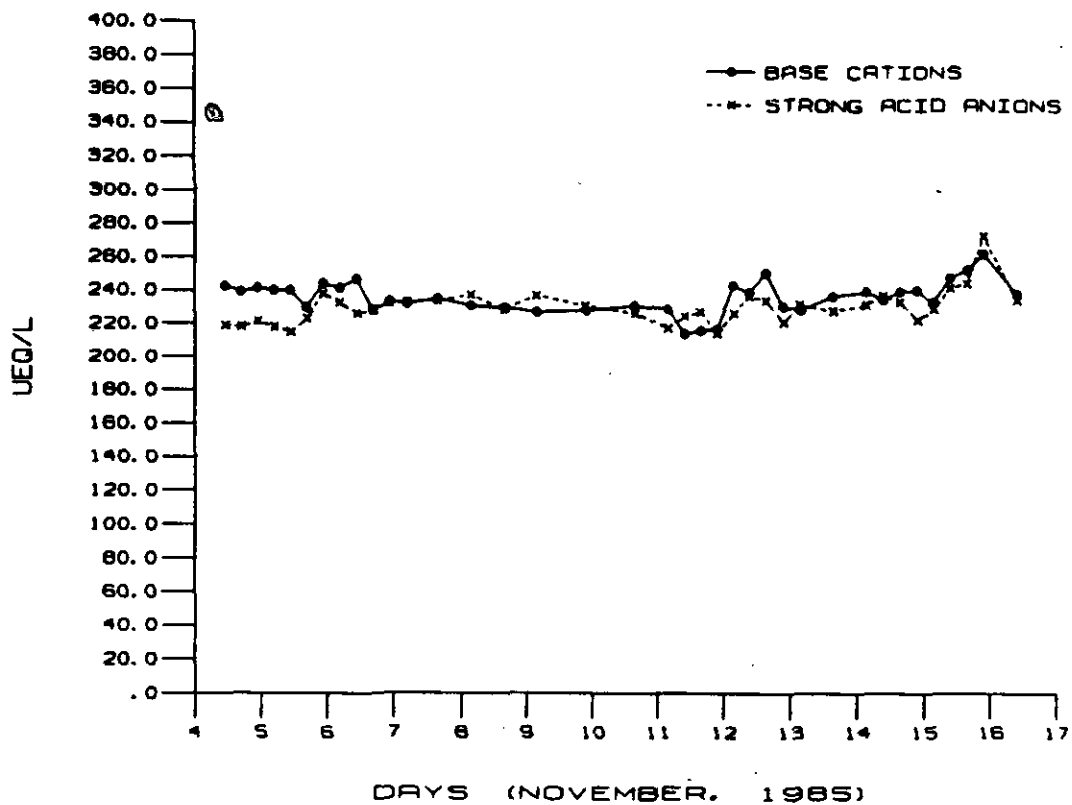


Figure 55. Charge equivalence, in micro-equivalence per liter, of base cations to strong acid anions for site 3 the downstream site.

toxic during moderate to intense rainfall events. The wetland stream, on the other hand, pH changes seems to be buffered by the organic acids present, which in turn complexes available aluminum and decreases its toxicological effect. The downstream site is usually well below toxic limits.

Soil Chemistry Analysis

Aluminum is an important element in the soil environment. Aluminum is incorporated into the granitic parent material and is released into the soil horizons by weathering. Biocycling can bring aluminum to the surface where it then is involved with the natural soil development process. It has been hypothesized that acid rain alters the natural soil development process have been made to explain the movement of aluminum from the soil to the stream environment (Cronan and Schofield, 1979; Driscoll, 1985).

The procedures used for soil sampling and analyses are presented in Chapter III with a summary of these results in Table 7. There are two major soil types in this watershed: spodosols and enceptisols. All of the soils sampled in this study had a fragipan or an apparent fragipan layer within one meter of the surface. Fragipan soils are typical in glacial till washout areas, and are important because they influence the hydrologic flowpath of the catchment, as most of the rainfall will not

Table 7

Summary of the soil analytical results where depth is in centimeters, pH_w is water pH, pH_s is salt pH, %org is percent organic matter content, Ca is exchangeable calcium (meq/100 g soil), Mg is exchangeable magnesium (meq/100 g soil), K is exchangeable potassium (meq/100 g soil), Na is exchangeable sodium (meq/100 g soil), Fe is exchangeable iron (meq/100 g soil), Al is exchangeable aluminum (meq/100 g soil), H is exchangeable hydrogen ion (meq/100 g soil).

SITE 1 - PAXTON

horizon	depth	pH _w	pH _s	%org	Ca	Mg	K	Na	Fe	Al	H
OI	MAT	****	****	67.0	1.25	.63	.34	.08	.01	3.29	1.45
OA	2.5- 0.0	3.55	2.80	34.4	.35	.23	.24	.22	.02	5.95	.69
A	0.0- 6.5	3.70	3.10	18.2	.06	.08	.14	.02	.01	5.99	.42
BW1	6.5-11.5	4.10	3.85	11.1	.06	.02	.04	.01	0.00	1.94	0.00
BW2	11.5-37.0	4.35	4.00	5.6	.05	.01	.03	.01	0.00	.83	.02
BC	37.0-54.5	4.45	4.25	2.7	.04	.01	.03	.01	0.00	.58	.01
CR	54.5-	4.70	4.10	1.0	.10	.02	.09	.02	0.00	.74	.01

SITE 2 - HARLOW

horizon	depth	pH _w	pH _s	%org	Ca	Mg	K	Na	Fe	Al	H
OA	16.5- 0.0	3.35	2.80	41.0	.20	.16	.25	.03	0.00	4.57	1.36
E	0.0- 5.0	3.90	3.00	4.6	.05	.02	.10	.01	.02	3.13	.26
BHS	5.0- 7.5	4.00	3.10	9.6	.09	.04	.09	.02	.01	6.09	.06
BS	7.5-16.5	4.15	3.80	11.3	.05	.01	.04	.01	0.00	2.47	0.00
BW	16.5-32.0	4.35	4.10	9.4	.05	.01	.02	.01	0.00	1.17	0.00

SITE 3 - MERRIMAC

horizon	depth	pH _w	pH _s	%org	Ca	Mg	K	Na	Fe	Al	H
A	0.0- 7.5	3.75	2.85	18.5	.09	.08	.17	.02	.01	4.72	.89
E	7.5-15.0	4.25	3.25	2.2	.02	.01	.03	.01	0.00	3.15	0.00
BW1	15.0-30.5	4.45	4.00	10.0	.03	.01	.03	.01	0.00	1.59	0.00
BW2	30.5-48.5	4.45	4.30	5.1	.02	.01	.02	.01	0.00	.50	.02
BW3	48.5-76.0	4.50	4.30	3.1	.02	0.00	.01	.01	0.00	.30	.01
C	76.0-	4.55	4.40	1.2	.02	0.00	.01	.01	0.00	.31	.02

SITE 4 - CANTON

horizon	depth	pH _w	pH _s	%org	Ca	Mg	K	Na	Fe	Al	H
A	0.0- 6.5	3.55	2.65	22.5	.10	.11	.23	.06	.02	6.21	1.05
E	6.5- 9.0	3.75	2.90	7.2	.05	.08	.10	.03	.21	4.85	.69
BW	9.0-38.0	4.25	3.65	14.7	.05	.04	.05	.02	0.00	2.67	0.00

SITE 5 - RAYPOLE

horizon	depth	pH _w	pH _s	%org	Ca	Mg	K	Na	Fe	Al	H
A	0.0-18.0	3.85	3.35	37.0	.06	.06	.14	.04	0.00	5.87	.01
BW	18.0-33.0	4.05	3.55	9.7	.03	.02	.04	.02	0.00	2.69	0.00
BO	33.0-45.5	4.30	3.90	9.8	.05	.01	.03	.02	0.00	1.55	0.00
CG1	45.5-61.0	4.30	3.95	4.1	.07	.01	.02	.03	0.00	.94	.02
CG2	61.0-81.5	4.50	4.25	3.1	.04	.01	.02	.03	0.00	.39	.01

Table 7 (continued)

SITE 6 - SCITUATE

horizon	depth	pHw	pHs	Sorg	Ca	Mg	K	Na	Fe	Al	H
AP	0.0-25.5	3.95	3.60	16.4	.14	.03	.08	.02	0.00	1.97	.06
BW1	25.5-45.5	4.20	3.85	6.7	.07	.02	.03	.02	0.00	1.31	0.00
BW2	45.5-63.5	4.55	4.10	4.0	.05	.02	.02	.01	0.00	.29	0.00
C	63.5-	4.90	4.50	1.2	.19	.01	.04	.02	0.00	.17	.02

SITE 7 - RIDGEBURY

horizon	depth	pHw	pHs	Sorg	Ca	Mg	K	Na	Fe	Al	H
A	0.0-18.0	3.90	3.65	19.9	.10	.05	.14	.04	0.00	3.01	.01
BG	18.0-33.0	4.35	4.00	7.5	.11	.02	.03	.03	0.00	1.27	.06
CG	33.0-	4.60	4.15	2.1	.06	.01	.03	.02	0.00	.45	0.00

SITE 8 - WHITMAN

horizon	depth	pHw	pHs	Sorg	Ca	Mg	K	Na	Fe	Al	H
A	0.0-20.5	4.10	3.65	18.4	.12	.08	.14	.05	0.00	3.34	0.00
BG	20.5-35.0	4.30	3.90	9.3	.11	.04	.07	.03	0.00	1.75	.08
CG	35.0-	4.40	3.85	13.1	.21	.07	.10	.04	0.00	3.10	.12

SITE 9 - WOODBRIDGE

horizon	depth	pHw	pHs	Sorg	Ca	Mg	K	Na	Fe	Al	H
A	0.0-5.0	4.40	3.85	29.9	.19	.31	.31	.05	.39	6.40	1.91
BW1	5.0-11.5	4.55	3.85	9.4	.06	.07	.15	.03	0.00	2.54	.03
BW2	11.5-18.0	4.60	4.00	8.0	.04	.03	.03	.02	0.00	1.97	0.00
BW3	18.0-30.5	4.65	4.10	5.2	.05	.02	.04	.01	0.00	1.35	0.00
BW4	30.5-53.5	4.70	4.05	4.8	.05	.02	.03	.01	0.00	1.09	.01

flow below this layer. Since more of the precipitation passes through the top meter of soil because of the fragipan layer, discussion of the soil survey will focus on this surficial material.

Nine different soil sites were sampled. Their approximate locations are shown in Figure 2. These nine sites are in the lowland area between the upstream confluence and the downstream sampling site. Nine different soil types along the one kilometer stream segment illustrate the complexity of assessing the importance of the soil horizons.

As seen in Table 7, the soils in this watershed are very acidic. Soil water pH values range from 3.35 to 4.90 with levels generally increasing with increasing depth. The most acidic soil horizon is the upper organic layer.

The percent organic matter content of these soils varies greatly, ranging from 67% in the organic litter layer to 1% in the mineral C horizon. Evidence of podsolization is seen in the Marlow, Merrimac, and Canton soils with a wash out of organics from the E horizon to the lower B horizons. The Whitman muck soil also shows a transport of organic matter from upper to lower horizons. The majority of the organic matter in these soils is in the upper horizons, thus suggesting that the increase in streamwater DOC during storm events is due to rainwater traveling mostly through the upper soil horizons.

Further evidence of podsolization can be seen when examining the exchangeable cations. The Marlow, Merrimac, and Canton soils show a transport of aluminum from the E to the B horizons. In addition, the

Whitman soil shows a similar response. Some of the base cations in these soils have also translocated, but in general the exchangeable base cations decrease with increasing depth.

Soil analyses also show that aluminum dominates the exchangeable cations for all soil types and horizons. The average base saturation for these soils is approximately 10% with the other 90% of the exchangeable cations being primarily aluminum. The exchangeable hydrogen ion is only important in the upper O and A horizons while the exchangeable acid cation iron is insignificant in this soil system.

In conclusion, these soils are very acidic with aluminum dominating the exchangeable cations. Because of the low base saturation of these soils, it becomes apparent that an increase in soil-water anions by acid rain will result in an increase in soil-water acid cations such as aluminum. The upper soil horizons have more organic matter and aluminum as compared to the lower horizons. This suggests that most of the rainwater travels through the upper soil horizons during intensive storms before entering the stream. Soil organic substances can increase the transport of aluminum by complexation reactions as well as by increasing the negative charge in the soil water, thus allowing more cations into solution.

Simulation Model

A mathematical simulation model was developed to gain insight into the various aluminum transport mechanisms within a watershed. The

purpose of the model is to obtain a better understanding of the processes. With additional testing and verification this model may be useful as a predictive tool. The model is presently designed to simulate the kilometer stream segment between the confluence of the mountain and wetland streams and the downstream sampling sites on the West Wachusett Brook. A physical configuration of the study area is depicted in Figure 14. Data from the first week of November were used to test the model. Model inputs consist of precipitation volume and chemistry, stream flow and chemistry, partial pressure of CO₂, and equilibrium constants, as discussed in Chapter IV. The following sections discuss input parameter estimations and model results.

Input Parameter Estimations

Physical properties of the soil environment are needed to simulate the soil compartment submodel. Table 8 lists the model's physical property inputs along with simulated values. The drainage basin area for this portion of the stream is estimated from a topographic map. The soil compartment depth approximates the depth of the O and A horizons. Thus, knowing the drainage basin area and the soil depth, the soil compartment volume can be determined. Minimum and maximum soil-water volumes are determined from soil moisture characteristics. Bulk density, field capacity moisture content, and saturation moisture content are presented in Table 9 with their mean values used in the

Table 8

Simulation Model Inputs

Physical Inputs to the Simulation Model

drainage basin area (m ²)	700,000.
soil compartment depth (cm)	10.
bulk density (gm-m ⁻³)	1.00
soil moisture content	
field capacity	.29
saturation	.58
soil compartment release rate (day ⁻¹)	.38

Chemical Inputs to the Simulation Model

sulfate partitioning coefficient (mg-Kg ⁻¹ /mg-L ⁻¹)	0.5
selectivity coefficients	
$2Al^{3+} + 3MX_2 = 2AlX_2 + 3M^{2+}$	2.5
$M^{2+} + 2KX = MX_2 + 2K^+$	-4.8
partial pressure of CO ₂	
soil	-2.5
atmosphere	-3.5

Initial Conditions

moisture content	.295
soil compartment total sulfate (Kg)	400

Direct Inputs

precipitation	volume and SO ₄ ²⁻
mountain stream	flow, SO ₄ ²⁻ , M ²⁺ , and K ⁺
wetland stream	flow, SO ₄ ²⁻ , M ²⁺ , and K ⁺
soil compartment	DOC
stream compartment	temperature, DOC, TF, Na ⁺ , and Cl ⁻

Table 9

Summary of the soil physical properties where depth is in centimeters, sden is density of solids (gm/cm^3), bden is dry bulk density (gm/cm^3), wet is moisture content (%), fwet is field capacity moisture content (%), swet is saturated moisture content (%).

SITE 1 - PAXTON

horizon	depth	sden	bden	wet	fwet	swet
OI	MAT	****	****	****	****	****
OA	2.5- 0.0	1.47	.98	.19	.17	.33
A	0.0- 6.5	****	****	****	****	****
BW1	6.5-11.5	2.04	.76	.33	.26	.63
BW2	11.5-37.0	****	****	****	****	****
BC	37.0-54.5	****	****	****	****	****
CR	54.5-	****	****	****	****	****

SITE 2 - MARLOW

horizon	depth	sden	bden	wet	fwet	swet
OA	16.5- 0.0	2.57	1.30	.34	.23	.49
E	0.0- 5.0	****	****	****	****	****
BHS	5.0- 7.5	****	****	****	****	****
BS	7.5-16.5	****	****	****	****	****
BW	16.5-32.0	2.80	.78	.45	.42	.72

SITE 3 - MERRINAC

horizon	depth	sden	bden	wet	fwet	swet
A	0.0- 7.5	****	****	****	****	****
E	7.5-15.0	2.26	1.03	.30	.24	.54
BW1	15.0-30.5	****	****	****	****	****
BW2	30.5-48.5	2.39	1.13	.27	.19	.52
BW3	48.5-76.0	****	****	****	****	****
C	76.0-	****	****	****	****	****

SITE 4 - CANTON

horizon	depth	sden	bden	wet	fwet	swet
A	0.0- 6.5	****	****	****	****	****
E	6.5- 9.0	.96	.31	.39	.28	.67
BW	9.0-38.0	2.03	.61	.54	.42	.70

SITE 5 - RAYPOLE

horizon	depth	sden	bden	wet	fwet	swet
A	0.0-18.0	1.65	.37	.70	.51	.78
BW	18.0-33.0	****	****	****	****	****
BG	33.0-45.5	****	****	****	****	****
CG1	45.5-61.0	****	****	****	****	****
CG2	61.0-81.5	****	****	****	****	****

SITE 6 - SCITUATE

horizon	depth	sden	bden	wet	fwet	swet
AP	0.0-25.5	2.27	.68	.43	.34	.70
BW1	25.5-45.5	****	****	****	****	****
BW2	45.5-63.5	****	****	****	****	****
C	63.5-	****	****	****	****	****

Table 9 (continued)

SITE 7 - RIDGEBURY

<u>horizon</u>	<u>depth</u>	<u>sden</u>	<u>bden</u>	<u>wet</u>	<u>fwet</u>	<u>swet</u>
A	0.0-18.0	2.05	.69	.56	.43	.67
BG	18.0-33.0	####	####	####	####	####
CG	33.0-	2.54	1.52	.36	.13	.40

SITE 8 - WHITMAN

<u>horizon</u>	<u>depth</u>	<u>sden</u>	<u>bden</u>	<u>wet</u>	<u>fwet</u>	<u>swet</u>
A	0.0-20.5	####	####	####	####	####
BG	20.5-35.0	2.37	1.23	.42	.22	.48
CG	35.0-	####	####	####	####	####

SITE 9 - WOODBRIDGE

<u>horizon</u>	<u>depth</u>	<u>sden</u>	<u>bden</u>	<u>wet</u>	<u>fwet</u>	<u>swet</u>
A	0.0- 5.0	####	####	####	####	####
BW1	5.0-11.5	####	####	####	####	####
BW2	11.5-18.0	####	####	####	####	####
BW3	18.0-30.5	1.74	..85	.24	.21	.51
BW4	30.5-53.5	####	####	####	####	####

simulation run listed in Table 8. The soil compartment is modeled as a simple linear reservoir with the first order release rate determined from hydrograph analysis (see Figure 17).

Chemical inputs to the simulation model are also presented in Table 8. The sulfate partitioning coefficient is essentially a calibration parameter. The value selected for this lumped parameter is within the range of typical literature values (Barrow, 1967; Singh, 1984). Furthermore, a preliminary sulfate adsorption study by Thorogood (1986) and personal communications with Dr. John Baker confirmed that the value used is reasonable. Selectivity coefficients are also incorporated into the modeling framework as calibration parameters since they are difficult to measure and may change temporally (over seasons and years). The partial pressure of CO_2 in the soil environment is assumed to be 10 times the atmospheric level because of microbial activity (Dr. John Baker, personal communication). Soil partial pressure levels can be as much as 100 times atmospheric (Stumm and Morgan, 1982).

Since this is a time-variable model, simulating periods up to a week in length, initial conditions for the soil compartment's moisture content and total sulfate are needed to start the simulation. Initial conditions for the November simulation are listed in Table 8. The values for these initial conditions are determined by calibration.

A summary of direct inputs to the model are also listed in Table 8. All of these inputs, except for the soil compartment DOC which is estimated by a mass balance analysis using upstream and downstream conditions, are directly measured in the field. The negative charge

associated with the soil-water DOC is assumed to be the same as the streamwater organic charge presented in Chapter IV (i.e., 7.0 meq/mg DOC). Equilibrium constants and enthalpy data used for the simulation are listed in Appendix B.

Precipitation volumes and chemistry, in particular SO_4^{2-} , are needed to drive the hydrologic and the soil chemistry submodels. Hourly precipitation volumes, obtained from the National Weather Service's gauging station located at the Worcester Municipal Airport, are used in the simulation runs. An on-site rain gauge is also used for comparison purposes. Corrections to the National Weather Service's gauge are made, based on the watershed's gauge. Precipitation sulfate concentrations were measured on a daily basis from rainwater collected at the study site.

Continuous stream flow was gauged only at the downstream site, therefore continuous flows for the two upstream sites were estimated from the downstream site. The estimation was performed by regressing the daily single point measurements of the upstream sites on the downstream site. Stream flows at all three stream sites were generally measured within a one-hour period and thus assumed to be simultaneous measurements. This assumption seems reasonable for low-flow conditions when the stream flows are not changing rapidly, but during high-flow periods this may not be valid. Nonetheless, regression of the mountain stream and the wetland stream on the downstream site were performed with the following results.

$$Q_1 = 0.0567 + 0.3039 \times Q_3 \quad (5.1)$$

(n=36, correlation coefficient r=.95)

$$Q_2 = -0.1222 + 0.5440 \times Q_3 \quad (5.2)$$

(n=36, correlation coefficient r=.97)

where:

Q_1 = mountain stream flow (m^3-s^{-1})

Q_2 = wetland stream flow (m^3-s^{-1})

Q_3 = downstream flow (m^3-s^{-1})

As seen from the slopes of the regression lines, approximately 85% of the downstream flow comes from the two upstreams with the remaining 15% coming from groundwater contributions.

The upstream SO_4^{2-} , M^{2+} , and K^+ input values are direct streamwater measurements. The streamwater compartment is assumed to be completely mixed, with input levels for temperature, total fluoride, DOC, Na^+ , and Cl^- assumed to be equal to their measured values at the downstream site.

Results and Discussion

Results of the hydrologic submodel for the first week of November are presented in Figures 56 and 57. This simple model predicts the downstream flow and groundwater contribution quite well. Calibration simulations, though, showed a stream flow lag of approximately four hours. This lag is due to the simple one box model not taking into account the travel time of the rainwater through the soil horizons.

SITE 3 STREAM FLOW SIMULATED VS MEASURED

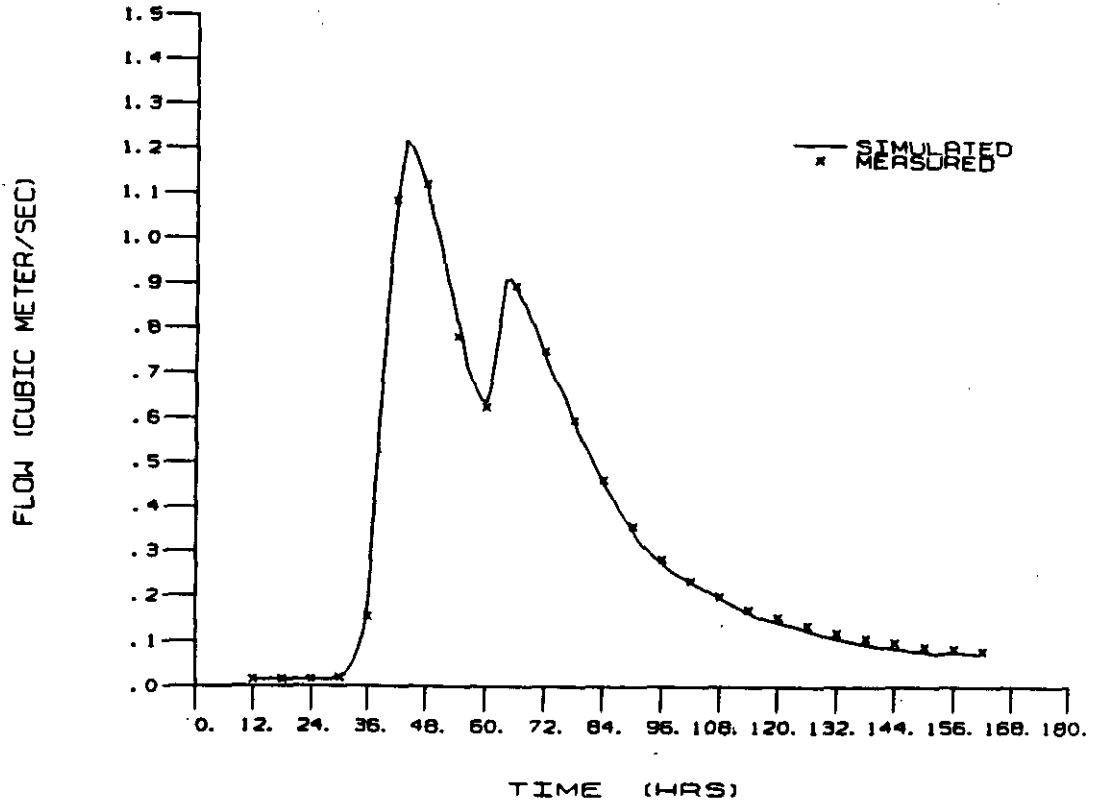


Figure 56. Simulated verses measured streamflow at the downstream site. Time starts on 4 November 1985.

GROUNDWATER FLOW SIMULATED VS MEASURED

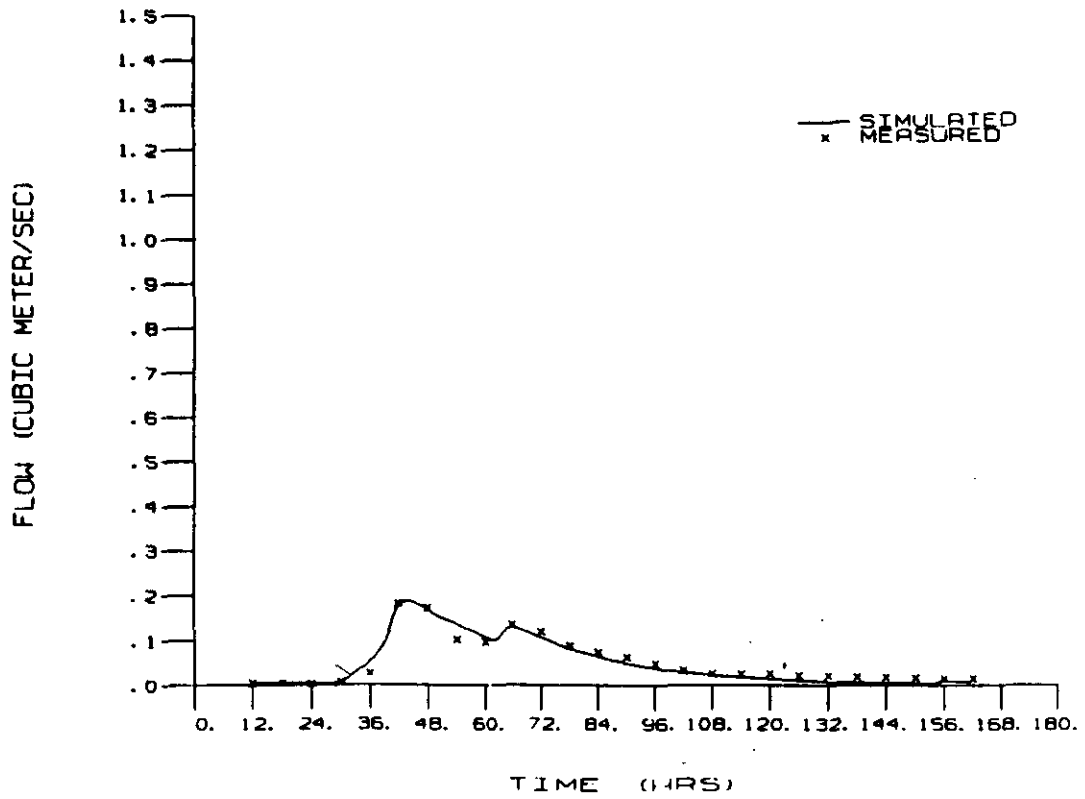


Figure 57. Simulated versus measured groundwater flow. Time starts on 4 November 1985.

Thus, a modification to the original model formulation was made, by incorporating a lag term, to enable a better prediction. Essentially, the lag model releases water from the soil compartment based on the volume four hours previously. This lag represents the average travel time that a water molecule spends in the soil compartment. Conceptually it can be thought of as the rain falling during hour four pushing the rain that fell during hour one out of the soil compartment and into the stream compartment. Since approximately 85% of the downstream flow is an input from the two upstreams, the hydrologic model depends on the soil compartment to make up the difference. The simple linear reservoir model simulates the groundwater contribution quite well.

Next the conservative anion and cations (i.e., SO_4^{2-} , M^{2+} , and K^+) in the streamwater compartment were calibrated. Since the two upstream concentrations are fixed at their measured levels, predicting the downstream concentrations depends on calibrating the soil chemistry submodel. Plots of the upstream input variables are shown in Appendix F.

The sulfate model was calibrated by adjusting the partitioning coefficient and the initial total mass of sulfate in the soil compartment. The results of this parameter estimation are presented in the previous section. The sulfate model was also modified to include a lag term, using the same lag response as used in the hydrologic model. Results of this run are shown in Figure 58. The simulation run underestimates the downstream sulfate concentration during the storm. Considering the simplicity of the model, though, the prediction is good

with an absolute error of less than 5 $\mu\text{mol/L}$ corresponding to a relative error of approximately 7%.

The base cations were calibrated next with simulation plots of the divalent cations and potassium in Figures 59 and 60, respectively. Selectivity coefficients were used as calibration parameters for the base cations with their final calibrated values presented in Table 8. There was good prediction, except during the peak of the storm, of the streamwater's divalent cations throughout the study period. This discrepancy during peak runoff could either be due to analytical measurement errors or perhaps the absence of a major component in the soil chemistry submodel. For the divalent cations to drop in the soil water an equivalent drop in anionic charge must occur. A decrease in soil-water negative charge could be attributed to the uncertainty of the organic anion charge in the soil water. McDowell and Wood (1984) found an inverse relationship between DOC and soil-water volume in a New Hampshire spodosol A2 horizon. Thus, during the peak of the storm, DOC levels in the soil water could be less than simulated and in turn the negative charge associated with the DOC could be less. The potassium simulation predicted the measured data quite well. It should be noted, though, the dominance of the wetland stream on this simulation with potassium levels approaching those of calcium on a mole basis in the wetland stream during the peak of the storm. See Appendix F for input levels.

SITE 3 SULFATE SIMULATED VS MEASURED

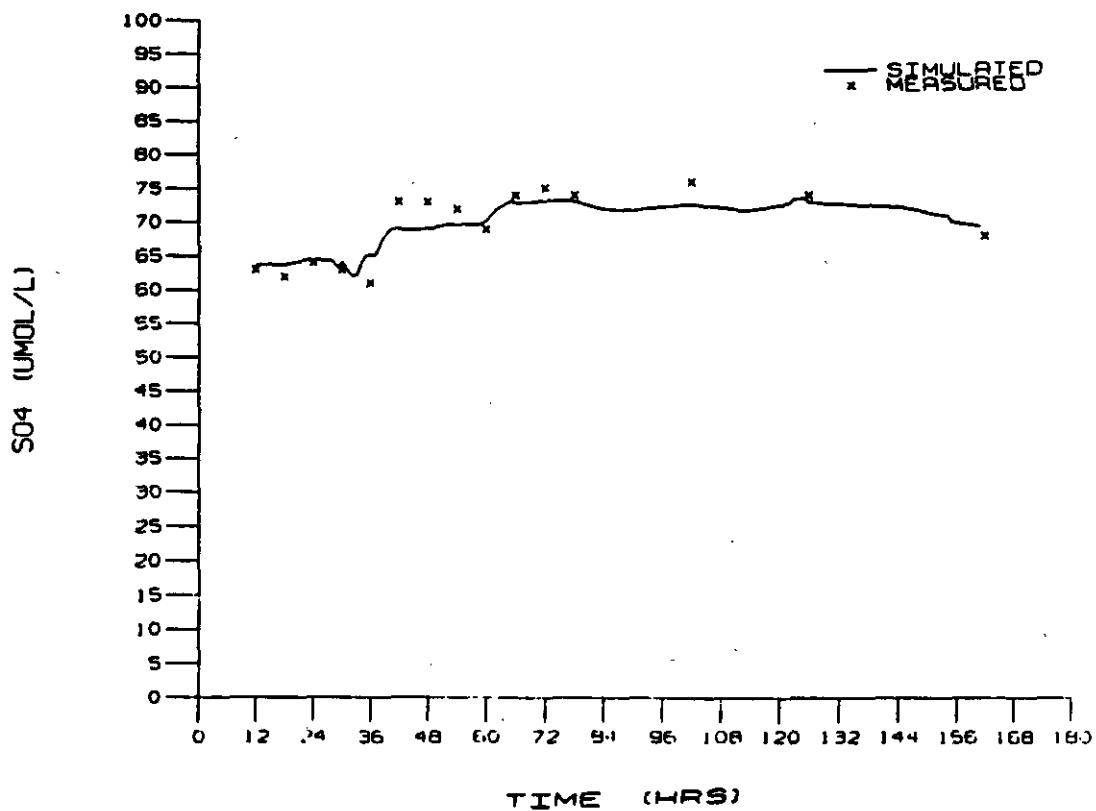


Figure 58. Simulated versus measured sulfate concentration at the downstream site. Time starts on 4 November 1985.

SITE 3 DIVALENT CATIONS

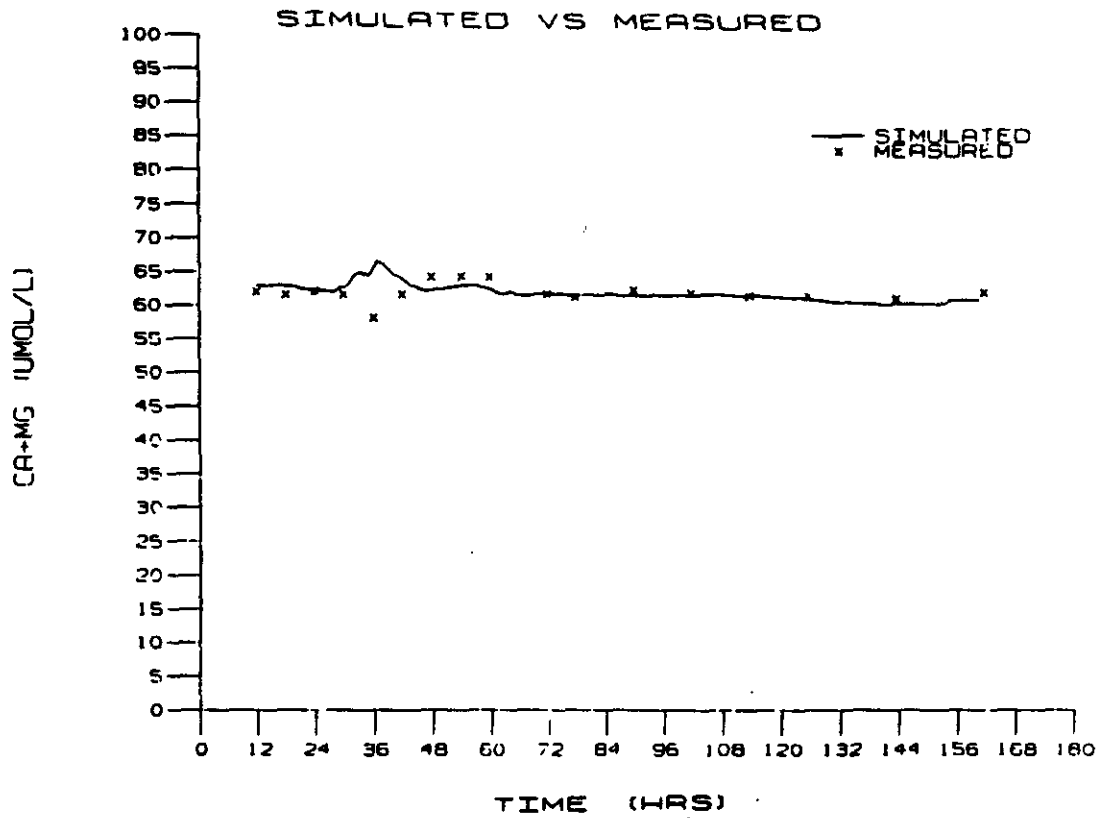


Figure 59. Simulated verses measured divalent cation concentration at the downstream site. Time starts on 4 November 1985.

SITE 3 POTASSIUM SIMULATED VS MEASURED

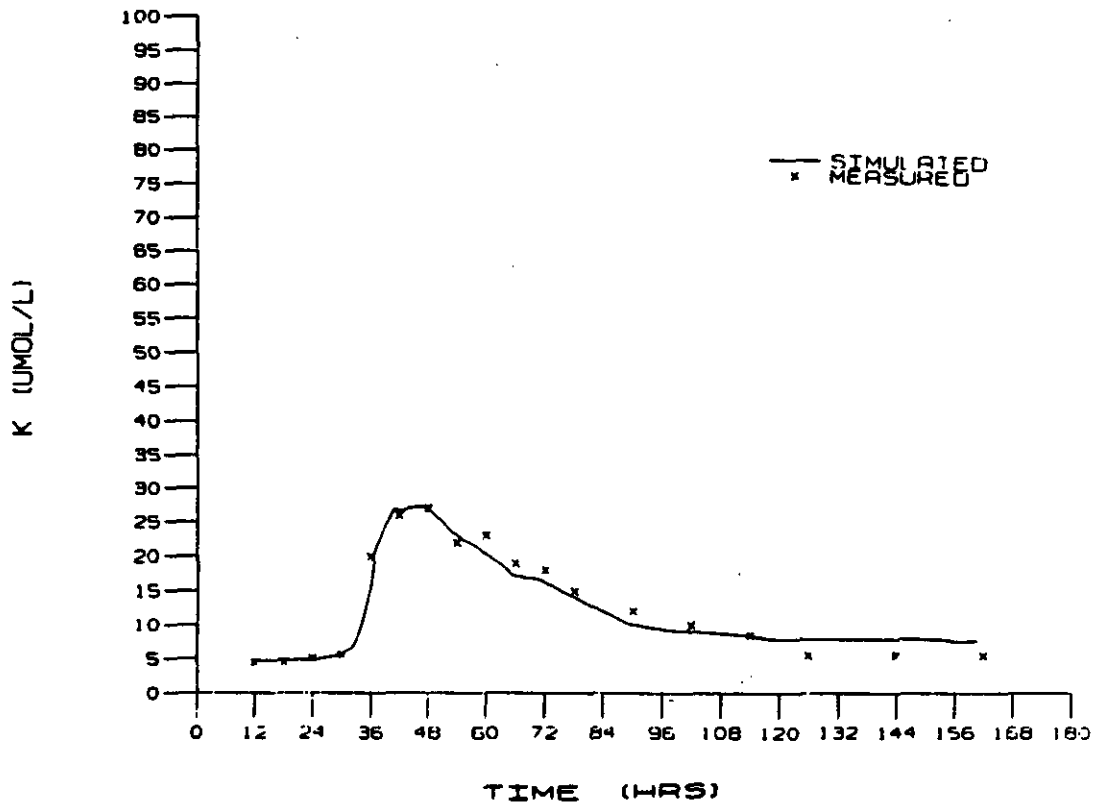


Figure 60. Simulated verses measured potassium concentration at the downstream site. Time starts on 4 November 1985.

With the conservative elements calibrated, the next step is to simulate the non-conservative state variables pH, ANC, monomeric aluminum, and organic monomeric aluminum. Results of these simulations are presented in Figures 61 through 64. In performing this calibration a major assumption on the controlling mineral phase was made. It appears that when the streamwater pH is less than 4.75 another mineral, besides gibbsite, may actually control the free aluminum concentration (see the aluminum solubility plot in Figure 65). Thus, to simulate this change in controlling mineral phase without completely rewriting the model, it was assumed that when the pH exceeds 4.75 natural gibbsite controls free aluminum concentration and at lower pH levels synthetic gibbsite controls. Essentially this adjustment lowers the levels of pH and aluminum when the pH drops below 4.75. Nordstrom and Ball (1986) also demonstrated a transition from gibbsite equilibrium when aqueous systems were above pH 4.6-4.9 to a disequilibrium when below these levels.

Another modification to the original model formulation was the inclusion of sodium and chloride in the streamwater compartment. It was determined from statistical analysis that these two ions did not balance each other on an equivalence basis as was originally assumed and thus could not be ignored. These two ions were not modeled, but were direct inputs to the streamwater compartment. Plots of these two ions are in a separate document.

SITE 3 PH SIMULATED VS MEASURED

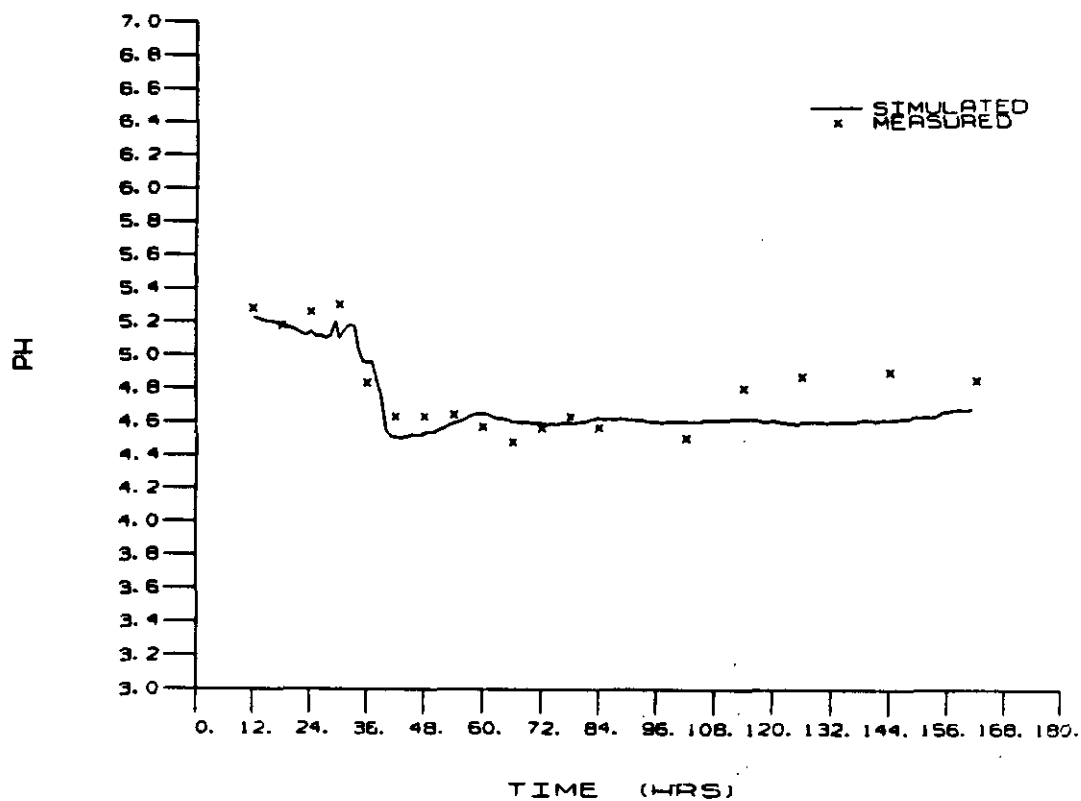


Figure 61. Simulated verses measured pH levels at the downstream site. Time starts on 4 November 1985.

SITE 3 ANC SIMULATED VS MEASURED

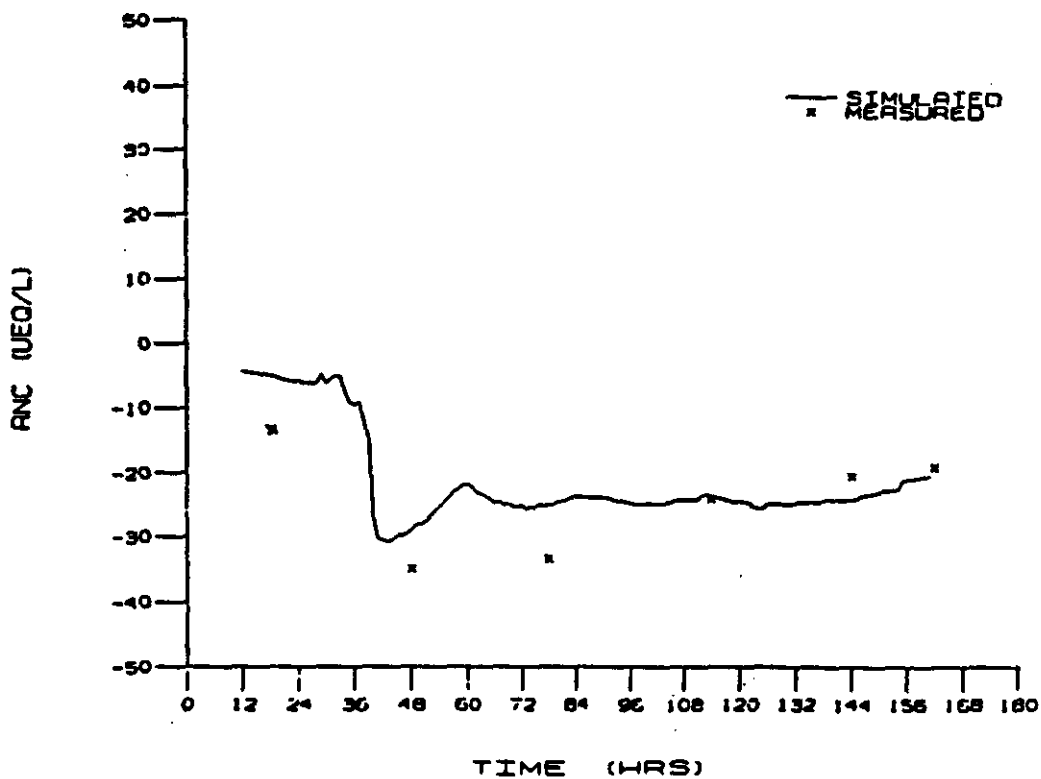


Figure 62. Simulated verses measured acid neutralizing capacity (ANC) at the downstream site. Time starts on 4 November 1985.

SITE 3 MONOMERIC AL SIMULATED VS MEASURED

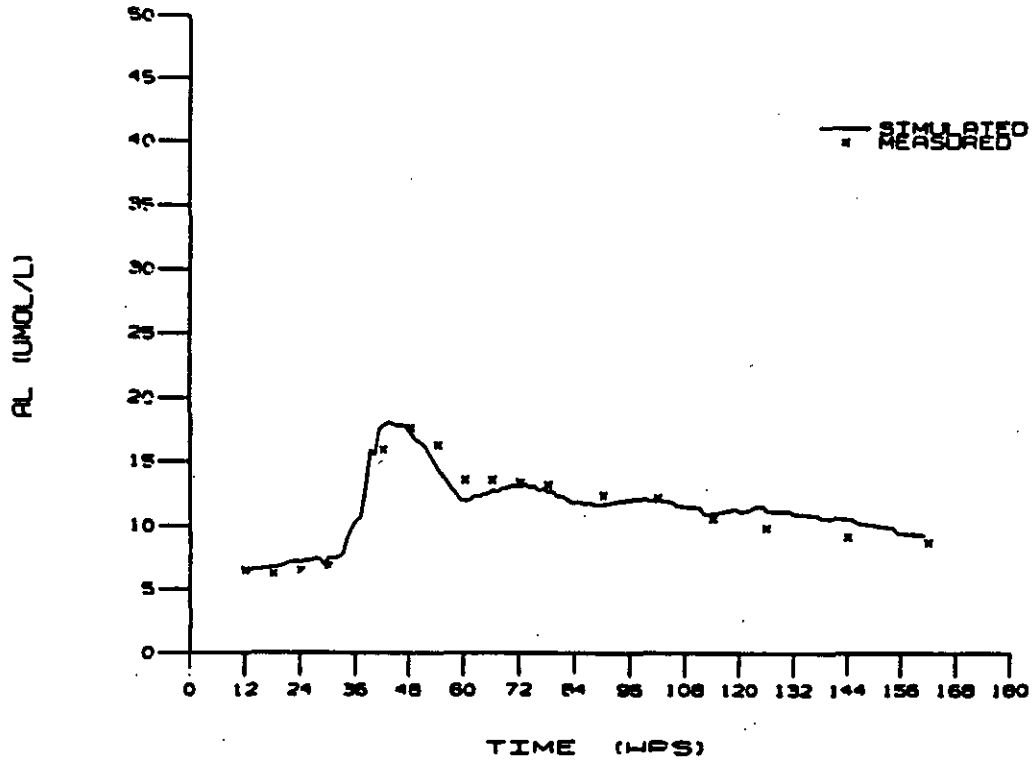


Figure 63. Simulated versus measured total monomeric aluminum at the downstream site. Time starts on 4 November 1985.

SITE 3 ORGANIC AL SIMULATED VS MEASURED

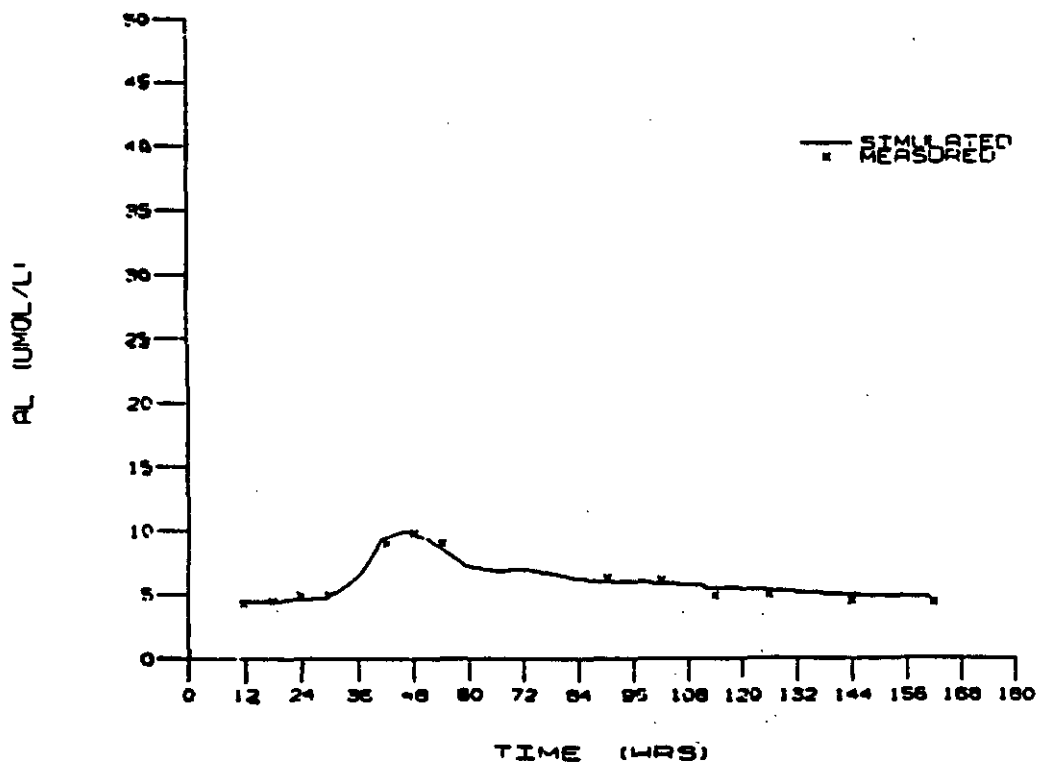


Figure 64. Simulated verses measured organic monomeric aluminum at the downstream site. Time starts on 4 November 1985.

SOLUBILITY PLOT FOR SITES

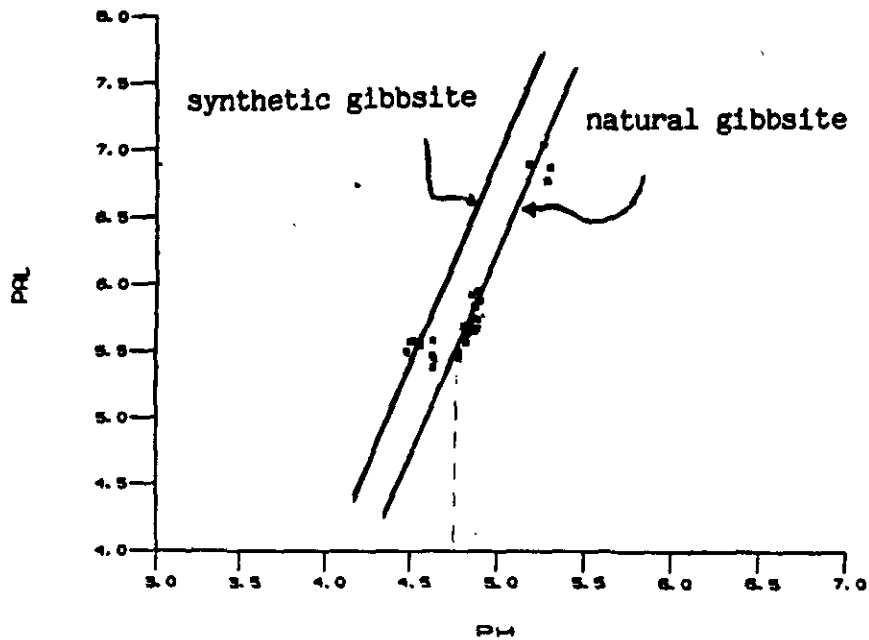


Figure 65. Solubility plot for the downstream site with $-\log(\text{Al}^{3+})$ plotted against $-\log(\text{H}^+)$.

The organic anion charge and the organic aluminum fraction were modeled by the relationships discussed in Chapter IV. These empirical formulations work quite well for this particular system.

In conclusion, the model describes the transport of aluminum extremely well during the peak of the storm. The two most important factors controlling aluminum during the storm are the organic anion, since it is needed to balance Al, and the change in mineral phase solubility around pH 4.75. The organic anion charge regulates the aluminum concentration at the downstream site as the base cations balance the strong acid anions (Figure 55). Thus, the increase of H^+ and Al^{3+} during the storm corresponds to the increase in DOC and its associated negative charge. The change in mineral phase solubility around pH 4.75 is also important since the model would over-estimate aluminum and under-estimate pH if natural gibbsite were used during the peak of the storm. This apparent change in solubility is an important consideration when modeling streamwater pH levels below 5. The simulation model is helpful in defining the important processes of aluminum transport and streamwater acidification. Understanding the role of the base cations, the strong acid anions, the organic acids, and the controlling solubility mineral phase is fundamental to describing the fate of aluminum in a watershed system. The model seems to account for the major acidification mechanisms by describing streamwater chemistry in a small Massachusetts brook.

CHAPTER VI
CONCLUSIONS AND RECOMMENDATIONS

Conclusions

Based on the results of this study the following conclusions are made.

1. The West Wachusett Brook is an acid-sensitive second order stream with its measured acid neutralizing capacity rarely exceeding zero. ANC values are positive only during the summer months at the wetland stream and downstream sites. Measured streamwater pH levels during this study ranged from a low of 4.2 at the mountain stream site to a high of 5.9 at the downstream site.
2. The hydrologic flowpath through the various soil horizons greatly influences streamwater quality. For example, during summer low-flow periods the rainwater has more time to react with the lower soil horizons resulting in higher streamwater pH levels, whereas during the spring and fall high runoff periods the rainwater has less contact time (mostly with the upper soil horizons) resulting in lower streamwater pH levels.
3. Rainfall volume influences streamwater acidity more than does rainfall acidity in this particular brook. Evidence of this is from the high runoff November hurricane storm in which a volume-weighted average

rainwater pH of 5.04 lowered the mountain stream's pH from 5.1 to 4.2. More acidic and less intense rains from the Midwest, in May and the second week of November, had less of an effect.

4. Equivalent charges of the base cations and the strong acid anions are important in regulating streamwater aluminum levels. An excess of strong acid anions (relative to base cations) must be balanced by acid cations (e.g., Al^{3+} and H^+). Moreover, if the equivalent charge of the strong acid anions are less than the base cations, aluminum is controlled by the amount of organic anion charge in solution. In this study the mountain stream's aluminum level is regulated mostly by the imbalance of inorganic charge, whereas the wetland stream and the downstream sites are controlled more by the organic anion charge.

5. High volume storms occurring after dry periods, have the potential of flushing high levels of organic substances from the ecosystem. These organic acids buffer pH changes as well as regulate aluminum levels by complexation reactions and by increasing the anionic charge in the soil and stream water.

6. The soil in this catchment is quite acidic with pH levels ranging from 3.35 to 4.90. Aluminum dominates the exchangeable cations with an average soil base saturation of approximately 10%. Thus, the primary source of aluminum appears to be from the soil environment.

7. The upper soil horizons (O and A) have considerably more organic matter and aluminum than do the lower soil horizons (B and C). Thus, soil chemistry suggests that during intensive storm events, i.e., when streamwater, DOC and aluminum levels increase significantly, the rainwater travels mostly through the upper soil horizons before entering the stream.

8. Aluminum speciation shows the mountain stream to exhibit the potential for aluminum toxicity, but only during moderate-to-intense rainfall events. The wetland stream, on the other hand, dominated by the organo-aluminum fraction shows a minimal toxicological effect on aquatic organism.

9. The wetland with its organic acids has an amazing ability to mitigate the effects of acid rain, especially if one assumes the stream feeding the wetland has similar chemical composition to that of the mountain stream, by buffering pH changes as well as chelating aluminum.

10. The simulation model describes the transport of aluminum within the West Wachusett Brook quite well, thus suggesting that the major mechanisms controlling the fate of aluminum have been included.

11. The simulation modeling effort revealed that the two most important processes controlling aluminum at the downstream site are the organic anion charge and the disequilibrium with an aluminum trihydroxide

mineral phase at low pH levels. The organic anion charge regulates aluminum at the downstream site because the base cations are in balance with the the strong acid anions. The importance of the disequilibrium with natural gibbsite at low pH levels is seen in the solubility plot (Figure 60).

12. Understanding the role of the base cations, the strong acid anions, the organic acids, and the controlling mineral phase is fundamental in describing the fate of aluminum within a watershed system.

Recommendations

Based on the results of this study the following recommendations are made.

1. A detailed study should be performed focusing on the hydrologic flowpath as well as the subsequent transport of organics, aluminum, base cations, and strong acid anions through the soil horizons, both spatially and temporally, during a storm event.
2. Further study should focus on the wetland's buffering effects, especially the role of organic acids, by sampling upstream and downstream of the wetland during a storm event.
3. Future modifications to the modeling framework could include: the incorporation of another mineral phase besides gibbsite to control

aluminum levels under low pH conditions, explicitly including organic transport in the soil and stream compartments, adding a base flow compartment to the soil submodel, and including snow hydrology so that the snowmelt responses could be addressed.

4. Future studies should include intensive sampling during both the winter and summer runoff periods so that acidification at these time periods could be investigated.

5. A laboratory fish bioassay study should be conducted that simulates actual time-series responses of natural streamwater conditions.

BIBLIOGRAPHY

- Andelman, J. B., "Incidence, Variability, and Controlling Factors for Trace Elements in Natural Fresh Waters," In: Trace Metals and Metal-Organic Interactions in Natural Waters, Edited by Philip C. Singer, Ann Arbor Science (1973).
- Baker, J. P. and C. L. Schofield, "Aluminum Toxicity to Fish as Related to Acid Precipitation and Adirondack Surface Water Quality," in Proceedings of the International Conference on Ecological Impacts of Acid Precipitation, D. Drablos and A. Tollan, Eds., Norway, SNSF Project (1980).
- Baker, J. P., "Aluminum Toxicity to Fish as Related to Acidic Precipitation and Adirondack Surface Water Quality at Ithaca, N. Y.," Ph.D. Thesis, Cornell University, (1981).
- Baker, J. P., and C. L. Schofield, "Aluminum Toxicity to Fish in Acidic Waters," Water, Air, and Soil Pollution, Vol. 18, 289-309 (1982).
- Ball, D. F., "Loss-On-Ignition as an Estimate of Organic Matter and Organic Carbon in Non-Calcareous Soils," Journal of Soil Science, Vol. 15, No. 1, 84-92 (1964).
- Ball, J. W., D. K. Nordstrom, and E. A. Jenne, "Additional and Revised Thermochemical Data and Computer Code for WATEQ-2 Computerized Chemical Model for Trace and Major Element Speciation and Mineral Equilibria of Natural Waters," U. S. Geological Survey Water Resources Investigations WRI 78-116 (1980).
- Barnard, T. E. and J. J. Bisogni, "Errors in Gran Function Analysis of Titration Data for Dilute Acidified Water," Water Research, Vol. 19, No. 3, 393-399 (1985).
- Barnes, R. B., "The Determination of Specific Forms of Aluminum in Natural Water," Chemical Geology, Vol. 15, 177-191 (1975).
- Barrow, N. J., "Studies on the Adsorption of Sulfate by Soils," Soil Science, Vol. 104, No. 5, 342-349 (1967).
- Berner, R. A., "Kinetics of Weathering and Diagenesis," Reviews in Mineralogy, Vol. 8, 111-134 (1981).
- Bloom, P. R., M. B. McBride, and Chadbourne, "Adsorption of Aluminum by a Smectite: I. Surface Hydrolysis During Ca^{2+} - Al^{3+}

- Exchange," Soil Science Society of America Journal, Vol. 41, 1068-1077 (1977).
- Bloom, P. R., M. C. McBride, and R. M. Weaver, "Aluminum Organic Matter in Acid Soils: Buffering and Solution Aluminum Activity," Soil Science Society of America Journal, Vol. 43, 488-493 (1979).
- Bohn, H. L., B. L. McNeal, and G. A. O'Connor, Soil Chemistry, A Wiley-Interscience Pub., John Wiley & Sons (1979).
- Brown, D., "The Effects of Various Cations on the Survival of Brown Trout, (*Salmo trutta*) at low pH's," Journal of Fish Biology, Vol. 18, 31-40 (1981).
- Buchanan, T. J. and W. P. Somers, Discharge Measurements at Gaging Stations, Techniques of Water-Resources Investigations of the United States Geological Survey, Book 3, Chapter A8, (1969).
- Burden, R. L. and J. D. Faires, Numerical Analysis, Prindle, Weber, and Schmidt Publishers, Boston, Massachusetts (1985).
- Butler, J. N., Ionic Equilibrium A Mathematical Approach, Addison-Wesley Publishing Company, Reading, Massachusetts (1964).
- Chen, C. W., J. D. Dean, S. A. Gherini, and R. A. Goldstein, "Acid Rain Model: Hydrologic Module," Journal of the Environmental Engineering Division, ASCE, Vol. 108, No. EE3, (1982).
- Chen, C. W., S. A. Gherini, R. J. M. Hudson, and J. D. Dean, "The Integrated Lake-Watershed Acidification Study, Volume 1: Model Principles and Application Procedures," Electric Power Research Institute, Palo Alto, California (1983).
- Christophersen, N. and R. F. Wright, "Sulfate Budget and a Model for Sulfate Concentrations in Stream Water at Birkenes, a Small Forested Catchment in Southernmost Norway," Water Resources Research, Vol. 17, No. 2, 377-389 (1981).
- Christophersen, N., H. M. Seip, and R. F. Wright, "A Model for Streamwater Chemistry at Birkenes, Norway," Water Resources Research, Vol. 18, No. 4, 977-996 (1982).
- Christophersen, N., L. H. Dymbe, M. Johannssen, and H. M. Seip, "A Model for Sulfate in Streamwater at Storgama, Southern Norway," Ecological Modelling, Vol. 21, 35-61 (1983/1984).

- Christophersen, N., S. Rustad, and H. M. Seip, "Modelling Streamwater Chemistry with Snowmelt," Royal Society of London, Philosophical Transaction, (1984).
- Cleveland, L., E. E. Little, S. J. Hamilton, D. R. Buckler, and J. B. Hunn, "Interactive Toxicity of Aluminum and Acidity to Early Life Stages of Brook Trout", Transactions of American Fisheries Society, Vol. 115, 610-620 (1986).
- Cosby, B. J., G. M. Hornberger, J. N. Galloway, and R. F. Wright, "Modeling the Effects of Acid Deposition: Assessment of a Lumped Parameter Model of Soil Water and Streamwater Chemistry," Water Resources Research, Vol. 21, No. 1, 51-63 (1985a).
- Cosby, B. J., R. F. Wright, G. M. Hornberger, and J. N. Galloway, "Modeling the Effects of Acid Deposition: Estimation of Long-Term Water Quality Responses in a Small Forested Catchment," Water Resources Research, Vol. 21, No. 11, 1591-1601 (1985b).
- Cronan, C. S. and C. L. Schofield, "Aluminum Leaching Response to Acid Precipitation: Effects on High-Elevation Watersheds in the Northeast," Science, Vol. 204, 304-305 (1979).
- Cronan, C. S., W. A. Reiners, and R. C. Reynolds, "The Impact of Acid Precipitation on Forest Canopies and Soils in the Northern U. S.," in Proceedings of the International Conference on Ecological Impacts of Acid Precipitation, D. Drablos and A. Tollan, Eds., Norway, SNSF Project (1980).
- Cronan, C. S., "Biogeochemical Responses of Forest Canopies to Acid Precipitation," In: Direct and Indirect Effects of Acidic Deposition on Vegetation, Edited by Rick A. Linthurst, Acid Precipitation Series, Vol. 5, Ann Arbor Science (1984).
- David, M. B. and C. T. Driscoll, "Aluminum Speciation and Equilibria in Soil Solutions of a Haplorthod in the Adirondack Mountains, New York," Geoderma, Vol. 33, 297-318 (1984).
- Davies, B. E., "Loss-On-Ignition as an Estimate of Soil Organic Matter," Soil Science Society of America Proceedings, Vol. 38, 150-151 (1974).
- Daye, P. G. and E. T. Garside., "Lethal Levels of pH for Brook Trout (Salvelinus fontinalis, Mitchill)," Canadian Journal of Zoology, Vol. 53, No. 5, 639-641 (1975).

- Deju, R. A., "A Model of Chemical Weathering of Silicate Minerals," Geological Society of American Bulletin, Vol. 82, 1055-1062 (1971).
- Dickson, W., "Some Effects of the Acidification of Swedish Lakes," International Association of Theoretical and Applied Limnology, Vol. 20, Part 2, 851-856 (1978).
- Drever, J. I., The Geochemistry of Natural Waters, Prentice-Hall, Englewood Cliffs, New Jersey (1982).
- Driscoll, C. T., "Chemical characterization of some dilute acidified lakes and streams in the Adirondack region of New York State," Ph.D. Thesis, Cornell University (1980).
- Driscoll, C. T., J. P. Baker, J. J. Bisogni, and C. L. Schofield, "Effects of Aluminum Speciation on Fish in Dilute Acidified Waters," Nature, Vol. 284, No. 5751, 161-164 (1980).
- Driscoll, C. T., J. R. White, G. C. Schafran, and J. D. Rendall, "CaCO₃ Neutralization of Acidified Surface Waters," Journal of Environmental Engineering, ASCE, Vol. 108, No. EE6, (1982).
- Driscoll, C. T. and J. J. Bisogni, "Weak Acid/Base Systems in Dilute Acidified Lakes and Streams of the Adirondack Region of New York State," Modeling Total Acid Precipitation Impacts, Acid Precipitation Series, Vol. 9, J. L. Schnoor, Ed., J. I. Teasley, Series Ed., Butterworth Publishers, Boston, 53-71 (1984).
- Driscoll, C. T., "Procedure for the Fractionation of Aqueous Aluminum in Dilute Acidic Waters," International Journal of Environmental Analytical Chemistry, Vol. 16, 267-283 (1984).
- Driscoll C. T. and W. D. Schecher, "Nature and Rates of Aluminum Removal in Acidic Surface Waters," ALBIOS 1984 Annual Report.
- Driscoll, C. T., N. van Breemen, and J. Mulder, "Aluminum Chemistry in a Forested Spodosol," Soil Science Society of America Journal, Vol. 49, 437-444 (1985).
- Driscoll, C. T., "Aluminum in Acidic Surface Waters: Chemistry, Transport, and Effects," Environmental Health Perspectives, Vol. 63, 93-104 (1985).
- Eshleman, K. N., "A biogeochemical approach to reservoir acidification by atmospheric deposition," MS Thesis, Massachusetts Institute of Technology, (1982).

- Eshleman, K. N. and H. F. Hemond, "The Role of Organic Acids in the Acid-Base Status of Surface Waters at Bickford Watershed, Massachusetts," Water Resources Research, Vol. 21, No. 10, 1503-1510 (1985).
- Eshleman, K. N., "Acid Deposition Effects on a Massachusetts Reservoir and Watershed," Ph.D. Dissertation, Massachusetts Institute of Technology, (1985).
- Freeman, R. A. and W. H. Everhart, "Toxicity of Aluminum Hydroxide Complexes in Neutral and Basic Media to Rainbow Trout," Transactions of the American Fisheries Society, Vol. 100, No. 4, 644-658 (1971).
- Frink, C. R. and G. K. Voight, "Potential Effects of Acid Precipitation on Soils in the Humid Temperate Zone," Water, Air, and Soil Pollution, Vol. 7, No. 3, 371-388 (1977).
- Fromm, P. O., "A Review of Some Physiological and Toxicological Responses of Freshwater Fish to Acid Stress," Environmental Biology of Fishes, Vol. 5, No. 1, 79-83 (1980).
- Gaines, G. L. and H. C. Thomas, "Adsorption Studies on Clay Minerals: II. Formulation of the Thermodynamics of Exchange Adsorption," Journal of Chemical Physics, Vol. 21, No. 4, (1953).
- Gapon, E. N., "On the Theory of Exchange Adsorption in Soils," (In Russian, original not seen) Journal of General Chemistry, U.S.S.R., Vol. 3, 144-163 (1933).
- Grahn, G., "Determination of the Equivalence Point in Potentiometric Titrations," International Congress on Analytical Chemistry, Vol. 77, No. 11, 661-667 (1952).
- Grahn, O., "Macrophyte Succession in Swedish Lakes Caused by Deposition of Airborne Acid Substances," Water, Air, and Soil Pollution, Vol. 7, No. 3, 295-305 (1977).
- Grahn, O., "Fishkills in Two Moderately Acid Lakes Due to High Aluminum Concentrations," in Proceedings of the International Conference on Ecological Impacts of Acid Precipitation, D. Drablos and A. Tollan, Eds., Norway, SNSF Project (1980).
- Hall, R. J., G. E. Likens, S. B. Fiance, and G. R. Hendrey, "Experimental Acidification of a Stream in the Hubbard Brook Experimental Forest, New Hampshire," Ecology, Vol. 61, 976-989 (1980).

- Hall, R. J., and G. E. Likens, "Chemical Flux in an Acid-Stressed Stream," Nature, Vol. 292, 329 (1981).
- Hem, J. D., Advances in Chemistry Series, 73, American Chemical Society, Washington D.C. (1968a).
- Hem, J. D., "Graphical Methods for Studies of Aqueous Aluminum Hydroxide, Fluoride, and Sulfate Complexes," U.S. Geological Survey Water Supply Paper 1827-B, (1968b).
- Hemond, H. F. and K. N. Eshleman, "Neutralization of Acid Deposition by Nitrate Retention at Bickford Watershed, Massachusetts," Water Resources Research, Vol. 20, No. 11, 1718-1724 (1984).
- Hendrey, G. R., K. Baalsrud, T. S. Traaen, M. Laake, and G. Raddum, "Acid Precipitation: Some Hydrobiological Changes," Ambio, Vol. 5, 224-227 (1976).
- Hillel, D., Introduction to Soil Physics, Academic Press, Orlando, Florida (1982).
- Holland, H. D., The Chemistry of the Atmosphere and Oceans, John Wiley and Sons, New York (1978).
- Hooper, R. P. and C. A. Shoemaker, "Aluminum Mobilization in an Acidic Headwater Stream: Temporal Variation and Mineral Dissolution Disequilibria," Science, Vol. 229, 463-465 (1985).
- Hooper, R. P. and C. T. Driscoll, "Comment on 'Modeling the Effects of Acid Deposition: Assessment of a Lumped Parameter Model of Soil Water and Streamwater Chemistry' by B. J. Cosby, G. M. Hornberger, J. N. Galloway, and R. F. Wright," Water Resources Research, (1986).
- Johannessen, M., "Aluminum, a Buffer in Acidic Waters," in Proceedings of the International Conference on Ecological Impacts of Acid Precipitation, D. Drablos and A. Tollan, Eds., Norway, SNSF Project (1980).
- Johnson, N. M., G. E. Likens, F. H. Borman, D. W. Fisher, and R. S. Pierce, "A Working Model for the Variation in Stream Chemistry at the Hubbard Brook Experimental Forest, New Hampshire," Water Resources Research, Vol. 5, 1353-1363 (1969).
- Johnson, N. M., C. T. Driscoll, J. S. Eaton, G. E. Likens, and W. H. McDowell, "'Acid Rain', Dissolved Aluminum and Chemical Weathering at the Hubbard Brook Experimental Forest, New

- Hampshire," Geochimica et Cosmochimica Acta, Vol. 45, 1421-1437 (1981).
- Johnson, D. W., J. Turner, and J. M. Kelly, "The Effects of Acid Rain on Forest Nutrient Status," Water Resources Research, Vol. 18, No. 3, 449-461 (1982).
- Johnson, N. M., "Acid Rain Neutralized by Geological Materials," In: Geological Aspects of Acid Deposition, Edited by Owen P. Bricker, Acid Precipitation Series, Vol. 7, Ann Arbor Science (1984).
- Kerr, R. A., "There is More to 'Acid Rain' Than Rain," Science, Vol. 211, 692-693 (1981).
- Krug, C. E., and C. F. Frink, "Acid Rain on Acid Soil: A New Perspective," Science, Vol. 221, 520-525 (1983).
- Leivestad, H., G. Hendrey, I. Muniz, and E. Snekvik, "Effects of Acid Precipitation on Freshwater Organisms," in Impact of Acid Precipitation on Forest and Freshwater Ecosystems in Norway, F. Braekke editor, SNSF Project Report, FR6, Oslo, Norway, 86-111 (1976).
- Leivestad, H., I. P. Muniz, and B. O. Rosseland, "Acid Stress in Trout from a Dilute Mountain Stream," in Proceedings of the International Conference on Ecological Impacts of Acid Precipitation, D. Drablos and A. Tollan, Eds., Norway, SNSF Project (1980).
- Linsey, R. K., M. A. Kohler, and J. L. H. Paulhus, Hydrology for Engineers, McGraw-Hill Book Company, (1975).
- Matthiessen, P. and A. E. Brafield, "The Effects of Dissolved Zinc on the Gills of the Stickleback (Gasterosteus aculeatus, L.)," Journal of Fish Biology, Vol. 5, No. 5, 607-613 (1973).
- Mattson, S. and J. B. Hester, "The Laws of Soil Colloidal Behavior: 12. The Amphoteric Nature of Soils in Relation to Aluminum Toxicity," Soil Science, Vol. 36, 229-244 (1933).
- May, H. M., P. A. Helmke, and M. L. Jackson, "Gibbsite Solubility and Thermodynamic Properties of Hydroxy-Aluminum Ions in Aqueous Solutions at 25 C," Geochimica et Cosmochimica Acta, Vol. 43, 861-868 (1979).
- McBride, M. B. and P. R. Bloom, "Adsorption of Aluminum by a Smectite: II. An Al^{3+} - Ca^{2+} Exchange Model," Soil Science Society of American Journal, Vol. 41, 1073-1077 (1977).

- McDowell, W. H. and T. Wood, "Podzolization: Soil Processes Control Dissolved Organic Carbon Concentrations in Stream Water," Soil Science, (1984).
- McQuaker, N. R., P. D. Kluckner, and D. K. Sandberg, "Chemical Analysis of Acid Precipitation: pH and Acidity Determinations," Environmental Science and Technology, Vol. 17, No. 7, 431-435 (1983).
- McWilliams, P. G. and W. T. W. Potts, "The Effects of pH and Calcium Concentrations on Gill Potentials in the Brown Trout (Salmo trutta)," Journal of Comparative Physiology, Vol. 126, No. 3, 277-286 (1978).
- McWilliams, P. G., D. J. A. Brown, G. D. Howells, and W. T. W. Potts, "Physiology of Fish in Acid Waters," in Proceedings of the International Conference on Ecological Impacts of Acid Precipitation, D. Drablos and A. Tollan, Eds., Norway, SNSF Project (1980).
- Methods of Soil Analysis, Part 2. Chemical and Microbiological Properties, Edited by A. L. Page, R. H. Miller, and D. R. Keemey, ASA-SSSA, Madison, Wisconsin, 2nd Edition (1982).
- Mount, D. I., "The Effects of Total Hardness and pH on Acute Toxicity of Zinc to Fish," Air and Water Pollution, Vol. 10, 49-56 (1966).
- Muniz, I. P. and H. Leivestad, "Toxic Effects of Aluminum on the Brown Trout (Salmo trutta L.)," in Proceedings of the International Conference on Ecological Impacts of Acid Precipitation, D. Drablos and A. Tollan, Eds., Norway, SNSF Project (1980).
- Muniz, I. P. and H. Leivestad, "Acidification-Effects on Freshwater Fish," in Proceedings of the International Conference on Ecological Impacts of Acid Precipitation, D. Drablos and A. Tollan, Eds., Norway, SNSF Project (1980).
- Nilsson, S. I. and B. Bergkvist, "Aluminum Chemistry and Acidification Processes in a Shallow Podzol on the Swedish Westcoast," Water, Air, and Soil Pollution, Vol. 20, 311-329 (1983).
- Nordstrom, D. K., "The Effects of Sulfate on Aluminum Concentrations in Natural Waters: Some Stability Relations in the System $Al_2O_3-SO_3-H_2O$ at 298 K," Geochimica et Cosmochimica Acta, 46, 681-692 (1982).

- Nordstrom, D. K. and J. W. Ball, "The Geochemical Behavior of Aluminum in Acidified Surface Waters," Science, Vol. 232, 54-56 (1986).
- Orion Research, Handbook of Electrode Technology, Cambridge, MA, (1982).
- Orion Research, Instruction Manual Ross pH Electrodes, Cambridge, MA (1984).
- Overrein, L. N., H. M. Seip, and A. Tollan, "Acid Precipitation - Effects on Forest and Fish," Final Report of the SNSF Project 1972-1980, (1981).
- Pleysier, J. L., A. S. R. Juo, and A. J. Herbillon, "Ion Exchange Equilibria Involving Aluminum in a Kaolinitic Ultisol," Soil Science Society of America Journal, Vol. 43, 875-880 (1979).
- Raddum, G. G., "Comparision of Benthic Invertebrates in Lakes With Different Acidity," in Proceedings of the International Conference on Ecological Impacts of Acid Precipitation, D. Drablos and A. Tollan, Eds., Norway, SNSF Project (1980).
- Record, F. A., D. V. Bubenick, and R. J. Kindya, Acid Rain Information Book, Noyes Data Corporation, Park Ridge, New Jersey, USA (1982).
- Reuss, J. O., "Simulation of Soil Nutrient Losses Resulting from Rainfall Acidity," Ecological Modeling, Vol. 11, 15-38 (1980).
- Reuss, J. O., "Implications of the Calcium-Aluminum Exchange System for the Effect of Acid Precipitation on Soils," Journal of Environmental Quality, Vol. 12, No. 4, (1983).
- Reuss, J. O. and D. W. Johnson, "Effect of Soil Processes on the Acidification of Water by Acid Deposition," Journal of Environmental Quality, Vol. 14, No. 1, (1985).
- Robertson, C. E., and J. D. Hem., "Solubility of Aluminum in the Presences of Hydroxide, Fluoride, and Sulfate," USGS Water Supply Paper 1827-C (1969).
- Roff, J. C., and R. E. Kwaitkowski, "Zooplankton and Zoobenthos Communities of Selected Northern Ontario Lakes of Different Acidities," Canadian Journal of Zoology, Vol. 55, 899-911 (1977).

- Rosenqvist, I. T., "Alternative Sources for Acidification of River Water in Norway," The Science of the Total Environment, Vol. 10, 39-49 (1978).
- Rosenqvist, I. T., P. Jorgensen, and H. Rveslatten, "The Importance of Natural pH Production for Acidity in Soil and Water," in Proceedings of the International Conference on Ecological Impacts of Acid Precipitation, D. Drablos and A. Tollan, Eds., Norway, SNSF Project (1980).
- Rutter, A. J., K. A. Kershaw, P. C. Robins, and A. J. Morton, "A Predictive Model of Rainfall Interception in Forest: 1. Derivation of the Model from Observations in a Plantation of Corsican Pine," Agricultural Meteorology, Vol. 9, 367-384 (1971).
- Saar, R. A. and J. H. Weber, "Fulvic Acid: Modifier of Metal-Ion Chemistry," Environmental Science and Technology, Vol. 16, No. 9, 510A-517A (1982).
- Schaeckler, M., "A Fractionation Procedure for Aluminum Analysis in Natural Waters," Project Report, Environmental Engineering Program, University of Massachusetts/Amherst, (1985).
- Schofield, C. L., Research Technical Completion Report A-072-NY, Office of Water Research and Technology, Dept. of the Interior, Washington D. C., (1977).
- Schofield, C. L., and J. R. Trojnar, "Aluminum Toxicity to Brook Trout (*Salvelinus fontinalis*) in Acidified Waters," Pollution Rain, Edited by T. Y. Toribara, M. W. Miller, and P. E. Morrow, Plenum Press, 341-363 (1980).
- Seip, H. M., "Deposition-Soil-Water Interactions Summary Document," Ecological Effects of Acid Deposition, National Swedish Environmental Protection Board, Report PM 1636 (1983).
- Shaffer, P. W. and J. N. Galloway, "Acid Precipitation: The Impact on Two Headwater Streams in Shenandoah National Park, Virginia," International Symposium on Hydrometeorology, American Water Resources Association, (June, 1982).
- Singh, B. R., "Effects of Acid Precipitation on Soil and Forest. 3. Sulfate Sorption by Acid Forest Soils," in Proceedings of the International Conference on Ecological Impacts of Acid Precipitation, D. Drablos and A. Tollan, Eds., Norway, SNSF Project (1980).

- Singh, B. R., G. Abrahamsen, and A. Stuanes, "Effect of Simulated Acid Rain on Sulfate Movement in Acid Forest Soils," Soil Science Society of America Journal, Vol. 44, 75-80 (1980).
- Singh, B. R., "Sulfate Sorption by Acid Forest Soils: 1. Sulfate Adsorption Isotherms and Comparison of Different Adsorption Equations in Describing Sulfate Adsorption," Soil Science, Vol. 138, No. 3, 189-197 (1984).
- Smith, R. M. and A. E. Martell, Critical Stability Constants, Volume 4: Inorganic Complexes, Plenum Press, New York (1974).
- SNSF Project 1972-1980, Acid Precipitation-Effects on Forest and Fish, Edited by L. N. Overrein, H. M. Seip, and A. Tollon, Oslo, Norway (1981).
- Stevenson, F. J., and J. H. Butler, "Chemistry of Humic Acids and Related Pigments," Organic Geochemistry, Edited by G. Elinton and M. T. J. Murphy, Springer-Verlag (1969).
- Standard Methods for the Examination of Water and Wastewater, American Public Health Association, 16th Edition, Washington D.C. (1985).
- Stone, B. D., Preliminary map of surficial deposits of the Gardner Quadrangle, Worcester County, Massachusetts. U. S. Geol. Survey Open-file report 78-379 (1978).
- Stumm, W. and J. J. Morgan, Aquatic Chemistry, Wiley Interscience (1981).
- Stumm, W., J. J. Morgan, and J. L. Schnoor, "Acid Rain-A Result of Disruptions in Hydrogeochemical Processes," Naturwissenschaften, Vol. 70, 216-223 (1983).
- Thorogood, A., "A Sulfate Adsorption Study on Selected Massachusetts Soils," Independent Study Report, Environmental Engineering Program, University of Massachusetts/Amherst, (1986).
- Truesdell, A. H. and B. F. Jones, "WATEQ, A Computer Program for Calculating Chemical Equilibria of Natural Waters," Journal of Research U.S. Geological Survey, Vol. 2, No. 2, 233-248 (1974).
- United States Department of Agriculture, "Inventory of Potential and Existing Reservoir Sites, Chicopee Study Area, Massachusetts," Soil Conservation Service and Massachusetts Water Resources Commission (1973).

- United States Environmental Protection Agency, Acid Rain, EPA Office of Research and Development, Washington D. C., EPA-600/9-79-036 (July, 1980).
- United States Fish and Wildlife Service, "Effects of Acid Precipitation on Aquatic Resources: Results of Modeling Workshop," U.S. FWS, Biological Services Program, FWS/obs-80/40.12 (1982).
- United States Geological Survey, Department of Interior, Bedrock Geology Map of Massachusetts, (1983).
- Voight, G. K., "Acid Precipitation and Soil Buffering Capacity," in Proceedings of the International Conference on Ecological Impacts of Acid Precipitation, D. Drablos and A. Tollan, Eds., Norway, SNSF Project (1980).
- Wagman, D. D., W. H. Evans, V. B. Parker, I. Halow, S. M. Baily, and R. H. Schumm, "Selected Values of Chemical Thermodynamic Properties," Technical Note 270-3, U.S. Department of Commerce, (1968).
- Westall, J. C., J. L. Zachary, and F. M. M. Morel, "MINEQL: A Computer Program for the Calculation of Chemical Equilibrium Composition of Aqueous Systems," Ralph M. Parsons Laboratory for Water Resources and Environmental Engineering, Department of Civil Engineering, Massachusetts Institute of Technology, Technical Note No. 18 (1976).
- Wigley, T. M. L., "WATSPEC: A Computer Program for Determining the Equilibrium Speciation of Aqueous Solutions," British Geomorphological Research Group, Technical Bulletin No. 20 (1977).
- Wright, R. F., "Norwegian Models for Surface Water Chemistry: An Overview," Modeling Total Acid Precipitation Impacts, Acid Precipitation Series, Vol. 9, J. L. Schnoor, Ed., J. I. Teasley, Series Ed., Butterworth Publishers, Boston, 73-87 (1984).
- Zinke, P. J., "Forest Interception Studies in the United States," Forest Hydrology, Edited by W. E. Sopper and H. W. Lull, Pergamon, Oxford, 137-161 (1967).

APPENDIX A

ANC COMPUTER PROGRAM LISTING WITH
SAMPLE INPUT AND OUTPUT

APPENDIX B

EQUILIBRIUM CONSTANTS AND ENTHALPY DATA
USED IN THIS STUDY

APPENDIX C

EQUAL COMPUTER PROGRAM LISTING WITH
SAMPLE INPUT AND OUTPUT

APPENDIX D

SIMULATION MODEL COMPUTER PROGRAM LISTING
WITH SAMPLE INPUT AND OUTPUT

APPENDIX E

RAW DATA COLLECTED
FOR THIS STUDY

APPENDIX F

PLOTS OF STREAMWATER IONS